8-2017

Resolving Spatial and Temporal Variability in Dissolved Organic Matter Characteristics within Combined Agricultural and Stormwater Conveyances

Bryce A. Mihalevich

RESOLVING SPATIAL AND TEMPORAL VARIABILITY IN DISSOLVED ORGANIC MATTER CHARACTERISTICS WITHIN COMBINED AGRICULTURAL AND STORMWATER CONVEYANCES

by

Bryce A. Mihalevich

A thesis submitted in partial fulfillment
of the requirements for the degree

of

MASTER OF SCIENCE

in

Civil and Environmental Engineering

Approved:

_____	_____
Jeffery S. Horsburgh, Ph.D. Major Professor	Michelle A. Baker, Ph.D. Committee Member
_____	_____
David K. Sevens, Ph.D. Committee Member	Mark R. McLellan, Ph.D. Vice President for Research and Dean of the School of Graduate Studies

UTAH STATE UNIVERSITY
Logan, Utah

2017

ABSTRACT

RESOLVING SPATIAL AND TEMPORAL VARIABILITY IN DISSOLVED ORGANIC MATTER CHARACTERISTICS WITHIN COMBINED AGRICULTURAL AND STORMWATER CONVEYANCES

by

Bryce A. Mihalevich, Master of Science

Utah State University, 2017

Major Professor: Dr. Jeffery S. Horsburgh
Department: Civil and Environmental Engineering

Dissolved organic matter (DOM) plays an important role in the cycling of nutrients within aquatic ecosystems; however, excess amounts can have detrimental effects on aquatic organisms. Stormwater runoff events in urban areas can contribute high concentrations of DOM to receiving waters, posing potential impairment to the aquatic ecosystems of urban streams and downstream water bodies. Characterizing compositional changes in DOM due to storm events is important for understanding potential downstream water quality effects and has been well studied in forested, agricultural, and urban landscapes. However, *in situ* sensors have not been widely applied to monitor stormwater contributions in urbanized areas, leaving the spatial and temporal characteristics within these systems poorly understood. Using laboratory measurements

of dissolved organic carbon (DOC) concentration and excitation emission matrix spectroscopy (EEMS), fluorescent DOM (FDOM) sensors, and a mobile water quality sensing platform, this study investigated changes in DOM quantity and sources within the Northwest Field Canal (NWFC), an urban water conveyance located in Logan, Utah, USA that receives runoff during storm events. Under baseflow conditions, FDOM decreased and exhibited dampened diurnal variability as the summer irrigation season progressed, while FDOM values at the upstream and downstream monitoring sites were relatively similar. During storm events, FDOM concentrations were rapidly elevated to values orders of magnitude greater than in baseflow measurements, and DOC concentrations were more than 3 times greater at the downstream site than those at the upstream site due to high contributions of DOC being discharged from outfalls. Compositional changes in DOM indicated a shift during storm events from a more autochthonous, less degraded DOM in baseflow to more decomposed and terrestrially derived DOM in stormwater flows. These observations were consistent with results from custom, *in situ* fluorometers, which also revealed a seasonal transition to a more microbially derived composition in baseflow conditions as the summer season progressed. Deployment of a mobile sensing platform during stormflow conditions confirmed that contributions of DOM were associated with the locations of outfalls discharging runoff into the canal and revealed spatial changes in DOM composition and concentration along canal transects.

(131 pages)

PUBLIC ABSTRACT

RESOLVING SPATIAL AND TEMPORAL VARIABILITY IN DISSOLVED ORGANIC MATTER CHARACTERISTICS WITHIN COMBINED AGRICULTURAL AND STORMWATER CONVEYANCES

Bryce A. Mihalevich

In many urban areas, stormwater runoff can threaten the ecological health of streams and downstream water bodies. Due to the increased impervious nature of urban landscapes, runoff is more "flashy" and as a result, high concentrations of pollutants can be transported in shorter periods of time than in more natural environments. One pollutant of concern is dissolved organic matter (DOM). DOM is important within aquatic ecosystems, but excess amounts can cause depletion in dissolved oxygen concentrations and can negatively affect aquatic organisms. This study investigated changes in DOM quantity and sources within the Northwest Field Canal (NWFC), an urban water conveyance located in Logan, Utah, USA that receives runoff during storm events. DOM was monitored at upstream and downstream locations within the canal and at selected stormwater outfalls within the study reach. During storm events, DOM concentrations were rapidly elevated to values orders of magnitude greater than in baseflow measurements, and were greater at the downstream site than at the upstream site, triggered by contributions from outfalls discharging into the canal. Changes in DOM composition during storm events confirmed that DOM is more terrestrially derived,

whereas it is normally more microbially derived during baseflow conditions in the canal. These results provide better understanding of the composition of DOM in the canal system and may provide crucial information for future management of stormwater runoff that can potentially lead to the improvements of water quality in downstream water bodies.

ACKNOWLEDGMENTS

I express many thanks to Dr. Jeff Horsburgh, for providing me the opportunity to carry out this research. I appreciate his opinions, expertise, and mentorship throughout my graduate studies. I also would like to thank my graduate committee members, Dr. David Stevens and Dr. Michelle Baker, for the time given to review my work and provide meaningful feedback and guidance.

I am grateful for the materials and laboratory equipment that were made available to me in order to carry out critical aspects of my research. Thank you to all who provided guidance to my questions, and assistance in data collection, laboratory analysis, and long nights in the field, including Tony Melcher, Amber Jones, Caleb Buahin, Julie Kelso, Rachel Gabor, Phil Suiter, Tyler King, and Hyrum Tennant. I am grateful to the City of Logan and the Northwest Field Canal Company for allowing access to monitoring sites. I also thank my parents for their support and encouragement in pursing my goals.

I am also very appreciative of the generous funding that supported my research and graduate schooling including the Utah Water Research Laboratory and Department of Civil and Environmental Engineering at Utah State University. Sampling equipment and data collection support was facilitated by the U.S. National Science Foundation under EPSCoR grant IIA-1208732 awarded to Utah State University, as part of the State of Utah EPSCoR Research Infrastructure Improvement Award. Any opinions, findings, and conclusions or recommendations expressed in this material are those of the authors and do not necessarily reflect the views of the National Science Foundation.

Bryce A. Mihalevich

CONTENTS

Page

ABSTRACT iii

PUBLIC ABSTRACT v

ACKNOWLEDGMENTS vii

LIST OF TABLES x

LIST OF FIGURES xi

CHAPTER

1. INTRODUCTION 1

    References 7

2. LITERATURE REVIEW 9

    2.1 Study Area Description 9
    2.2 Dissolved Organic Matter in Aquatic Environments 10
    2.3 Excitation Emission Matrix Spectroscopy 15
    2.4 EEM Peaks and Fluorescence Indices 16
    2.5 Continuous *in situ* Fluorescence Monitoring 19
    2.6 Remote Sensing of Water Quality 22
    References 24
    Tables 31

3. INVESTIGATING STORMWATER IMPACTS ON DISSOLVED ORGANIC MATTER IN AN URBAN WATER SYSTEM 32

    Abstract 32
    3.1 Introduction 33
    3.2 Methods 36

        3.2.1 Study Area 36
        3.2.2 Data Collection 37
        3.2.3 Sample Preparation 39
        3.2.4 Sample Analysis 40
        3.2.5 Data Analysis 42

    3.3 Results and Discussion 45

3.3.1 Dissolved Organic Carbon Concentrations 45
3.3.2 Excitation Emission Matrix Spectroscopy 46
3.3.3 Fluorescence Indices 47

3.4 Conclusions 52
Acknowledgments 55
References 56
Tables 61
Figures 66

4. HIGH FREQUENCY MEASUREMENTS REVEAL SPATIAL AND TEMPORAL PATTERNS OF DISSOLVED ORGANIC MATTER IN AN URBAN WATER CONVEYANCE 76

Abstract 76
4.1 Introduction 77
4.2 Methods 80

4.2.1 Study Area 80
4.2.2 Sampling and Laboratory Analysis 81
4.2.3 Continuous Data Collection 84
4.2.4 Mobile Sensing Platform 86
4.2.5 Data Analysis 87

4.3 Results 89

4.3.1 Temporal Changes of DOM 89
4.3.2 High Resolution Spatial Variability of DOM 91

4.4 Discussion 92

4.4.1 Continuous FDOM Measurements 92
4.4.2 Custom Fluorometers for in situ FI 95
4.4.3 High Resolution Spatial Characteristics 99

4.5 Conclusions 101
Acknowledgments 103
References 104
Tables 109
Figures 112

5. SUMMARY AND CONCLUSION 121

6. ENGINEERING SIGNIFICANCE 126

7. RECOMMENDATIONS FOR FUTURE RESEARCH 129

LIST OF TABLES

Table		Page
2-1	Commonly used excitation/emission peak regions used in EEMS analyses	31
2-2	Commonly used fluorescence indices	31
3-1	Threshold criteria used to trigger automated sampling	61
3-2	Sampling conducted during the 2015 and 2016 irrigation seasons	61
3-3	Storm event characteristics of sampled storms at the continuously monitored outfall sites	62
3-4	Mean and standard deviation of measured DOC concentrations for each sampling location and flow condition	63
3-5	Mean and standard deviation of calculated fluorescence indices	64
3-6	Calculated $SUVA_{254}$ values for each sampling location and flow condition.	65
4-1	Instrumentation at the canal and outfall monitoring sites	109
4-2	Instrumentation of the mobile sensing platform	110
4-3	Summary of monthly FDOM statistics for baseflow conditions at the upstream and downstream continuous monitoring locations	111

LIST OF FIGURES

Figure		Page
3-1	Site map of the Northwest Field Canal showing locations of sampling sites and land use categories	66
3-2	Box and whisker plot of DOC concentrations in the Northwest Field Canal under baseflow and stormflow conditions	67
3-3	Box and whisker plot comparing the calculated volumes under the EEM for sampling locations and flow conditions	68
3-4	Correlation between EEM fluorescence volume and DOC concentrations	69
3-5	Change in relative contributions of known EEM peaks across sampling locations and flow conditions	70
3-6	Subtraction of normalized EEMs for each flow condition from the normalized baseflow EEM at the 200 S site	71
3-7	Box and whisker plot of the FI values in the Northwest Field Canal under baseflow and stormflow conditions	72
3-8	Box and whisker plot of HIX values in the Northwest Field Canal under baseflow and stormflow conditions	73
3-9	Box and whisker plot of BIX values in the Northwest Field Canal under baseflow and stormflow conditions	74
3-10	Boxplot of $SUVA_{254}$ values in the Northwest Field Canal under baseflow and stormflow conditions	75
4-1	Operation of the mobile sensing platform during stormflow conditions	112
4-2	Comparison of raw and corrected FDOM with DOC samples during a storm event at the 1800 N monitoring location	113
4-3	*In situ* measurements of FDOM in log scale and rainfall during the two irrigation seasons in the NWFC	114
4-4	Mean and standard deviation of the diurnal cycle of FDOM during baseflow conditions for each month at the continuous canal monitoring sites during the 2016 field season	115

4-5 Seasonal change of $FI_{n\text{-}situ}$ measured in the NWFC at the upstream and downstream monitoring locations during baseflow conditions 116

4-6 Comparison of lab measured and FIin-situ values during a storm event at the 1800 N monitoring location 117

4-7 Baseflow runs with the mobile sensing platform.....118

4-8 Two stormflow runs with the mobile sensing platform where spikes in FDOM are associated with the locations of outfalls discharging into the canal 119

4-9 Comparison between the response of FDOM and $FI_{in\text{-}situ}$ to outfall contributions during a stormflow run with the mobile sensing platform.....120

CHAPTER 1

INTRODUCTION

In urban areas, stormwater runoff can pose serious threats to the ecological health of streams and downstream water bodies. Urban catchments can have large areas of impervious surfaces and drainage connectivity that routes runoff directly to receiving waters, which can make them much more "flashy" when compared to the characteristics of forested and agricultural watersheds. In more natural or agricultural watersheds, runoff from stormwater may also be buffered by riparian vegetation, which allows opportunity for some pollutants to be removed and for some of the runoff to infiltrate into groundwater aquifers. The lack of infiltration in urban areas induces faster pollutant export, allowing little or no time for terrestrial processing to influence the quality of stream water (Hatt et al., 2004). As a result, significant fluxes of pollutants can be exported during stormwater runoff events in urban watersheds (Goldman et al., 2014; Nguyen et al., 2010). While these nonpoint source (NPS) contributions may be individually relatively small in nature compared to point sources, the cumulative effect over large areas has been suggested to be a dominant source of biological degradation in urban catchments (Paul and Meyer, 2001).

In Logan, UT, where this study took place, stormwater is directed from city streets and parking lots into irrigation canals and transported downstream and out of the city. Under baseflow conditions, these canals serve as irrigation water conveyances for downstream agricultural users. However, during rainfall events that contribute large

volumes of runoff to the canals, water quality may degraded to the point that it is inadequate for some agricultural uses.

Furthermore, downstream of Logan, UT and agricultural areas is Cutler Reservoir, which is listed as having impaired water quality in the State of Utah's list of impaired waters compiled by the Utah Department of Environmental Quality (DEQ), Division of Water Quality (DWQ), in compliance with Section 303(d) of the Clean Water Act (Utah DWQ, 2004; Utah Office of Administrative Rules, 2017). The primary water quality constituent of concern is excess total phosphorus as targeted in the recent total maximum daily load (TMDL) study (Utah DWQ, 2010). However, the underlying issue for which Cutler Reservoir was included on Utah's 303(d) list is low dissolved oxygen (DO) concentrations within the reservoir, which have a number of ecological impacts, including adverse effects on fish and other aquatic species. The TMDL targeted phosphorus under the premise that excess nutrients promote algal growth that can lead to subsequent oxygen depletion in the reservoir. The TMDL pointed out that potential sources of phosphorus in the area are primarily from point sources, agricultural practices, stream bank and shoreline erosion, and stormwater runoff from developed areas. The study noted potential divers for low DO to be from decaying organic matter originating from algal and macrophyte growth, sediment oxygen demand (SOD), climactic factors (i.e., wind mixing suspending bottom sediments with high SOD), and elevated temperatures within Cutler Reservoir. However, no quantitative linkage between low DO and total phosphorus could be determined in the study. The TMDL concluded that if low DO concentrations persisted after implementation of point source reductions and NPS

management measures aimed at reducing phosphorus loading to the reservoir, other factors, such as organic matter loading, should be investigated.

Biological oxygen demand (BOD) exerted during decomposition of organic matter (primarily by bacteria) can cause a subsequent drop in DO concentrations (Boyd, 2000), contributing to impacts on aquatic ecosystems. This threat can be amplified in urban watersheds, where contributions of organic matter are flushed out during stormwater runoff events, leading to short episodes of hypoxia in receiving streams and potentially longer term effects on downstream water bodies like Cutler Reservoir (Mallin et al., 2006). Thus, there is a need to need to study potential DOM contributions to waters like Cutler Reservoir that are experiencing low DO concentrations. DOM can also have other adverse effects on water quality, including problems with coloration, taste, and odor in natural waters.

DOM is ubiquitous in nature. It is a heterogeneous mixture of organic compounds, making it sometimes difficult to characterize (Baker and Spencer, 2004). Although excess DOM can contribute to water quality impairment, DOM is very important as it is one of the largest sources of biologically available carbon in aquatic ecosystems and, therefore, has a significant importance in the cycling of nutrients in aquatic food webs (Fellman et al., 2010). DOM also plays critical roles in the transport of toxic metals from the environment (McKnight et al., 2001; Corbett, 2007).

There is a growing body of literature aimed at characterizing DOM in runoff from agricultural, forested, and urban watersheds. Characterization is often done by dissolved organic carbon (DOC) concentration analysis, excitation emission matrix spectroscopy

(EEMS), or by using *in situ* sensors measuring fluorescent DOM (FDOM). EEMs have been widely used to characterize the source, age, quality, and composition of DOM in aquatic samples (Goldman et al., 2014; McElmurry et al., 2014; Nguyen et al., 2010). The application of *in situ* sensors has become more prevalent with improvements in technology; however, most application of *in situ* monitoring have been in forested and agricultural watersheds (Saraceno et al., 2009; Spencer et al., 2007). The benefits associated with continuous monitoring are numerous, including the ability to: 1) capture a much broader range of hydrologic conditions, 2) customize data collection frequency and create a much larger number of observations than could be analyzed in a laboratory, 3) identify and characterize short-term hydrologic events that are difficult to sample, and 4) reduce the cost per observation. However, the application of *in situ* fluorescence monitoring for better characterizing and quantifying water quality effects of urban stormwater has yet to be thoroughly examined.

The potential for DOM transport in stormwater runoff from Logan City is significant, as with most urbanized watersheds. The overall objective of the research presented in this thesis was to quantify and better characterize the contributions of DOM from urban stormwater runoff to the combined stream/agricultural/stormwater conveyances in Logan, which are also common in other cities in the western U.S. (City of Grand Junction, 2016; City of Sequim, 2016). We measured DOM under baseflow and stormflow conditions within one of the major canal systems in Logan to provide a better understanding of contributions from stormwater outfalls, combined effects after mixing with water diverted from the Logan River for agricultural uses, and potential downstream

effects on canal water users and in Cutler Reservoir. Although not addressed by this thesis, this study was conducted in companion with a dissertation that examined sediment and phosphorus exports via stormwater from the Logan City urban area (Melcher and Horsburgh, 2017).

This study was conducted over the course of the two summer irrigation seasons to characterize the DOM in the Northwest Field Canal (NWFC), an urban water conveyance located in Logan City, that receives stormwater inputs. The scope of this study included quantifying DOM concentrations and determining DOM compositional changes between baseflow and stormflow samples collected at upstream and downstream ends of the study reach and between stormflow samples collected from outfalls discharging directly to the canal. Specifically, we hypothesized that 1) the concentrations of DOM in stormwater runoff contributed to the canal would be greater than the concentrations of DOM during baseflow conditions in the canal, and 2) the DOM in samples collected from the outfalls during stormwater runoff would have a different composition than the DOM in samples collected from the canal during baseflow conditions. To test these first two hypotheses, we collected samples from within the canal and from storm drains during baseflow and storm runoff conditions and analyzed them for DOC concentration and using EEMS.

We also hypothesized that 3) FDOM concentrations would change seasonally within the canal and would be different at the upstream and downstream end of the canal, 4) the sources contributing or producing DOM within the system would change temporally and seasonally in the canal, and 5) DOM concentration and composition within the canal would be effected by contributions from outfalls discharging into the

canal during stormwater runoff. To test hypotheses 3 – 5, continuous high-frequency measurements of FDOM and fluorescence at custom spectral regions were made using *in situ* sensors at the upstream and downstream ends and along the length of the study reach using a mobile sensing platform to capture spatial and temporal changes in DOM concentration and composition.

This research demonstrated that changes in composition and concentration of DOM are occurring in the NWFC due to stormwater runoff discharging into the canal. We were able to observe seasonal changes and diurnal fluctuations in the amount of DOM being contributed to the NWFC from the upstream Logan River. Lastly, we examined the spatial differences in DOM along select transects of the canal and revealed contributions that were associated with the discrete locations of outfalls discharging into the canal that would have otherwise gone unobserved. We anticipate that the results of this work will be of interest to stormwater managers and the broader water quality management community.

References

Baker, A., and R. G. M. Spencer (2004), Characterization of dissolved organic matter from source to sea using fluorescence and absorbance spectroscopy, *Sci. Total Environm.*, *333*, 217–232, doi: 10.1016/j.scitotenv.2004.04.013.

Boyd, C. E. (2000), *Water quality: An introduction*. Kluwer Academic Publishers, Boston, MA.

City of Grand Junction (2016), Grand Junction Municipal Code Volume II: Development Regulations; Title 28: Stormwater Management Manual; Chapter 28.52: Irrigation/Drainage Structures. Grand Junction, Colorado. <http://www.codepublishing.com/CO/GrandJunction/html2/GrandJunction28/GrandJunction2852.html#28.52> (Feb. 8, 2017).

City of Sequim (2016), *Storm and Surface Water Master Plan*. Sequim, Washington <http://www.sequimwa.gov/DocumentCenter/View/7735> (Feb. 8, 2017).

Corbett, C. A. (2007), Colored dissolved organic matter (CDOM) workshop summary, *Reports*, 2. http://scholarcommons.usf.edu/basgp_report/2

Fellman, J. B., E. Hood, and R. G. M. Spencer (2010), Fluorescence spectroscopy opens new windows into dissolved organic matter dynamics in freshwater ecosystems: A review, *Limnol. Oceanogr.*, *55*(6), 2452–2462, doi: 10.4319/lo.2010.55.6.2452.

Goldman, J. H., S. A. Rounds, M. K. Keith, and S. Sobieszczyk (2014), Investigating organic matter in Fanno Creek, Oregon, Part 3 of 3: Identifying and quantifying sources of organic matter to an urban stream, *J. Hydro.*, *519*, 3028–3041, doi: 10.1016/j.jhydrol.2014.07.033.

Hatt, B. E., T. D. Fletcher, C. J. Walsh, and S. L. Taylor (2004), The influence of urban density and drainage infrastructure on the concentrations and loads of pollutants in small streams, *J. Environ. Manage.*, *34*(1), 112–124, doi: 10.1007/s00267-004-0221-8.

Mallin, M. A., V. L. Johnson, S. H. Ensign, and T. A. MacPherson (2006), Factors contributing to hypoxia in rivers, lakes, and streams, *Limnol. Oceanogr.*, *51*(1, part 2), 690–701, doi: 10.4319/lo.2006.51.1_part_2.0690.

McElmurry, S. P., D. T. Long, and T. C. Voice (2014), Stormwater dissolved organic matter: Influence of land cover and environmental factors, *Environ. Sci. Technol.*, *48*(1), 45–53, doi: 10.1021/es402664t.

McKnight, D. M., E. W. Boyer, P. K. Westerhoff, P. T. Doran, T. Kulbe, and D. T. Andersen (2001), Spectrofluorometric characterization of dissolved organic matter for indication of precursor organic material and aromaticity, *Limnol. Oceanogr.*, *46*(1), 38–48, doi: 10.4319/lo.2001.46.1.0038.

Melcher, A. A., and J. S. Horsburgh (2017), An urban observatory for quantifying phosphorus and suspended solids loads in combined natural and stormwater conveyances, *Environ. Monit. Assess.*, *2017,* 189-285, doi: 10.1007/s10661-017-5974-7.

Nguyen, H. V.-M., J. Hur, and H.-S. Shin (2010), Changes in spectroscopic and molecular weight characteristics of dissolved organic matter in a river during a storm event, *Water Air Soil Pollut.*, *212*(1–4), 395–406, doi: 10.1007/s11270-010-0353-9.

Paul, M. J., and J. L. Meyer (2001), Streams in the urban landscape, *Annu. Rev. Ecol. Syst.*, *32*(1), 333–365, doi: 10.1146/annurev.ecolsys.32.081501.114040.

Saraceno, J. F., B. A. Pellerin, B. D. Downing, E. Boss, P. A. M. Bachand, and B. A. Bergamaschi (2009), High-frequency in situ optical measurements during a storm event: Assessing relationships between dissolved organic matter, sediment concentrations, and hydrologic processes, *J. Geophys. Res.*, *114*, G00F09, doi: 10.1029/2009JG000989.

Spencer, R. G. M., B. A. Pellerin, B. A. Bergamaschi, B. D. Downing, T. E. C. Kraus, D. R. Smart, R. A. Dahlgren, and P. J. Hernes (2007), Diurnal variability in riverine dissolved organic matter composition determined by in situ optical measurement in the San Joaquin River (California, USA), *Hydrol. Processes*, *21*(23), 3181–3189, doi: 10.1002/hyp.6887.

Utah Depatment of Environmental Quality, Division of Water Quality (2004), *Utah's 2004 303(d) List of Impaired Waters*, Salt Lake City, UT.

Utah Depatment of Environmental Quality, Division of Water Quality (2010), *Middle Bear River and Cutler Reservoir Total Maximum Daily Load (TMDL)*, Salt Lake City, UT.

Utah Office of Administrative Rules (2017), R317-2. Standards of Quality for Waters of the State. Salt Lake City, UT.

CHAPTER 2

LITERATURE REVIEW

2.1 Study Area Description

Logan, UT, located in the state's northern region, has a population of about 50,371 (U.S. Census Bureau, 2016), making it the largest city in Utah's Cache County. The Logan River enters city boundaries from the east as the river finishes its course through Logan Canyon. The Logan River watershed (United States Geological Survey Hydrologic Unit Code 1601020303) is part of the larger Bear River basin. As the Logan River enters the city it runs through what is known as the Logan "Island" district. At River Hollow Park, a portion of the Logan River is diverted into a mixed natural/lined channel called the Little Logan River. The Little Logan River then travels through the heart of the city, receiving stormwater from notable city features such as Merlin Olson Park and the Main Street City Center. The Little Logan River then flows west to Logan High School. Just west of Logan High School, the Little Logan River is diverted into the Northwest Field Canal (NWFC), the study site for this research.

The NWFC flows north, first through residential and mixed residential neighborhoods and then through primarily commercial and mixed-use, receiving stormwater from much of Logan's city center and commercial zones. Drainage subcatchments in Logan City are bordered by four irrigation canals, all of which are diverted from the Logan River and flow north through the city, with stormwater generally following the slope of the landscape, which is primarily from east to west. Many Logan City residents have the option of irrigating their lawns and gardens with canal water, thus

irrigation water is diverted from the canals and is conveyed through the city's gutters. Water is diverted from the canal east of a neighborhood and either returns directly or is applied for irrigation and later runs off into the canal to the west.

2.2 Dissolved Organic Matter in Aquatic Environments

DOM is present in all natural aquatic environments (Stedmon and Markager, 2005). It is significant because of the role it plays in nutrient sequestration and supply and because it is an available carbon source for aquatic biota (Goldman et al., 2012). Some DOM has metal-binding properties that are important in the transport of toxic metals from the environment, preventing harm to biological organisms (McKnight et al., 2001; Corbett, 2007). Additionally, DOM affects the color, taste, and odor of natural waters (Nguyen et al., 2010).

In aquatic ecosystems, DOM is generally characterized as being autochthonous (from the stream) or allochthonous (from terrestrial sources) in nature. For the majority of freshwater ecosystems, natural allochthonous inputs are the predominant contributor to the DOM pool (Carpenter et al., 2013; Sobieszczyk et al., 2014). This is usually attributed to terrestrial DOM (e.g., riparian vegetative biomass, atmospheric dust and gases, root exudates, and soil organic matter) being more recalcitrant, derived of heterogeneous, refractory organic substances of higher molecular weight and more resistant to biological degradation (Ylla et al., 2012). In contrast, autochthonous inputs are the most labile and bioavailable forms of DOM in the stream, resulting in lower residence times (Ylla et al., 2012). Common autochthonous sources include

decomposition from microbes and other aquatic species (e.g., phytoplankton, periphyton, and macrophytes) (Bertilsson and Jones, 2003). Both DOM sources are comprised of complex organic compounds that vary greatly in chemical composition, and the presence and concentration of these compounds are dependent on climate and regional factors such as land use, photolysis, hydrology, soil characteristics, and water residence time (Wright and Reddy, 2012). The addition and eventual degradation of DOM are essential to ecosystem function.

DOM is predominately made up of dissolved organic carbon (DOC), but can also be in the organic forms of nitrogen, sulfur, and phosphorus. Within natural aquatic systems, the chemical composition of DOM consists of humic substances, macromolecular hydrophilic acids, or low molecular weight organics. Humic substances, which make up approximately 50% of all terrestrially derived DOC, include fulvic acids and humic acids. Fulvic acids are a result of microbial degradation of plant and animal remains with a high portion of fatty acids and are high in aliphatic and carboxyl groups. Humic acids are characteristic of aromatic groups such as methoxyls and phenolics. Macromolecular hydrophilic acids compose approximately 30% of the terrestrial DOC pool. These consist of lower molecular weight organics, carbohydrates, carboxylic acids, and amino acids. The remaining portion (~20%) is made up of identifiable lower molecular weight organics such as carbohydrates (Aitkenhead-Peterson et al., 2003). The DOM produced from decaying algae and macrophytes consists of lower-molecular weight compounds, is biologically labile, and is readily used as an energy source by heterotrophic bacteria (Bertilsson and Jones, 2003). Microbial and photochemical

processes remove some of these constituents as fast as they are produced, making their concentration only measurable indirectly as bacterial production and respiration (Søndergaard and Thomas, 2004).

DOM is also a major component in carbon cycling. Due to its ability to make molecular bonds, DOM varies in chemical quality and quantity in stream water and contributes to the transport and cycling of nutrients in aquatic food webs. Often, in lotic systems, DOM bonded with nutrients is transported from productive to less productive areas. Excessive quantities of exported DOM can be detrimental to an aquatic ecosystem by creating increased nutrient bioavailability and high oxygen demand (Goldman et al., 2014). Yet, DOM is essential and provides numerous benefits to an ecosystem. Many marine ecosystems depend on terrestrial sources of DOM as a source of energy and nutrients (Fellman et al., 2010). In aquatic environments, DOM is transferred into higher trophic levels through predation, providing energy and nutrients across the food web. The residence time of DOM is a function of chemical characteristics like molecular weight, as well as the likelihood that organisms in the food web will consume it. Therefore, characterizing DOM is important for understanding how it may alter an aquatic ecosystem.

In many ecosystems, DOM provides some protection from ultraviolet (UV) radiation for algae and plankton (Coble, 2007; Wright and Reddy, 2012). However, high exposure to UV light can cause photodegradation of the DOM pool. The extent to which this occurs is dependent upon the concentration of DOM and the amount of light energy to which the DOM is exposed. Photodegradation of DOM has been shown to be a

dominant driver for DOM removal in estuaries and large rivers (Moran et al., 2000; Hernes and Benner, 2003; Coble, 2007). Additionally, increased light penetration can increase the photosynthesis of phytoplankton, potentially contributing to harmful algal blooms (Conley et al., 2009). In smaller streams, riparian shading can offer UV protection from photodegradation due to forested canopy; however, riparian shading tends to be less abundant in urban areas. This may contribute to UV light having a greater influence on DOM alterations in urban streams and especially urban canals having little overhead canopy.

Although the importance of DOM in aquatic ecosystems is well recognized and much work has been done to characterize it in more natural settings such as streams and rivers, less is known about DOM sources, composition, and residence time in urban stormwater runoff and in urban water conveyances. In general, the greater imperviousness and drainage connections in urban areas induce faster exports of pollutants, allowing little or no time for terrestrial processing and the bypassing of natural riparian buffers that might otherwise influence the quality of runoff reaching a stream (Hatt et al., 2004). Land use has also been shown to greatly influence the molecular weight and concentration of allochthonous DOM in surface water runoff (McElmurry et al., 2014). As a result, significant fluxes of carbon export occurring during stormwater runoff in urban watersheds have been reported (Goldman et al., 2014; Nguyen et al., 2010). While these nonpoint source (NPS) contributions may be relatively small in nature compared to point sources, the cumulative effect has been suggested to be a dominant source of biological degradation in urban catchments (Paul and Meyer, 2001).

The seasonal first flush, which varies temporally due to geographic climates (e.g., spring snowmelt or fall monsoons), and subsequent flush events from storms have been shown to produce the highest concentrations of DOM additions (Hood et al., 2005; Goldman et al., 2014). Goldman et al. (2014) also found soil and leaf litter additions to be the major source of DOM contributions during storm events in an urban stream in northwest Oregon. The pre-processing of organic matter in gutters and junction boxes of storm drain networks within urban areas may result in contributions of organic matter in forms that are bioavailable, which may cause water quality issues due to the subsequent increase of biological oxygen demand (BOD) in receiving water bodies (Kaushal and Belt, 2012). It is widely known that organic matter exerts a BOD, which, in high amounts, can lower dissolved oxygen (DO) concentrations and stress the aquatic ecosystem (Boyd, 2000; Keith et al., 2014). With most contributions of organic matter in urban areas being flushed out during brief and potentially infrequent stormwater runoff periods, short episodes of hypoxia in receiving streams and downstream water bodies can occur that are difficult to characterize without continuous data (Mallin et al., 2006). These episodes can be detrimental to aquatic ecosystems, and, therefore, understanding the quantity and quality of DOM contributed to urban streams from stormwater runoff is important for understanding the potential effects in receiving waters. This study directly addresses this need.

2.3 Excitation Emission Matrix Spectroscopy

While extensive oceanic and coastal estuary research has been conducted on DOM characteristics with the use of spectroscopic fluorescence analysis (Baker and Spencer, 2004; Stedmon and Markager, 2005; Søndergaard and Thomas, 2004), the advancement of fluorescence spectroscopy and *in situ* fluorescence sensor technology is now enabling new research applications in freshwater rivers and lakes (e.g., Waiser and Robarts, 2000; Spencer et al., 2007; Nguyen et al., 2010) and other environments. The optical properties of DOM can provide insight into the nature and source of the overall composition of DOM in an aquatic system, or DOM pool (Goldman et al., 2012). When many organic molecules are exposed to certain wavelengths of light, the molecules become excited and will fluoresce and emit light with different wavelengths and intensities, but at different spectral regions depending on the molecules. The intensity of the emitted fluorescence at each wavelength can be measured, revealing some information about the chemical composition of a sample. These principles are the basis of excitation emission matrix spectroscopy (EEMS), which measures the fluorescence of a water sample. By using a set range of excitation wavelengths to excite organic molecules in a sample and recording the emitted light at a range of wavelengths for each excitation wavelength, an EEM can be created.

However, not all organic matter molecules contained in a sample are captured in an EEM. Some molecules may be light absorbing but non-fluorescing, and therefore are not detected by the emission detector. Instead, information on non-fluorescent

compounds in the water sample can be provided by the absorbance data collected by the transmission detector of the fluorescence spectrometer (Horiba Jobin Yvon, 2013).

2.4 EEM Peaks and Fluorescence Indices

The measured fluorescence intensity values from an EEMS scan of a sample can be used to quantifiably characterize the nature of the DOM in the sample. A common EEM analysis technique, often referred to as "peak-picking," consists of extracting intensity values of identified fluorescence peaks from regions of the emission spectra that have been linked to ecologically meaningful characteristics of DOM. The intensity of EEM peaks can be used as a surrogate measure of the concentration of the fluorophore to ppm or ppb levels, depending upon the fluorophore. In recent years, "peak-picking" has been used less frequently due to the growing popularity of parallel factor analysis (PARAFAC) to model EEM components. However, recent uses of the method have been applied to water quality studies of treated sewage effluent (Hudson et al., 2008; Hur et al., 2008), and end-member mixing of flow contributions (Goldman et al., 2012). Table 2-1 lists peaks that are commonly used in EEMS analysis of water samples from aquatic environments (Parlanti et al., 2000; Coble, 2007). EEM peaks are extracted from corrected EEMS that account for differences in spectral, absorbance, and intensity properties of samples (Lakowicz, 2006; Lawaetz and Stedmon, 2009).

Comparison of specific excitation and emission wavelength pairs captured in an EEM has also been used to characterize quality, age, and source of the organic material in a sample. These relationships between known pairs are commonly referred to as fluorescence indices. Table 2-2 lists a subset of the fluorescence indices commonly used

in analysis of DOM characteristics in aquatic samples and indicates how each index is interpreted (Gabor et al., 2014). Slight changes in fluorescence index (FI) have been attributed to relative shifts in the DOM precursor material, with reported values usually ranging between 1.2 and 1.8 (McKnight et al., 2001; Cory et al., 2010; Carpenter et al., 2013; Goldman et al., 2014). The FI has also been reported to decrease during storm events (Saraceno et al., 2009, Carpenter et al., 2016). While reported FI values within the literature very among fluorescence measurement methods and spectrofluorometers, the relative trends in FI values, irrespective of the absolute value of the FI, can be interpreted to represent changes in the source of DOM (Cory et al., 2010).

The humification index (HIX) has also been used to describe the source of DOM by using the values as an indication of the degree of microbial processing of terrestrial material. Greater values indicate greater humification of source material (Ohno, 2002; Fellman et al., 2009; Goldman et al., 2014). Commonly reported values of the HIX range between <1 and 30. Soil derived DOM has been shown to have greater HIX values compared to plant litter derived DOM values (Kalbitz et al., 2003). Nguyen et al. (2010) attributed high HIX values during a storm event to soil leaching, the primary factor controlling DOM composition at peak discharges.

The freshness index (BIX; sometimes reported as β:α) is the ratio of protein-like to humic-like DOM components, representing the proportion of biologically produced to terrestrially derived DOM, with higher values indicating more recently microbially produced DOM (Parlanti et al., 2000; Gabor et al., 2014). Values for BIX have been reported between 0.41 and 0.69 in boreal lakes (Kothawala et al., 2012), between 0.55

and 0.68 in a montane headwater tributary and 0.98 in the groundwater of the same watershed (Burns et al., 2016), and between 0.73 and 0.92 in urban stormwater ponds (Williams et al., 2013). Furthermore, Wilson and Xenopoulos (2008) compared the BIX to land uses, showing that decreases in wetland coverage and increases in cropland coverage correlated positively to recently produced DOM. However, the BIX has not been readily applied to characterizing changes in stream DOM composition due to stormwater inputs.

Another useful characterization method for DOM is specific UV absorbance at 254 nm of excitation ($SUVA_{254}$). $SUVA_{254}$ is a commonly used method applied with fluorescence spectroscopy and DOC analysis that can reveal information about the aromaticity of DOM in aquatic samples (Weishaar et al., 2003; Hood et al., 2005; Saraceno et al., 2009; Goldman et al., 2014). Higher $SUVA_{254}$ values indicate the presence of organic molecules with cyclic, aromatic rings that are thought to be stable and less biologically reactive, making the DOM more recalcitrant. Lower values indicate more labile and bioavailable composition of DOM. $SUVA_{254}$ is calculated by dividing the absorbance coefficient (in units of cm^{-1}; λ_{ex} = 254 nm) by the DOC concentration of the same sample in mg C L^{-1} and multiplying by 100, and is reported in units of Liter per milligram of carbon per meter. Values of $SUVA_{254}$ for riverine ecosystems have been reported between 1.8 L mg C^{-1} m^{-1} (more labile; less aromatic) and 4.8 L mg C^{-1} m^{-1} (more recalcitrant; more aromatic) (Creed et al., 2015). As previously mentioned, autochthonous sources of DOM are more labile while allochthonous sources are generally more recalcitrant, thus $SUVA_{254}$ can provide some information about likely

DOM source characteristics. $SUVA_{254}$ has been used in a wide range of surrogate applications for DOM, correlating it with changes in humic-like fluorescence (Fellman et al., 2009) and DOC concentration (Goldman et al., 2012).

2.5 Continuous *in situ* Fluorescence Monitoring

Fluorescence spectroscopy is a common method for assessing DOM composition in water samples (e.g., McKnight et al., 2001; Parlanti et al., 2000; Zsolnay et al., 1999); however, it is not well suited for high frequency measurements because it requires laboratory analysis of physical samples. Because of this, in the past several years *in situ* methods for measuring DOM have started to become more common as sensor technology has emerged. The most common method for measuring DOM *in situ* uses FDOM sensors. Studies conducted with FDOM sensors in freshwater environments have shown diurnal patterns in FDOM (Spencer et al., 2007), quantified the contributions of DOM to an urban stream during season flushing (e.g., spring snowmelt, first storm of the autumn season) (Goldman et al., 2014), and characterized temporal trends and seasonal exports from a forested first order stream (Wilson et al., 2013). FDOM has also been used as a surrogate for DOC concentrations, allowing for continuous estimates of DOC export in streams (Carpenter et al., 2013; Goldman et al., 2014; Saraceno et al., 2009; and others).

The effects of individual storm events on FDOM concentrations have also been evaluated in an agricultural watershed (Saraceno et al., 2009) and a forested stream (Wilson et al., 2013), with observations including the significance of the first flush for causing rapid increases in FDOM concentrations characterized by a steep rising limb and

a slower falling limb of a storm hydrograph. Wilson et al. (2013) also concluded that the largest contribution of DOM being exported in the system they studied occurred during storm events, with contributions due to seasonal snowmelt runoff being the second largest contributor to DOM exports. While there have been efforts aimed at characterizing DOM during storm events in urban settings (e.g., McElmurry et al., 2014), only a few studies have been conducted using *in situ* sensors within urban water systems (e.g., Goldman et al., 2014). Therefore, this study focused on determining the spatial and temporal dynamics of FDOM using high frequency data in an urban water conveyance that receives stormflows from outfalls along the channel.

FDOM sensors only capture a narrow portion of the EEM spectrum. Because of this, compositional changes in DOM (i.e., the presence or absence of specific classes of organic chemicals) cannot be detected using a single FDOM sensor. Carpenter et al. (2013) implemented custom fluorometers manufactured at selected wavelengths to represent discrete regions of the EEM spectra to determine changes in the source and composition of DOM with some success. However, the availability of custom fluorometers capable of deployment in stream or riverine environments is relatively new, and few applications of custom fluorometers in these types of environments exist. Therefore, there is a need to further evaluate the effectiveness of using custom manufactured fluorometers to indirectly quantify DOM composition and provide new relational environmental proxies to laboratory measurements (i.e., EEMS). Part of this study was aimed at continuing the evaluation of custom fluorometers to detect changes in DOM source composition.

One of the biggest challenges in applying fluorometers in stream and riverine systems is that other water quality characteristics and constituents (e.g., temperature and turbidity) can disrupt the true value of FDOM and, therefore, require corrections to be applied in post-processing of the data. Saraceno et al. (2009) was the first to recognize that high levels of turbidity reduced the measured FDOM of an unfiltered sample relative to a filtered sample, causing discrepancy between lab and *in situ* measured FDOM values. This reduction is due to absorption and scattering effects caused by light attenuated by suspended particles. Since then, recent work has indicated that *in situ* FDOM measurements are also sensitive to temperature changes, with the raw FDOM signal being amplified by low temperatures and requiring that FDOM data also be corrected for temperature in post processing of the data (Watras et al., 2011; Downing et al., 2012; Lee et al., 2015; Saraceno et al., 2017). Inner filtering by high concentrations of colored dissolved substances has also been shown to attenuate the FDOM signal, but, due to a general lack of *in situ* data required to correct for this phenomenon (e.g., absorbance of ultraviolet light at 254 nm), corrections for the potential interferences from high levels of dissolved constituents have not been readily applied (Downing et al., 2012). The optical properties of FDOM have also been shown to be affected by pH, but only due to large variations and, therefore, are not a concern in aquatic environments that have relatively consistent pH levels (Patel-Sorrentino et al., 2002). Corrections to raw FDOM measurements have implications for studies estimating organic matter transport, since FDOM is commonly used as proxy for DOC. Without correcting FDOM measurements in post processing of the data, analyses using the data may be incorrect.

2.6 Remote Sensing of Water Quality

Discrete grab sampling coupled with stationary, *in situ* sensors have been used to characterize the chemical composition of the DOM pool in aquatic systems (Goldman et al., 2012; Hood et al., 2005; Nguyen et al., 2010). Strategic deployment of multiple, continuous, remote monitoring sites within an aquatic ecosystem can improve our ability to measure how DOM changes spatially (Glasgow et al., 2004). However, since the DOM pool can change rapidly in both space and time, there is a need for methods that can obtain higher resolution data that can be used to investigate how the composition changes over space and time. While the use of *in situ* fluorometers at many locations is one option for monitoring spatiotemporal changes in DOM, fluorometers are expensive, and this technique would become very costly as the number of data collection sites grows. Additionally, data collected at fixed monitoring sites may still be unable to characterize spatial changes due to choice and availability of monitoring locations. Therefore, new methods are needed for obtaining high-resolution spatial and temporal DOM data while minimizing the cost of implementation.

The application of mobile sensing platforms, sometimes referred to as autonomous surface vessels (ASVs), unmanned surface vehicles (USVs), or remotely operated vehicles (ROVs), for detecting spatial changes in water have been widely tested. These platforms can provide a Lagrangian context, with the potential to effectively follow a parcel of water through an aquatic system and measure changes in water quality in both space and time. Mobile platforms used to conduct experiments can be equipped with environmental and meteorological sensors to capture necessary data. In freshwater systems, several research groups have applied ASVs and ROVs with a common

motivation of mapping harmful algal blooms in water bodies (Dunbabin and Grinham, 2010; Low et al., 2009; Podnar et al., 2010). Others have designed ASV's with the capability to take measurements at a range of depths for limnological lake studies (Hitz et al., 2012). They have also been used to map spatial changes of several water quality parameters in an urban river (Casper et al., 2012). However, mobile platforms have not been widely applied to studies of DOM, and, thus, outfitting a vessel with a payload of onboard fluorometers poses an innovative approach for resolving spatiotemporal patterns in the DOM pool. Furthermore, mobile platforms have not been used in urban streams during episodic stormflow periods, during which water quality changes rapidly in space and time with stormwater contributions. Therefore, we designed and implemented a mobile sensing platform and deployed it during baseflow and stormflow conditions to collect high-resolution data that fills the gaps between fixed sampling sites and allows for the detection of unique spatial changes in FDOM and other water quality parameters.

References

Aitkenhead-Peterson, J. A., W. H. Mcdowell, and J. C. Neff (2003), Sources, production and regulation of allochthonous dissolved organic matter inputs to surface waters, in *Aquatic ecosystems: Interactivity of dissolved organic matter*, edited by S. E. G. Findlay and R. L. Sinsabaugh, pp. 26– 70, Aquatic Ecology Series, Academic Press.

Baker, A., and R. G. M. Spencer (2004), Characterization of dissolved organic matter from source to sea using fluorescence and absorbance spectroscopy, *Sci. Total Environm.*, *333*, 217–232, doi: 10.1016/j.scitotenv.2004.04.013.

Bertilsson, S., and J. B. Jones (2003), Supply of dissolved organic matter to aquatic ecosystems: Autochthonous sources, in *Aquatic ecosystems: Interactivity of dissolved organic matter*, edited by S. E. G. Findlay and R. L. Sinsabaugh, pp. 3–25, Aquatic Ecology Series, Academic Press.

Boyd, C. E. (2000), *Water quality: An introduction*. Kluwer Academic Publishers, Boston, MA.

Burns, M. A., H. R. Barnard, R. S. Gabor, D. M. McKnight, and P. D. Brooks (2016), Dissolved organic matter transport reflects hill slope to stream connectivity during snowmelt in a montane catchment, *Water Resour. Res.*, *52*, 1–20, doi: 10.1002/2015WR017878.

Carpenter, K. D., T. E. C. Kraus, J. H. Goldman, J. F. Saraceno, B. D. Downing, B. A. Bergamaschi, G. McGhee, and T. Triplett (2013), Sources and characteristics of organic matter in the Clackamas River, Oregon, related to the gormation of disinfection by-products in treated drinking water. U.S. Geological Survey Scientific Investigations Report 2013-5001, 78.

Casper, A. F., B. Dixon, E. T. Steimle, M. L. Hall, and R. N. Conmy (2012), Scales of heterogeneity of water quality in rivers: Insights from high resolution maps based on integrated geospatial, sensor and ROV technologies, *Appl. Geog.*, *32*(2), 455–464, doi: 10.1016/j.apgeog.2011.01.023.

Coble, P. G. (2007), Marine optical biogeochemistry: The chemistry of ocean color. *Chem. Rev.*, *107*(2), 402–418, doi: 10.1021/cr050350+.

Conley, D. J., H. W. Paerl, R. W. Howarth, D. F. Boesch, S. P. Seitzinger, K. E. Havens, C. Lancelot, and G. E. Likens (2009), Controlling eutrophication: nitrogen and phosphorus, *Science*, *323*, 1014–1015, doi: 10.1126/science.1167755.

Corbett, C. A. (2007), Colored dissolved organic matter (CDOM) workshop summary, *Reports*, 2. http://scholarcommons.usf.edu/basgp_report/2

Cory, R. M., M. P. Miller, D. M. McKnight, J. J. Guerard, and P. L. Miller (2010), Effect of instrument-specific response on the analysis of fulvic acid fluorescence spectra, *Limnol. Oceanogr. Methods*, *8*, 67–78, doi: 10.4319/lom.2010.8.0067.

Creed, I. F., D. M. McKnight, B. A. Pellerin, M. B. Green, B. A. Bergamaschi, G. R. Aiken, D. A. Burns, S. E. G. Findlay, J. B. Shanley, R. G. Striegl, B. T. Aulenbach, D. W. Clow, H. Laudon, B. L. Mcglynn, K. J. Mcguire, R. A. Smith, and S. M. Stackpoole (2015), The river as a chemostat : fresh perspectives on dissolved organic matter flowing down the river continuum, *Can. J. Fish. Aquat. Sci.*, *14*, 1–14, doi: 10.1139/cjfas-2014-0400.

Downing, B. D., B. A. Pellerin, B. A. Bergamaschi, J. F. Saraceno, and T. E. C. Kraus (2012), Seeing the light: The effects of particles, dissolved materials, and temperature on in situ measurements of DOM fluorescence in rivers and streams, *Limnol. Oceanogr. Methods*, *10*, 767–775, doi: 10.4319/lom.2012.10.767.

Dunbabin, M., and A. Grinham (2010), Experimental evaluation of an autonomous surface vehicle for water quality and greenhouse gas emission monitoring, paper presented at: *IEEE International Conference on Robotics and Automation (ICRA)*, 5268–5274, May 3-8, Anchorage, AK, doi: 10.1109/ROBOT.2010.5509187.

Fellman, J. B., E. Hood, R. T. Edwards, and D. V. D'Amore (2009), Changes in the concentration, biodegradability, and fluorescent properties of dissolved organic matter during stormflows in coastal temperate watersheds, *J. Geophys. Res.*, *114*, G01021, doi:10.1029/2008JG000790.

Fellman, J. B., E. Hood, and R. G. M. Spencer (2010), Fluorescence spectroscopy opens new windows into dissolved organic matter dynamics in freshwater ecosystems: A review, *Limnol. Oceanogr.*, *55*(6), 2452–2462, doi: 10.4319/lo.2010.55.6.2452.

Gabor, R. S., A. Baker, D. M. McKnight, and M. P. Miller (2014), Fluorescence Indices and Their Interpretation, in *Aquatic Organic Matter Fluorescence*, edited by P. G. Coble, J. Lead, A. Baker, D. M. Reynolds, and R. G. M. Spencer, pp. 303-338, Cambridge Environmental Chemistry Series, Cambridge University Press. Cambridge, MA, doi:10.1017/CBO9781139045452.015.

Glasgow, H. B., J. M. Burkholder, R. E. Reed, A. J. Lewitus, and J. E. Kleinman (2004), Real-time remote monitoring of water quality: A review of current applications, and advancements in sensor, telemetry, and computing technologies, *J. Exp. Mar. Biol. Ecol.*, *300*(1–2), 409–448, doi: 10.1016/j.jembe.2004.02.022.

Goldman, J. H., S. A. Rounds, and J. A. Needoba (2012), Applications of fluorescence spectroscopy for predicting percent wastewater in an urban stream, *Environ. Sci. Technol.*, *46*, 4374–4381, doi: 10.1021/es2041114.

Goldman, J. H., S. A. Rounds, M. K. Keith, and S. Sobieszczyk (2014), Investigating organic matter in Fanno Creek, Oregon, Part 3 of 3: Identifying and quantifying sources of organic matter to an urban stream, *J. Hydrol.*, *519*, 3028–3041, doi: 10.1016/j.jhydrol.2014.07.033.

Hatt, B. E., T. D. Fletcher, C. J. Walsh, and S. L. Taylor (2004), The influence of urban density and drainage infrastructure on the concentrations and loads of pollutants in small streams, *J. Environ. Manage.*, *34*(1), 112–124, doi: 10.1007/s00267-004-0221-8.

Hernes, P. J., and R. Benner (2003), Photochemical and microbial degradation of dissolved lignin phenols: Implications for the fate of terrigenous dissolved organic matter in marine environments, *J. Geophys. Res.*, *108*(C9), 3291, doi: 10.1029/2002JC001421.

Hitz, G., F. Pomerleau, M.-E. Garneau, C. Pradalier, T. Posch, J. Pernthaler, and R. Y. Siegwart (2012), Autonomous inland water monitoring: Design and application of a surface vessel, *IEEE Rob. Autom. Mag.*, *19*, 62–72, doi: 10.1109/MRA.2011.2181771.

Hood, E., M. W. Williams, and D. M. Mcknight (2005), Sources of dissolved organic matter (DOM) in a Rocky Mountain stream using chemical fractionation and stable isotopes, *Biogeochemistry*, *74*, 231–255, doi: 10.1007/s10533-004-4322-5

Horiba Jobin Yvon (2013), *Aqualog Operation Manual*. Edison, New Jersey.

Hudson, N., A. Baker, D. Ward, D. M. Reynolds, C. Brunsdon, C. Carliell-Marquet, and S. Browning (2008), Can fluorescence spectrometry be used as a surrogate for the Biochemical Oxygen Demand (BOD) test in water quality assessment? An example from South West England, *Sci. Total Environ.*, 391(1), 149–158, doi: 10.1016/j.scitotenv.2007.10.054.

Hur, J., S.-J. Hwang, and J-K. Shin (2008), Using synchronous fluorescence technique as a water quality monitoring tool for an urban river, *Water Air Soil Pollut.*, *191*(1), 231–243, doi: 10.1007/s11270-008-9620-4.

Kalbitz, K., J. Schmerwitz, D. Schwesig, and E. Matzner (2003), Biodegradation of soil-derived dissolved organic matter as related to its properties, *Geoderma*, *113*(3–4), 273–291, doi: 10.1016/S0016-7061(02)00365-8.

Kaushal, S. S., and K. T. Belt (2012), The urban watershed continuum: Evolving spatial and temporal dimensions, *Urban Ecosyst.*, *15*(2), 409–435, doi: 10.1007/s11252-012-0226-7.

Keith, M. K., S. Sobieszczyk, J. H. Goldman, and S. A. Rounds (2014), Investigating organic matter in Fanno Creek, Oregon, Part 2 of 3: Identifying and quantifying sources of organic matter to an urban stream, *J. Hydrol.*, *519*, 3010–3027, doi: 10.1016/j.jhydrol.2014.07.027.

Kraus, T. E. C., C. A. Anderson, K. Morgenstern, B. D. Downing, B. A. Pellerin, and B. A. Bergamaschi (2010), Determining sources of dissolved organic carbon and disinfection byproduct precursors to the McKenzie River, Oregon, *J. Environ. Qual.*, *39*, 2100–2112, doi: 10.2134/jeq2010.0030.

Lakowicz, J. R. (2006), *Principles of fluorescence spectroscopy*, 3rd Ed., Springer USA, New York, NY, doi: 10.1007/978-0-387-46312-4.

Lawaetz, A. J., and C. A. Stedmon (2009), Fluorescence intensity calibration using the raman scatter peak of water, *Appl. Spectrosc.*, *63*(November), 936–940, doi: 10.1366/000370209788964548.

Lee, E.-J., G.-Y. Yoo, Y. Jeong, K.-U. Kim, J.-H. Park, and N.-H. Oh (2015), Comparison of UV-VIS and FDOM sensors for in situ monitoring of stream DOC concentrations, *Biogeosciences*, *12*(10), 3109–3118, doi: 10.5194/bg-12-3109-2015.

Low, K. H., G. Podnar, S. Stancliff, J. M. Dolan, and A. Elfes (2009), Robot boats as a mobile aquatic sensor network, paper presented at: *Workshop on Sensor Networks for Earth and Space Science Applications (ESSA)*, Apr. 16, San Francisco, CA.

Mallin, M. A., V. L. Johnson, S. H. Ensign, and T. A. MacPherson (2006), Factors contributing to hypoxia in rivers, lakes, and streams, *Limnol. Oceanogr.*, *51*(1, part 2), 690–701, doi: 10.4319/lo.2006.51.1_part_2.0690.

McElmurry, S. P., D. T. Long, and T. C. Voice (2014), Stormwater dissolved organic matter: Influence of land cover and environmental factors, *Environ. Sci. Technol.*, *48*(1), 45–53, doi: 10.1021/es402664t.

McKnight, D. M., E. W. Boyer, P. K. Westerhoff, P. T. Doran, T. Kulbe, and D. T. Andersen (2001), Spectrofluorometric characterization of dissolved organic matter for indication of precursor organic material and aromaticity, *Limnol. Oceanogr.*, *46*(1), 38–48, doi: 10.4319/lo.2001.46.1.0038.

Moran, M. A., W. M. Sheldon, and R. G. Zepp (2000), Carbon loss and optical property changes during long-term photochemical and biological degradation of estuarine dissolved organic matter, *Limnol. Oceanogr.*, *45*(6), 1254–1264, doi: 10.4319/lo.2000.45.6.1254.

Nguyen, H. V.-M., J. Hur, and H.-S. Shin (2010), Changes in spectroscopic and molecular weight characteristics of dissolved organic matter in a river during a storm event, *Water Air Soil Pollut.*, *212*(1–4), 395–406, doi: 10.1007/s11270-010-0353-9.

Ohno, T. (2002), Fluorescence inner-filtering correction for determining the humification index of dissolved organic matter, *Environ. Sci. Technol.*, *36*(4), 742–746, doi: 10.1021/es0155276.

Parlanti, E., K. Worz, L. Geoffroy, and M. Lamotte (2000), Dissolved organic matter fluorescence spectroscopy as a tool to estimate biological activity in a coastal zone submitted to anthropogenic inputs, *Org. Geochem.*, *31*, 1765–1781, doi: 10.1016/S0146-6380(00)00124-8.

Patel-Sorrentino, N., S. Mounier, and J. Y. Benaim (2002), Excitation-emission fluorescence matrix to study pH influence on organic matter fluorescence in the Amazon basin rivers, *Water Res.*, *36*(10), 2571–2581, doi: 10.1016/S0043-1354(01)00469-9.

Paul, M. J., and J. L. Meyer (2001), Streams in the urban landscape, *Annu. Rev. Ecol. Syst.*, *32*(1), 333–365, doi: 10.1146/annurev.ecolsys.32.081501.114040.

Podnar, G., J. M. Dolan, K. H. Low, and A. Elfes (2010), Telesupervised remote surface water quality sensing, paper presented at: *IEEE Aerospace Conference*, 1–9. Mar. 6-13, Big Sky, MT, doi: 10.1109/AERO.2010.5446668.

Saraceno, J. F., B. A. Pellerin, B. D. Downing, E. Boss, P. A. M. Bachand, and B. A. Bergamaschi (2009), High-frequency in situ optical measurements during a storm event: Assessing relationships between dissolved organic matter, sediment concentrations, and hydrologic processes, *J. Geophys. Res.*, *114*, G00F09, doi: 10.1029/2009JG000989.

Saraceno, J. F., J. B. Shanley, B. D. Downing, and B. A. Pellerin (2017), Clearing the waters: Evaluating the need for site-specific field fluorescence corrections based on turbidity measurements, *Limnol. Oceanogr. Methods*, *15*(4), 408-416. dio: 10.1002/lom3.10175.

Sobieszczyk, S., M. K. Keith, S. A. Rounds, and J. H. Goldman (2014), Investigating organic matter in Fanno Creek , Oregon , Part 1 of 3 : Estimating annual foliar biomass for a deciduous-dominant urban riparian corridor, *J. Hydrol.*, *519*, 3001–3009, doi: 10.1016/j.jhydrol.2014.06.054.

Spencer, R. G. M., B. A. Pellerin, B. A. Bergamaschi, B. D. Downing, T. E. C. Kraus, D. R. Smart, R. A. Dahlgren, and P. J. Hernes (2007), Diurnal variability in riverine dissolved organic matter composition determined by in situ optical measurement in the San Joaquin River (California, USA), *Hydrol. Processes*, *21*(23), 3181–3189, doi: 10.1002/hyp.6887.

Stedmon, C. A., and S. Markager (2005), Resolving the variability of dissolved organic matter fluorescence in a temperate estuary and its catchment using PARAFAC analysis, *Limnol. Oceanogr.*, *50*(2), 686–697, doi: 10.4319/lo.2005.50.2.0686.

Søndergaard, M., D.N. Thomas, (2004), *Dissolved organic matter (DOM) in aquatic ecosystems: A study of european catchments and coastal waters*. The DOMAINE project, Bristol, UK.

U.S. Census Bureau, Population Division (2016), Annual Estimates of the Resident Population: April 1, 2010 to July 1, 2015. <https://factfinder.census.gov/faces/tableservices/jsf/pages/productview.xhtml?src=bkmk> (Apr. 26, 2017).

Waiser, M. J., and R. D. Robarts (2000), Changes in composition and reactivity of allochthonous DOM in a prairie saline lake, *Limnol.Oceanogr.*, *45*(4), 763–774, doi: 10.4319/lo.2000.45.4.0763.

Watras, C. J., P. C. Hanson, T. L. Stacy, K. M. Morrison, J. Mather, Y.-H. Hu, and P. Milewski (2011), A temperature compensation method for CDOM fluorescence sensors in freshwater, *Limnol. Oceanogr. Methods*, *9*, 296–301, doi: 10.4319/lom.2011.9.296.

Weishaar, J. L., G. R. Aiken, B. A. Bergamaschi, M. S. Fram, R. Fujii, and K. Mopper (2003), Evaluation of specific ultraviolet absorbance as an indicator of the chemical composition and reactivity of dissolved organic carbon, *Environ. Sci. Technol.*, *37*(20), 4702–4708, doi:10.1021/es030360x.

Williams, C. J., P. C. Frost, and M. A. Xenopoulos (2013), Beyond best management practices: Pelagic biogeochemical dynamics in urban stormwater ponds, *Ecol. Appl.*, *23*(6), 1384–1395, doi: 10.1890/12-0825.1.

Wilson, H. F., and M. A. Xenopoulos (2008), Effects of agricultural land use on the composition of fluvial dissolved organic matter, *Nat. Geosci.*, *2*(1), 37–41, doi: 10.1038/ngeo391.

Wilson, H. F., J. E. Saiers, P. A. Raymond, and W. V. Sobczak (2013), Hydrologic drivers and seasonality of dissolved organic carbon concentration, nitrogen content, bioavailability, and export in a forested new england stream, *Ecosystems*, *16*, 604–616, doi: 10.1007/s10021-013-9635-6.

Wright, A. L., and K. R. Reddy (2009), Dissolved organic matter in wetlands, *University of Florida, Institue of Food and Argrigultural Sciences Extension*, SR 294, 1–3.

Ylla, I., A. M. Romaní, and S. Sabater (2012), Labile and recalcitrant organic matter utilization by river biofilm under increasing water temperature, *Microb. Ecol.*, *64*(3), 593–604, doi: 10.1007/s00248-012-0062-6.

Zsolnay, A., E. Baigar, M. Jimenez, B. Steinweg, and F. Saccomandi (1999), Differentiating with fluorescence spectroscopy the sources of dissolved organic matter in soils subjected to drying, *Chemosphere*, *38*(1), 45–50, doi: 10.1016/S0045-6535(98)00166-0.

Tables

Table 2-1. Commonly used excitation/emission peak regions used in EEMS analyses.

Component	Peak Name	Excitation (nm)	Emission (nm)	Description/Source
Tyrosine-like, protein-like	B	270-280	300-320	Fluorescence peak similar to free tyrosine, amino acids, more degraded peptide material, autochthonous
Tryptophan-like, protein-like	T	270-280	320-350	Fluorescence peak similar to free tryptophan, amino acids, less degraded peptide material, autochthonous
UVC humic-like	A	250-260	380-480	Humic, terrestrial, allochthonous
UVA marine humic-like	M	290-310	370-410	Anthropogenic from wastewater and agriculture
UVA humic-like	C	320-360	420-460	Terrestrial, anthropogenic, agriculture

Table 2-2. Commonly used fluorescence indices.

Index	Calculation	Usage
Fluorescence Index (FI) (McKnight et al., 2001)	Calculated as the ratio of the emission intensities at 470 nm and 520 nm with excitation intensity at 370 nm.	Indicative of microbial (FI ~ 1.8) or terrestrially derived (FI ~1.2) DOM. Shifts in the FI indicate changes in DOM production sources.
Humification Index (HIX) (Zsolnay et al., 1999)	Calculated as the ratio of the area under emission 435-480 nm divided by the area under emission 300-345 nm at excitation 254 nm.	Characterizes the degree of humification, with higher values being more soil derived DOM and lower being more plant litter derived DOM.
Freshness Index (BIX) (Parlanti et al., 2000)	Calculated as the ratio between the beta peak and alpha peak; the intensity at emission 380 nm divided by the max intensity between emission 420 nm and emission 435 nm at excitation 310 nm.	Indicates the age of the DOM, with higher values indicating more recently created OM (characterized by the magnitude of the beta peak) and lower values indicating older, more decomposed OM (characterized by the magnitude of the alpha peak).

CHAPTER 3

INVESTIGATING STORMWATER IMPACTS ON DISSOLVED ORGANIC MATTER IN AN URBAN WATER SYSTEM

Abstract

Dissolved organic matter (DOM) plays an important role in the aquatic environment and can have significant effects on aquatic organisms. Characterizing the composition of DOM within urban receiving waters and the contributions of DOM from urban stormwater runoff is important for understanding potential downstream water quality effects. We conducted this study to characterize the DOM in an urban water conveyance that receives stormwater inputs during runoff events. Baseflow samples were collected at upstream and downstream ends of a study reach, and stormflow samples were collected from outfalls discharging to the study reach. DOM was characterized by measuring dissolved organic carbon (DOC) concentration and using excitation emission matrix spectroscopy (EEMS). During storm events, DOC concentrations were more than 3 times greater at the downstream site than those at the upstream site due to high contributions of DOC being discharged from outfalls. EEMS results and fluorescence indices indicated that DOM composition shifted during storm events from a more autochthonous, less degraded DOM in baseflow to more decomposed and terrestrially derived DOM in stormwater flows and that these changes were driven by outfall specific runoff contributions and DOM compositions. While the magnitude of fluorescence response was much greater in stormwater samples than baseflow and there were compositional changes between existing fluorescence peaks, we did not observe any new

peaks in stormwater samples that were not already present in the baseflow samples within the range of excitation and emission we tested.

3.1 Introduction

Dissolved organic matter (DOM) in the aquatic environment originates from living and decaying organisms and anthropogenic sources (Goldman et al., 2012). DOM plays a significant role in the availability of dissolved nutrients, sequestration of metals from the environment, and optical properties in aquatic ecosystems (Spencer et al., 2007), all of which affect aquatic organisms. For example, DOM can change water clarity, introduce stresses from oxygen demand (Keith et al., 2014), and ultimately impair aquatic ecosystems. The source and chemical composition of DOM are influenced by numerous factors, including land use, hydrology, and water residence time (Wright and Reddy, 2012). Other factors also effect changes in DOM, such as microbial degradation and photodegradation.

Within urban water systems, significant fluxes of anthropogenic DOM can be contributed to receiving waters with stormwater runoff (McElmurry et al., 2014). Urban stormwater discharges have been shown to increase pollutant concentrations and alter aquatic chemistry, leading to degradation in the quality of receiving waters (Kaushal and Belt, 2012; Kim et al., 2003; Paul and Meyer, 2001). However, relatively few studies have examined the amount and quality of DOM contributions from urban stormwater runoff versus DOM in natural streams and river systems, which have been studied more extensively (Buffam et al., 2001; Wilson et al., 2013; Creed et al., 2015). Characterizing the DOM pool within urban receiving waters and the contributions of DOM from urban

stormwater runoff is important for understanding the potential downstream water quality effects of urban stormwater runoff.

The purpose of this study was to improve understanding of DOM contributions from stormwater inputs within urban water systems. More specifically, we studied the characteristics of DOM in the Northwest Field Canal (NWFC), an urban water conveyance of combined stream, irrigation, storm, and agricultural return flow in Logan, Utah, USA. Understanding the characteristics of the DOM pool and how it changes during storm events may lead to more informed management decisions and more accurate assessment of compliance with water quality standards set by state and federal regulatory agencies.

The NWFC discharges into Cutler Reservoir, which is listed as having impaired water quality in the State of Utah's list of impaired waters compiled by the Utah Department of Environmental Quality (DEQ), Division of Water Quality (DWQ), in compliance with Section 303(d) of the Clean Water Act (Utah DWQ, 2004; Utah Office of Administrative Rules, 2017). A total maximum daily load (TMDL) study was recently completed that targeted excess total phosphorus loading to the reservoir as a primary cause of the water quality impairment (Utah DWQ, 2010). However, Cutler Reservoir was listed for low dissolved oxygen (DO) concentrations within the reservoir, and potential effects on aquatic organisms were identified as the driver for the TMDL. While excess phosphorus is a primary water quality concern, DOM contributions during storm runoff events may also be of concern for both the quality of the water in the canal with respect to what is desirable for canal water users and with respect to potential

downstream effects in Cutler Reservoir. This is a pattern that is repeated in many western cities where population centers grew within areas historically used for agriculture and where agricultural canals now serve dual purpose as both agricultural and stormwater conveyances (City of Grand Junction, 2016; City of Logan, 2016; City of Sequim, 2016). Indeed, urban stormwater runoff has proven to be a major contributor of sediment, nutrients, and other pollutants to receiving water bodies in many areas of the U.S. (National Research Council, 2009).

In this study, we studied the DOM pool in the NWFC over the course of two summer irrigation seasons (May – October) using sampling for dissolved organic carbon (DOC) concentrations and excitation emission matrix spectroscopy (EEMS). Specifically, we sought to determine the extent to which DOC concentrations in the NWFC were impacted by stormwater inflows and the extent to which excitation emission matrices, which are characteristic of and serve as surrogates for concentrations of certain classes of organic chemicals, were different for DOM in samples collected from river water diverted for agriculture under non-storm conditions versus DOM in samples collected from urban stormwater runoff. We tested common EEMS analyses, including "peak picking" and calculation of common fluorescence indices for samples collected from storm and non-storm conditions to determine whether these simple analyses could provide information about the source of DOM and aid in quantifying the allochthonous and autochthonous inputs to the DOM pool in the canal under stormflow and baseflow conditions.

3.2 Methods

3.2.1 Study Area

Logan, UT, located in the state's northern region, has a population of about 50,371 (U.S. Census Bureau, 2016), making it the largest city in Utah's Cache County. The Logan River enters city boundaries from the east as the river finishes its course through Logan Canyon. The Logan River watershed (United States Geological Survey Hydrologic Unit Code 1601020303) is part of the larger Bear River basin. Stormwater runoff in Logan is primarily directed into four agricultural irrigation canals that run north, then west, and eventually empty into Cutler Reservoir. The study site for this research included the Logan City urban water system, but focused on the NWFC, which is the irrigation canal located farthest west in Logan (Figure 3-1). This canal was selected specifically because it receives runoff from a variety of land uses within its drainage area.

The Logan River enters the city from the east and runs through what is known as the Logan "Island" district. At River Hollow Park, a portion of the Logan River is diverted into a mixed natural/lined channel called the Little Logan River. The Little Logan River then travels through the heart of the city, receiving stormwater from notable city features such as Merlin Olson Park and the Main Street City Center. The Little Logan River then flows west to Logan High School. Just west of Logan High School, the Little Logan River is diverted into the NWFC. The NWFC flows north, first through residential and mixed residential neighborhoods and then through primarily commercial and mixed-use, receiving stormwater from much of Logan's city center and commercial zones. Drainage subcatchments in Logan City are bordered by the four irrigation canals,

with stormwater traveling primarily from east to west. Many Logan City residents have the option of irrigating their lawns and gardens with canal water, thus irrigation water is diverted from the canals and is conveyed through the city's gutters. Water is diverted from the canal east of a neighborhood and either returns directly or is applied for irrigation and later runs off into the canal to the west.

3.2.2 Data Collection

The NWFC was monitored from the 200 South 400 West intersection (upstream) to the 1800 North 200 West intersection (downstream) in Logan, a distance of approximately 2.7 miles. Monitoring sites along the canal consisted of stormwater outfall sites and canal sites. Canal monitoring sites were installed at the upstream and downstream ends of our study reach. Between the upstream and downstream canal sites, stormwater outfall sites were located at stormwater discharge points in the canal. At any time throughout the study period there were two stormwater outfall sites installed, and a total of six different outfall sites were monitored during this study.

We devised a sampling protocol that included both canal and stormwater outfall monitoring sites aimed at characterizing baseline flows in the canal, flow from stormwater outfalls, and combined flows within the canal during storm conditions. Periodic grab sampling was conducted during baseflow (i.e., non-storm) conditions to characterize water diverted from the Logan River for irrigation purposes. Samples were collected on a weekly basis, when possible, throughout the two irrigation seasons. Baseflow sampling was postponed during storm events or when storm runoff was influencing the conditions in the canal.

Stormwater sampling was carried out using automated samplers capable of collecting 24 – one Liter samples at a time at both stormwater outfall and canal sites. Stormwater outfall sites and canal sites were configured to work in pairs, such that the upstream canal site was associated with the more upstream outfall site and the downstream canal site was associated with the further downstream outfall site. Threshold criteria were developed for automated sample collection during storm flows based on weather conditions (Table 3-1). Samples were collected during periods where all threshold conditions were satisfied. If any of the criteria fell below its threshold, sampling was postponed. Once thresholds at a stormwater outfall site had been met, an automated signal was sent to its associated canal site initiating sampling at that site. Sampling intervals at stormwater outfall sites were varied to capture the bulk of the first flush of an event and the falling limb of the storm hydrograph. This resulted in a sampling interval of every 3 minutes for the first 5 samples followed by a sample every 15 minutes for the rest of the storm or until all 24 of the sample bottles had been filled. Outfall sampling intervals reflect the short and intense nature of many storms experienced in Logan and were set after monitoring several storms to determine the extent and duration of first flush effects.

After receiving a stormwater runoff event flag from an outfall site, the canal sites were programmed to initiate adaptive, event-based sampling. Samples were collected at canal sites according to a turbidity threshold sampling procedure. During storm events, samples were triggered as turbidity values rose above or fell below predefined thresholds. Threshold values were determined using methods described by Lewis (1996). A more

detailed description of coordinated sampling procedures in the canal is provided by Melcher and Horsburgh (2017).

3.2.3 Sample Preparation

Samples collected using the automated sampler were placed in coolers and transported to the Utah Water Research Laboratory to be filtered into amber vials. Samples collected by hand were filtered into amber vials in the field using a syringe and placed into a cooler with an ice pack and transported to the laboratory. All samples were filtered using Whatman glass microfiber filters, type GF/F, with pore size of 0.7 μm, syringed through reusable EMD Millipore Swinnex filter holders or vacuumed through Nalgene Reusable filter holders. Each filtered sample was stored in a 40 mL amber vial and refrigerated at 4° C at the laboratory prior to analysis. Filter holders, amber vial caps, and syringes were soaked in 10% HCl solution for at least two hours and rinsed thoroughly with deionized water before use. Amber vials and filters were ashed in a muffle furnace at 450° C or greater for at least 1 hour to remove any residual organic matter before sample collection. Samples to be analyzed for DOC were acidified with phosphoric acid ahead of time to preserve the sample. When possible, DOC samples were analyzed within 28 days of collection, and EEMS samples within 7 days of collection. Samples were allowed to warm to room temperature before DOC and EEMS analysis.

During the first field season, one 40 mL vial was filled per sample, to be used for both EEM and DOC analysis. This was changed in the second field season to two 40 mL vials containing the same sample (one vial per analysis) to reduce sample handling and provide duplicates for quality control.

3.2.4 Sample Analysis

DOC analysis was conducted on samples using a Teledyne Tekmar, Apollo 9000 Combustion TOC Analyzer. Carbon detection standards were made using potassium hydrogen phthalate with dilutions between 0.8 ppm to 25 ppm as C. Samples were diluted to a 1:10 ratio if a sample was diluted for an EEMS scan, which always preceded DOC analysis. Samples of deionized water and 5 - 10 ppm standard were run intermittently (every 5-10 samples) during sample analysis to verify good catalyst combustion for quality control.

EEMs and absorbance scan measurements were collected for samples using an Aqualog spectrofluorometer (Horiba Jobin Yvon, Edison, New Jersey). The sample signal was collected in ratio mode (sample/reference) to account for non-uniform output of the lamp over the excitation range (Cory et al., 2010). Samples were held in a standard 4 mL quartz cuvette cell with a path length of 10 mm. Excitation wavelengths spanned from 248 nm to 830 nm and were stepped at 2 or 6 nm increments and integrated from 0.5 to 4 seconds, depending on the sample. Emission wavelengths were collected between approximately 250 nm and 828 nm at a low charge-coupled device (CCD) gain and 8 pixel (~ 4.12 nm) increment. Some samples were analyzed at the University of Utah using a different model Aqualog while the Aqualog at USU was being repaired. Excitation wavelengths remained the same but emission wavelengths spanned between approximately 245 nm and 825 nm (~ 2.3 nm). These data were integrated to the same emission wavelengths measured by the USU Aqualog before analysis.

Since two different instruments were used in our EEMS analyses, intensity calibration was performed to convert data to Raman units (RU), as discussed below. The

maximum fluorescence intensity of a sample was checked after each scan to ensure that the chosen integration time was appropriate, thus integration times were altered on a per sample basis following the guidance of the Aqualog manual (Horiba Jobin Yvon, 2013). Dilutions were performed on a per sample basis to ensure that the absorbance coefficient was less than, but as close as possible to, 0.3 cm^{-1} at the excitation wavelength of 254 nm.

Corrections were performed on the resulting EEM of each sample to account for differences in spectral, absorbance, and intensity properties of samples. Milli-Q blanks were collected daily before running samples. EEMs were corrected for instrument specific response by the Aqualog as the ratio of the corrected reference signal to the corrected emission detector signal, resulting in a spectral corrected EEM after each measurement. Sample EEMs were corrected for the inner filter effect (Lakowicz, 2006). Milli-Q blank and sample EEMs were Raman-normalized by dividing the EEM by the area under the water-Raman curve at an excitation of wavelength 350 nm, converting the arbitrary units to RU (Lawaetz and Stedmon, 2009). Raman-normalized EEMs were then blank subtracted and corrected for dilution.

Table 3-2 summarizes the sampling and analysis efforts of the two irrigation seasons and provides the total number of samples collected at each site and within each flow condition. The final column in Table 3-2 provides the total number of storm events that were sampled at each location across the two seasons. Table 3-3 shows the characteristics of sampled storm events based on rainfall data collected from the outfall sites.

3.2.5 Data Analysis

We employed several data analysis techniques to determine the extent to which DOC concentrations and DOM composition in the NWFC were impacted by stormwater inflows. All samples were categorized within four flow conditions: 1) samples collected from the canal during baseflow, 2) samples collected from the canal consisting of combined canal and stormflow, 3) samples collected from outfalls during the first flush (i.e., the first 20 minutes after onset of a storm event) of stormflow, and 4) stormflow condition samples collected after the first flush of a stormwater runoff event. Additionally, samples were also categorized by their location along the canal, recorded as the nearest street intersection to the sampling site.

First, we compared DOC concentrations for samples collected in the canal during base flow conditions versus those collected from stormwater outfalls and in the canal during storm events to determine how DOC concentrations vary between baseflow, stormwater runoff, and combined flows in the canal. Distributions of DOC concentrations within each of the four sample categories were compared visually using box and whisker plots.

Initial inspection of EEMs showed that the overall magnitudes of the fluorescence intensities recorded in stormwater sample EEMs were much higher than those of baseflow samples, likely due to much greater overall concentrations of DOM. To illustrate this, we integrated the volume under the entire EEM spectra of each sample using methods similar to those described by Chen et al. (2003). This provided a single volume for each EEM sample (in units of nm^2 x RU), which was then compared between the flow conditions among sampling sites. The integrated volume of each EEM sample

was also compared to the sample DOC concentration to examine to degree to which the magnitudes of the integrated EEMs volumes were related to the concentration of DOM in a sample.

To examine whether there were compositional changes in DOM with stormwater runoff, we conducted an EEM peak analysis that involved examining the fluorescence response for 5 commonly analyzed fluorescence regions listed in Table 2-1. We again integrated the volume for each sample, but this time only under the identified peak regions. The remaining portion of the EEM (not recognized as a peak region) was also integrated but omitted from the comparison. Each peak region volume was multiplied by an area multiplication factor, equal to the fraction of peak region area to the total EEM area (not including areas where Rayleigh and Raman scatter were removed), to account for effects of secondary or tertiary responses in neighboring peak regions (Chen et al., 2003). EEMs were then normalized to a percentage scale by calculating the percent contribution of the total integrated volume for each peak region in each sample. We then calculated the average percentage compositions for all samples within each condition for comparison. This enabled us to examine the relative composition of the EEMs with respect to the five common peaks independent of the effects of DOM concentration differences to determine whether there were compositional changes that occurred across the five peaks for samples within each of the conditions.

An EEM fluorescence subtraction method was applied to determine whether any persistent peaks outside the five identified in Table 2-1 were visibly present in samples from stormflow conditions but not in baseflow samples. We first calculated an average

EEM for each flow condition and sample location combination by averaging all of the EEMs within each flow condition. Averaged EEMs were then normalized between 0 and 1 by min-max scaling, as shown in Equation 1:

$$x = \frac{x - \min(x)}{\max(x) - \min(x)} \quad (1)$$

where x is the averaged EEM, min(x) is the minimum value within the averaged EEM and max(x) is the maximum value within the averaged EEM. Each normalized average EEM was subtracted from the normalized average EEM of the baseflow condition at the upstream end of the canal to produce a "differenced EEM" for each flow condition. The result was a differenced EEM for each location and flow condition, where values greater than zero represent a greater abundance of a fluorophore in the baseflow sample and values less than zero represent a greater abundance of a fluorophore in the stormflow condition sample.

Lastly, fluorescence index values were compared as a means for characterizing the quality, age, and source of DOM with our samples. We calculated values for specific UV absorbance at 254 nm of excitation ($SUVA_{254}$) and the fluorescence indices listed in Table 2-2 for each of the samples within each of the flow conditions to better understand the chemical quality of DOM in the canal and compare how the values of these indices were impacted by stormwater runoff.

3.3 Results and Discussion

3.3.1 Dissolved Organic Carbon Concentrations

Figure 3-2 shows how DOC concentrations varied among sampling sites and flow conditions (also summarized in Table 3-4). Spatially, mean DOC concentrations had little change between the upstream and downstream sites (+0.57 mg C L^{-1}) during baseflow conditions, while during stormflow conditions the mean DOC concentrations rose by 5.50 mg C L^{-1} between the two sites. During stormflow conditions, the upstream site DOC concentrations were elevated by approximately 1.24 mg C L^{-1} while the downstream site increased by approximately 4.04 mg C L^{-1}. Therefore, the upstream to downstream increase in DOC (5.50 mg C L^{-1}) was greater than the increase at 1800 N alone, indicating that elevated DOC concentrations are being driven by stormwater inputs between 200 S and 1800 N.

DOC concentrations were greatest at outfall sites and were highest during the first flushes of storm events, which contributed to elevating the combined stormflow concentrations in the canal. The mean DOC concentration during the first flush at outfall sites was higher and decreased during post-first flush conditions. Stormflow DOC concentrations from outfall sites varied in magnitude, but for each outfall site the mean first flush contributions of DOC were all higher than the mean post-first flush DOC concentrations. We also observed that DOC concentrations in stormflow samples from the outfall sites had a much higher degree of variability than baseflow or combined flow samples in the canal, with first flush samples exhibiting the highest degree of variability. Depressed concentrations of DOC after the first flush of outfall sites are likely due to a

greater portion of the organic matter-rich detritus built up on the landscape or stored in the storm drains being flushed out with the onset of runoff. Contributions from outfall sites were also dependent on site specific characteristics, which may be attributed to land use or drainage area or both. In general, our observations are consistent with findings in the literature, where DOC is elevated due to stormwater runoff (Buffam et al., 2001; Hatt et al., 2004; and others).

3.3.2 Excitation Emission Matrix Spectroscopy

The volumes under the EEMs of stormflow condition samples were orders of magnitude greater than the volumes of the baseflow samples (Figure 3-3). To put the magnitude differences in perspective, the average EEM volumes of combined flow, stormflow, and first flush stormflow were 7.55, 33.71, and 71.78 times greater than the averaged EEM volume for baseflow conditions, respectively. As expected, the volume under the surface of the EEM was positively correlated with DOC concentration (R^2 = 0.81), verifying that the fluorescence intensities of samples increased as DOC concentrations increase (Figure 3-4). Data were log transformed prior to correlation analysis to account for non-uniform variance. Regression of the log transformed data was completed using the "fitnlm" function in MATLAB, after which the correlation coefficient was calculated. We hypothesize that this correlation was not stronger because different fluorophores fluoresce with differing intensities and DOM composition.

The normalized EEM peak values indicate that the DOM composition of the samples varied for each location and flow condition (Figure 3-5). Comparing baseflow

conditions, there appears to be little compositional change occurring over the reach of the canal. However, peak A and peak M had greater magnitude in stormflow samples than in baseflow samples. Peaks B and T had little to no change during stormflow conditions compared to baseflow peak B and peak T levels. Peak C levels decreased more than any other peak during stormflow conditions. Smaller peak C values in stormflow samples versus baseflow samples was an unexpected result given that peak C values indicate DOM that is typically reported as allochthonous, anthropogenic, or agriculturally derived (Coble, 2007). Aside from the observed decline in peak C during stormflow conditions, these results agree with the literature, where it has been suggested that humic-like fluorescence (i.e., peaks A and M) is more driven by hydrological processes, whereas biological processes control the amount of protein-like fluorescence (i.e., peaks B and T) (Fellman et al., 2010).

Figure 3-6 shows the result of the EEM fluorescence subtraction procedure. Areas in green (positive difference) represent areas that were generally higher in the baseflow condition, whereas areas in blue (negative difference) represent areas that were higher in the condition being compared. While Figure 3-4 does not appear to reveal any new information about the compositional differences in DOM of baseflow versus other conditions (e.g., no additional peaks are immediately apparent), it does further illustrate the compositional changes that have been described above.

3.3.3 Fluorescence Indices

Slight changes in fluorescence index (FI) have been attributed to relative shifts in the DOM precursor material, with reported values usually ranging between 1.2 and 1.8

(McKnight et al., 2001; Carpenter et al., 2013; Goldman et al., 2014). Calculated FI values were almost identical during baseflow conditions at 200 S and 1800 N, indicating that there is little change in the composition of DOM between the two sites during baseflow conditions (Figure 3-7; Table 3-5). More variation was seen between 200 S and 1800 N during stormflow conditions, where the mean FI decreased between the two canal sites, indicating a shift to more allochthonous derived DOM. FI varied even more among the outfall sites, with the lowest mean FI of 1.46 occurring at the 1400 N location. The first flush of an event did not have the same influence on the FI at each outfall or combined stormflow site, with some sites having lower FI values during the first flush (200 S, 300 N, 1400 N), other sites having lower FI values post-first flush (1300 N, 1800 N), and the rest having little to no change in FI values (800 N, 1000 N, 1250 N). In some instances, the recorded FI during stormflow exceeded the maximum observed FI during baseflow condition, with the highest FI of 1.78 being observed during the first flush at 1300 N. It is important to note that the outfall site at 1300 N was often partially submerged during stormflow conditions due to its orientation in the canal. Because of this, some stormflow samples from this outfall may have been mixed with canal flow (particularly when velocities in the outfall were low) leading to results that were not representative of unmixed stormflow. This was not an issue with other outfall sites.

Overall, the mean baseflow FI value of 1.62 decreased during stormflows to a mean of 1.51 from all outfall sites and 1.54 at the downstream site. The observed decline in FI during stormflow conditions is consistent with the observed increase in peaks A and M (Figure 3-5), which represent terrestrially derived, allochthonous DOM. Similar

studies have also shown that stormflow inputs decrease the instream FI (Saraceno et al., 2009; Nguyen et al., 2010; Goldman et al., 2014). While these reported FI values within the literature very among locations and fluorescence measurement methods and spectrofluorometers, the relative trends in FI values, irrespective of the absolute value of the FI, can be interpreted to represent changes in the source of DOM (Cory et al., 2010). Therefore, the shifts in FI observed in this study from higher to lower values indicate that more autochthonous and terrestrially derived source material is being contributed to the canal during runoff events.

The humification index (HIX) has also been used to describe the source of DOM by using the values as an indication of the degree of microbial processing of terrestrial material, with greater values indicating greater humification of source material (Zsolnay et al., 1999; Ohno, 2002; Fellman et al., 2009). Changes in the HIX values had a great deal of variation among the flow conditions and sampling locations (Figure 3-8). The average HIX values for baseflow were 5.95 at 200 S and 5.43 at 1800 N. However, the standard deviation of the HIX values were high for both canal sites during baseflow (Table 3-5), with observed maximum values of 31.73 and 21.26 at the upstream and downstream sites, respectively. During stormflows, the HIX decreased at the upstream site but increased slightly at the downstream sampling location compared to the baseflow conditions. The changes observed in the HIX values are similar to the changes observed in DOM composition where humic-like to protein-like contributions changed among sampling locations (Figure 3-5). The more upstream outfall sites (300 N and 800 N) are characterized as primarily residential land use while the downstream sites (1000 N –

1800 N) are far more commercial (Figure 3-1; note that 1000 N is outfall is located in a residential area but drains neighboring paved and commercial areas). The upstream outfall sites, as illustrated in Figure 3-1, had greater protein-like contributions than the downstream sites (Figure 3-5). The denominator in the HIX calculation (Em: 300-345/ Ex: 254) is a shoulder of protein-like peaks B and T while the numerator (Em: 435-480/ Ex: 254) is within the peak A region. Since compositional changes in peak A were minimal among the outfall sites, we attribute the changes in HIX values to protein-like contributions. While protein-like fluorescence has been attributed to animal wastes (Baker, 2002), we would not expect high animal waste contributions in the urban landscape. Therefore, we theorize that the contributions at the upstream outfalls during stormflows have a greater concentration of newer, less degraded plant litter and grass clippings, which has also been associated with more protein-like components (Kalbitz et al., 2003). At the downstream sites, we expect less plant litter contributions and more soil derived and older DOM, which we would expect to contain less protein-like components. It is also possible that the HIX values are best interpreted on a per-storm basis, as did Nguyen et al. (2010), given the great deal of variability in our results.

The freshness index (BIX; sometimes reported as β:α) is the ratio of protein-like to humic-like DOM components, representing the proportion of biologically produced to terrestrially derived DOM, with higher values indicating more recently microbially produced DOM (Parlanti et al., 2000; Gabor et al., 2014). BIX values were highest during baseflow conditions across all sites except for 1300 N, which had the highest BIX values during post first flush stormflow conditions (Figure 3-9; Table 3-5). All other sites saw a

decrease in BIX values during storm events, with 1000 N and 1400 N having the lowest. Each of the outfall sites had lower BIX values during the first flush and increased after first flush in stormflow conditions, indicating that the initial flush consists of older, more terrestrially derived DOM but starts to shift back to more freshly produced, microbially derived DOM after the initial onset of runoff. The changes from the baseflow condition and variation in BIX values are again site specific during stormflow events. Changes in the age of DOM have been related to changes in land use, as indicated by the BIX (Wilson and Xenopoulous, 2008), which supports our hypothesis that differences in BIX among outfalls are likely due to site specific characteristics. The high BIX observed at 1300 N is inconsistent in that it seems to indicate that the DOM is likely more recently biologically produced. This is similar to the result we observed for the FI and supports our thoughts that samples from 1300 N may have been contaminated by canal water during stormflow conditions.

$SUVA_{254}$ can reveal information about the aromaticity of DOM in aquatic samples, with higher $SUVA_{254}$ values indicating the presence of organic molecules with cyclic, aromatic rings that are stable and less reactive, making the DOM more recalcitrant and, thus, closely tied to terrestrial sources of DOM (Hood et al., 2005; Saraceno et al., 2009; Goldman et al., 2014). The maximum $SUVA_{254}$ values calculated in this study were higher than those often reported in the literature, especially for some of the outfall sites. Some studies have excluded high $SUVA_{254}$ results from analyses with the assumption that they contain inorganic substances (Kraus et al., 2010). Due to our large sample set, we believe that the median values are more representative of the $SUVA_{254}$,

since the potential contamination of inorganics (e.g., metals) in samples may have inflated mean $SUVA_{254}$. Therefore, this section compares median values of $SUVA_{254}$ instead of mean values but both are reported in Table 3-6.

Median $SUVA_{254}$ values in the baseflow condition were similar for 200 S and 1800 N, indicating that there is little change in the aromaticity of DOM in baseflow between these sites (Figure 3-10; Table 3-6). However, median $SUVA_{254}$ values during stormflow conditions increased between the two canal sites, indicating a shift to less labile and more aromatic DOM within the canal. The responses in median $SUVA_{254}$ values from the outfall sites varied in magnitude. $SUVA_{254}$ values during stormflow were higher than baseflow values (except at 800 N and 1300 N during the first flush) and in most sites were elevated to higher $SUVA_{254}$ values after the initial onset of runoff. Therefore, the higher downstream $SUVA_{254}$ values are being driven by the composition of the DOM from the outfall sites, especially after the first flush has taken place. This result agrees with the results from the FI values, where overall, stormflow contributions consisted of more allochthonous and terrestrially derived older organic matter.

3.4 Conclusions

Our results show how the characteristics of DOM in the NWFC changed due to stormwater influences. During baseflow conditions, only small changes were observed between the upstream and downstream monitoring sites, likely indicating that there are few sources of DOM along the length of the canal and that the travel time is insufficient for major changes to occur (e.g., via photodegredation). However, during stormflow conditions, DOC concentrations in the canal were elevated due to runoff being

discharged from outfall sites, and these discharges subsequently altered the DOM composition.

The analysis we performed by integrating the volume under each EEM surface and the high degree of correlation we observed between the integrated volumes and DOC concentrations indicate that the largest changes in DOM within the canal were concentration related (i.e., concentrations were much higher in flows from stormwater outfalls and in the combined flows within the canal under stormflow conditions than baseflow). However, our examination of the EEMs on a relative scale using a "peak picking" analysis showed that there were also compositional changes between the flow conditions. DOM from outfall sites had more fluorphores in the peak A and M regions, less in the peak C region, and little to no change in peaks B and T regions when compared to the baseflow DOM. This indicates that the DOM pool during storm events increases in humic-like composition, while protein-like chemical contributions decrease minimally or do not change. The similar changes between the peaks in combined stormflow at 200 S and 1800 N indicate that changes in DOM composition in the canal are driven by the contributions from the stormflow outfall sites during storm events.

Our EEMs subtraction procedure did not appear to reveal any new information about differences in EEMs peaks within the examined excitation and emission wavelength ranges that we did not see using other methods. The magnitude of the fluorescence response was much greater in stormflow samples than base flow samples, but it did not appear that there were fluorescence peaks in stormflows that were not present in baseflow. There are other, more sophisticated methods that can be used to

analyze EEM peaks, including principle components analysis (PCA) and parallel factor analysis (PARAFAC) modeling, that may reveal additional structure in our EEMs samples that we were not able to observe using these simpler methods.

The FI results showed that for the majority of the outfall sites (1300 N being the exception) the DOM is of allochthonous nature during stormflow conditions, while it is derived of more autochthonous DOM during baseflow conditions. The HIX and the BIX supported what we observed with the FI. HIX values suggest that there are differences in the degree of microbial processing of the DOM for the residentially dominant land use outfall sites versus those dominated by commercial land use. We attribute the lower values to a greater amount of plant material in the form of grass clippings and leaf litter from residential areas.

BIX values indicated that the stormwater inputs are of older and more terrestrially derived DOM, which may indicate that organic matter is stored in the storm drains until flushed out with the onset of additional runoff. Thus, the first flush of stormflows had the lowest BIX values but were elevated after the first flush due to the less degraded DOM being washed through the storm drains. BIX provided further information of the DOM composition and support to the conclusions made using the FI and HIX indices. Stormflow values for FI, HIX, and BIX at 1000 N and 1400 N always exhibited the greatest difference from baseflow, while 300 N and 800 N always had smaller differences, indicating that the fluorescence properties of DOM being contributed during storm events are site specific. $SUVA_{254}$ values were elevated in the canal during stormflow, indicating a change in chemical structure of the DOM to more aromatic

compounds, which are less labile in nature. The high variation in $SUVA_{254}$ values may have been caused by metal contamination, and therefore, only median values were analyzed for $SUVA_{254}$.

Our results provide information about the source, quantity, and quality of DOM that is contributed to an urban water conveyance via stormwater runoff. We anticipate that the behavior we observed is likely similar to that of many urban systems in the intermountain western U.S., with land use types, climate, and urban water systems that are similar to the one we monitored. These results provide better understanding of the composition of DOM in the canal system and may provide crucial information for future management of stormwater runoff that can potentially lead to the improvements of water quality in downstream water bodies.

Acknowledgments

This work was supported by funding from the Utah Water Research Laboratory at Utah State University and from United States National Science Foundation grant 1208732. Any opinions, findings, and conclusions or recommendations expressed are those of the authors and do not necessarily reflect the views of the National Science Foundation.

References

Baker, A. (2002), Fluorescence exciation emission characterization of some sewage-impacted rivers, *Water Res.*, *36*(1), 189-195, doi: 10.1016/S0043-1354(01)00210-X.

Buffam, I., J. N. Galloway, L. K. Blum, and K. J. McGlathery (2001), A stormflow/baseflow comparison of dissolved organic matter concentrations and bioavailability in an Appalachian stream, *Biogeochemistry*, *53*(3), 269–306, doi: 10.1023/A:1010643432253.

Carpenter, K. D., T. E. C. Kraus, J. H. Goldman, J. F. Saraceno, B. D. Downing, B. A. Bergamaschi, G. McGhee, and T. Triplett (2013), Sources and characteristics of organic matter in the Clackamas River, Oregon, related to the gormation of disinfection by-products in treated drinking water. U.S. Geological Survey Scientific Investigations Report 2013-5001, 78.

Chen, W., P. Westerhoff, J. A. Leenheer, and K. Booksh (2003), Fluorescence excitation-emission matrix regional integration to quantify spectra for dissolved organic matter, *Environ. Sci Technol.*, *37*, 5701–5710, doi: 10.1021/es034354c.

City of Grand Junction (2016), *Grand Junction Municipal Code Volume II: Development Regulations; Title 28: Stormwater Management Manual; Chapter 28.52: Irrigation/Drainage Structures.* Grand Junction, Colorado. <http://www.codepublishing.com/CO/GrandJunction/html2/GrandJunction28/GrandJunction2852.html#28.52> (Feb. 8, 2017).

City of Logan (2016), *Storm Water Management Plan*. Logan, Utah. <http://www.loganutah.org/SWMP%20Document%20Less%20Appendices_Final.pdf> (Feb. 8, 2017).

City of Sequim (2016), *Storm and Surface Water Master Plan*. Sequim, Washington <http://www.sequimwa.gov/DocumentCenter/View/7735> (Feb. 8, 2017).

Coble, P. G. (2007), Marine optical biogeochemistry: The chemistry of ocean color. *Chem. Rev.*, *107*(2), 402–418, doi: 10.1021/cr050350+.

Cory, R. M., M. P. Miller, D. M. McKnight, J. J. Guerard, and P. L. Miller (2010), Effect of instrument-specific response on the analysis of fulvic acid fluorescence spectra, *Limnol. Oceanogr. Methods*, *8*, 67–78, doi: 10.4319/lom.2010.8.0067.

Creed, I. F., D. M. McKnight, B. A. Pellerin, M. B. Green, B. A. Bergamaschi, G. R. Aiken, D. A. Burns, S. E. G. Findlay, J. B. Shanley, R. G. Striegl, B. T. Aulenbach, D. W. Clow, H. Laudon, B. L. Mcglynn, K. J. Mcguire, R. A. Smith, and S. M. Stackpoole (2015), The river as a chemostat : fresh perspectives on dissolved organic matter flowing down the river continuum, *Can. J. Fish. Aquat. Sci.*, *14*, 1–14, doi: 10.1139/cjfas-2014-0400.

Fellman, J. B., E. Hood, R. T. Edwards, and D. V. D'Amore (2009), Changes in the concentration, biodegradability, and fluorescent properties of dissolved organic matter during stormflows in coastal temperate watersheds, *J. Geophys. Res.*, *114*, G01021, doi:10.1029/2008JG000790.

Fellman, J. B., E. Hood, and R. G. M. Spencer (2010), Fluorescence spectroscopy opens new windows into dissolved organic matter dynamics in freshwater ecosystems: A review, *Limnol. Oceanogr.*, *55*(6), 2452–2462, doi: 10.4319/lo.2010.55.6.2452.

Gabor, R. S., A. Baker, D. M. McKnight, and M. P. Miller (2014), Fluorescence Indices and Their Interpretation, in *Aquatic Organic Matter Fluorescence*, edited by P. G. Coble, J. Lead, A. Baker, D. M. Reynolds, and R. G. M. Spencer, pp. 303-338, Cambridge Environmental Chemistry Series, Cambridge University Press. Cambridge, MA, doi:10.1017/CBO9781139045452.015.

Glasgow, H. B., J. M. Burkholder, R. E. Reed, A. J. Lewitus, and J. E. Kleinman (2004), Real-time remote monitoring of water quality: A review of current applications, and advancements in sensor, telemetry, and computing technologies, *J. Exp. Mar. Biol. Ecol.*, *300*(1–2), 409–448, doi: 10.1016/j.jembe.2004.02.022.

Goldman, J. H., S. A. Rounds, and J. A. Needoba (2012), Applications of fluorescence spectroscopy for predicting percent wastewater in an urban stream, *Environ. Sci. Technol.*, *46*, 4374–4381, doi: 10.1021/es2041114.

Goldman, J. H., S. A. Rounds, M. K. Keith, and S. Sobieszczyk (2014), Investigating organic matter in Fanno Creek, Oregon, Part 3 of 3: Identifying and quantifying sources of organic matter to an urban stream, *J. Hydrol.*, *519*, 3028–3041, doi: 10.1016/j.jhydrol.2014.07.033.

Hatt, B. E., T. D. Fletcher, C. J. Walsh, and S. L. Taylor (2004), The influence of urban density and drainage infrastructure on the concentrations and loads of pollutants in small streams, *J. Environ. Manage.*, *34*(1), 112–124, doi: 10.1007/s00267-004-0221-8.

Hood, E., M. W. Williams, and D. M. Mcknight (2005), Sources of dissolved organic matter (DOM) in a Rocky Mountain stream using chemical fractionation and stable isotopes, *Biogeochemistry*, *74*, 231–255, doi: 10.1007/s10533-004-4322-5

Horiba Jobin Yvon (2013), *Aqualog Operation Manual*. Edison, New Jersey.

Kalbitz, K., J. Schmerwitz, D. Schwesig, and E. Matzner (2003), Biodegradation of soil-derived dissolved organic matter as related to its properties, *Geoderma*, *113*(3–4), 273–291, doi: 10.1016/S0016-7061(02)00365-8.

Kaushal, S. S., and K. T. Belt (2012), The urban watershed continuum: Evolving spatial and temporal dimensions, *Urban Ecosyst.*, *15*(2), 409–435, doi: 10.1007/s11252-012-0226-7.

Keith, M. K., S. Sobieszczyk, J. H. Goldman, and S. A. Rounds (2014), Investigating organic matter in Fanno Creek, Oregon, Part 2 of 3: Identifying and quantifying sources of organic matter to an urban stream, *J. Hydrol.*, *519*, 3010–3027, doi: 10.1016/j.jhydrol.2014.07.027.

Kim, L., E. Choi, and M. K. Stenstrom (2003), Sediment characteristics, phosphorus types and phosphorus release rates between river and lake sediments, *Chemosphere*, *50*, 53–61, doi: 10.1016/S0045-6535(02)00310-7.

Kraus, T. E. C., C. A. Anderson, K. Morgenstern, B. D. Downing, B. A. Pellerin, and B. A. Bergamaschi (2010), Determining sources of dissolved organic carbon and disinfection byproduct precursors to the McKenzie River, Oregon, *J. Environ. Qual.*, *39*, 2100–2112, doi: 10.2134/jeq2010.0030.

Lakowicz, J. R. (2006), *Principles of fluorescence spectroscopy*, 3rd Ed., Springer USA, New York, NY, doi: 10.1007/978-0-387-46312-4.

Lawaetz, A. J., and C. A. Stedmon (2009), Fluorescence intensity calibration using the raman scatter peak of water, *Appl. Spectrosc.*, *63*(November), 936–940, doi: 10.1366/000370209788964548.

Lewis, J. (1996), Turbidity-controlled suspended sediment sampling and load estimation, *Water Resour. Res.*, *32*(7), 2299–2310, doi: 10.1029/96WR00991.

McElmurry, S. P., D. T. Long, and T. C. Voice (2014), Stormwater dissolved organic matter: Influence of land cover and environmental factors, *Environ. Sci. Technol.*, *48*(1), 45–53, doi: 10.1021/es402664t.

McKnight, D. M., E. W. Boyer, P. K. Westerhoff, P. T. Doran, T. Kulbe, and D. T. Andersen (2001), Spectrofluorometric characterization of dissolved organic matter for indication of precursor organic material and aromaticity, *Limnol. Oceanogr.*, *46*(1), 38–48, doi: 10.4319/lo.2001.46.1.0038.

Melcher, A. A., and J. S. Horsburgh (2017), An urban observatory for quantifying phosphorus and suspended solids loads in combined natural and stormwater conveyances, *Environ. Monit. Assess.*, *2017*, 189-285, doi: 10.1007/s10661-017-5974-7.

National Research Council (2009), *Urban Stormwater Management in the United States Committee on Reducing Stormwater Discharge Contributions to Water Pollution*. The National Academies Press, Washington, DC, doi: 10.17226/12465.

Nguyen, H. V.-M., J. Hur, and H.-S. Shin (2010), Changes in spectroscopic and molecular weight characteristics of dissolved organic matter in a river during a storm event, *Water Air Soil Pollut.*, *212*(1–4), 395–406, doi: 10.1007/s11270-010-0353-9.

Ohno, T. (2002), Fluorescence inner-filtering correction for determining the humification index of dissolved organic matter, *Environ. Sci. Technol.*, *36*(4), 742–746, doi: 10.1021/es0155276.

Parlanti, E., K. Worz, L. Geoffroy, and M. Lamotte (2000), Dissolved organic matter fluorescence spectroscopy as a tool to estimate biological activity in a coastal zone submitted to anthropogenic inputs, *Org. Geochem.*, *31*, 1765–1781, doi: 10.1016/S0146-6380(00)00124-8.

Paul, M. J., and J. L. Meyer (2001), Streams in the urban landscape, *Annu. Rev. Ecol. Syst.*, *32*(1), 333–365, doi: 10.1146/annurev.ecolsys.32.081501.114040.

Saraceno, J. F., B. A. Pellerin, B. D. Downing, E. Boss, P. A. M. Bachand, and B. A. Bergamaschi (2009), High-frequency in situ optical measurements during a storm event: Assessing relationships between dissolved organic matter, sediment concentrations, and hydrologic processes, *J. Geophys. Res.*, *114*, G00F09, doi: 10.1029/2009JG000989.

Spencer, R. G. M., B. A. Pellerin, B. A. Bergamaschi, B. D. Downing, T. E. C. Kraus, D. R. Smart, R. A. Dahlgren, and P. J. Hernes (2007), Diurnal variability in riverine dissolved organic matter composition determined by in situ optical measurement in the San Joaquin River (California, USA), *Hydrol. Processes*, *21*(23), 3181–3189, doi: 10.1002/hyp.6887.

U.S. Census Bureau, Population Division (2016), Annual Estimates of the Resident Population: April 1, 2010 to July 1, 2015. <https://factfinder.census.gov/faces/tableservices/jsf/pages/productview.xhtml?src=bkmk> (Apr. 26, 2017).

Utah Depatment of Environmental Quality, Division of Water Quality (2004), *Utah's 2004 303(d) List of Impaired Waters*, Salt Lake City, UT.

Utah Depatment of Environmental Quality, Division of Water Quality (2010), *Middle Bear River and Cutler Reservoir Total Maximum Daily Load (TMDL)*, Salt Lake City, UT.

Utah Office of Administrative Rules (2017), *R317-2. Standards of Quality for Waters of the State*. Salt Lake City, UT.

Wilson, H. F., J. E. Saiers, P. A. Raymond, and W. V. Sobczak (2013), Hydrologic drivers and seasonality of dissolved organic carbon concentration, nitrogen content, bioavailability, and export in a forested new england stream, *Ecosystems*, *16*, 604–616, doi: 10.1007/s10021-013-9635-6.

Wright, A. L., and K. R. Reddy (2009), Dissolved organic matter in wetlands, *University of Florida, Institue of Food and Argrigultural Sciences Extension*, SR 294, 1–3.

Zsolnay, A., E. Baigar, M. Jimenez, B. Steinweg, and F. Saccomandi (1999), Differentiating with fluorescence spectroscopy the sources of dissolved organic matter in soils subjected to drying, *Chemosphere*, *38*(1), 45–50, doi: 10.1016/S0045-6535(98)00166-0.

Tables

Table 3-1. Threshold criteria used to trigger automated sampling.

Site Type	Sampling Threshold Criteria
Stormwater Outfall Site	1. Stormwater depth of flow in the conduit is greater than the specified threshold (site specific)
	2. Stormwater velocity in the stormwater conduit is greater than the specified threshold (site specific)
	3. Rain has been recorded within the prior four hours (site specific)
Canal Site	Automated sampling has been initiated at the nearest outfall site

Table 3-2. Sampling conducted during the 2015 and 2016 irrigation seasons.

Sampling Location	Baseflow Samples[a]		First Flush Samples[b]		Stormflow Samples		Total Number of Samples		Number of Different Storms
	EEM	DOC	EEM	DOC	EEM	DOC	EEM	DOC	
200 S 400 N	23	20	-	-	57	53	80	73	20
300 N 300 W	-	-	14	12	17	9	31	21	11
800 N 150 W	-	-	25	25	41	41	66	66	14
1000 N 200 W	-	-	10	10	22	22	32	32	8
1250 N 200 W	-	-	13	11	32	27	45	38	16
1300 N 200 W	-	-	15	15	41	40	56	55	17
1400 N 200 W	-	-	10	10	24	24	34	34	8
1800 N 200 W	23	21	-	-	63	59	86	80	21

[a] Baseflow samples were not collected at outfall sites

[b] First flush condition only applies to outfall sites

Table 3-3. Storm event characteristics of sampled storms at the continuously monitored outfall sites.

Sampled Storm Dates[a]	Antecedent Dry Period[b] (days)	Runoff Duration[c] (hours)	Rainfall Depth (mm)	Average Rainfall Intensity (mm/hr)	Peak Rainfall Intensity (mm/hr)
19-May-2015[1, d]	0.39	5.73	-	-	-
23-May-2015[2]	1.36	8.97	11.94	1.20	6.10
03-Jun-2015[1,2]	6.24	1.53	5.21	3.03	38.10
10-Jun-2015[1,2]	4.08	32.64	24.13	2.69	47.24
05-Jul-2015[1,2]	2.74	7.48	3.18	0.90	7.62
08-Jul-2015[1,2]	1.96	6.98	3.18	0.83	7.62
27-Jul-2015[1,2]	13.17	0.49	2.29	2.05	9.14
14-Sep-2015[1,2]	3.74	10.73	5.84	1.27	22.86
15-Sep-2015[1]	0.27	10.55	6.86	0.64	12.19
16-Sep-2015[1,2]	0.38	14.53	30.73	2.23	22.86
03-Oct-2015[1,2]	9.36	10.53	2.54	1.94	9.14
22-Mar-2016[3]	4.76	9.80	9.91	0.94	9.14
10-Apr-2016[3]	9.60	2.32	5.59	2.10	12.19
13-Apr-2016[3]	2.83	17.67	11.68	0.63	15.24
14-Apr-2016[3]	0.46	11.55	25.15	2.11	12.19
23-Apr-2016 AM[3]	7.76	0.72	0.76	0.48	3.05
23-Apr-2016 AM[3]	0.24	0.97	1.02	0.76	9.14
23-Apr-2016 PM[3]	0.34	8.07	6.35	0.74	3.05
25-Apr-2016[3]	1.33	1.85	2.79	1.29	9.14
06-May-2016[3]	0.35	3.77	6.35	1.44	9.14
10-May-2016[3]	1.54	4.37	5.08	1.13	9.14
15-May-2016[3]	0.63	8.72	4.83	0.53	12.19
19-May-2016[3]	3.34	14.63	17.27	1.11	12.19
25-May-2016[3]	2.58	1.37	1.78	0.93	3.05
11-Jun-2016[4,5]	0.35	75.32	24.26	0.38	94.49
07-Aug-2016[4,5]	16.79	4.10	1.27	0.30	9.14
13-Sep-2016 AM[4,5]	22.45	7.22	4.45	0.59	6.10
13-Sep-2016 PM[4,5]	0.47	12.03	8.89	0.73	27.43
14-Sep-2016[4,5]	0.41	11.12	4.95	0.42	15.24
21-Sep-2016[4,5]	6.70	11.11	33.40	2.96	59.44
22-Sep-2016[4,5]	0.34	24.28	33.27	1.36	30.48

[a] Superscripts indicate sampling locations during storm; where 1 = 300 N 300 W, 2 = 1250 N 200 W, 3 = 800 N 150 W, 4 = 1000 N 200 W, and 5 = 1400 N 200 W.

[b] The antecedent dry period is the elapsed time between when water was last flowing in the outfall.

[c] Runoff duration is the amount of time the outfall was flowing during the storm.

[d] The storm on 19-May-2015 occurred before installation of the rainfall tipping bucket.

Table 3-4. Mean and standard deviation of measured DOC concentrations[a] for each sampling location and flow condition.

Sample Location	Baseflow DOC[b]	Combined Flow and Stormflow DOC	Stormflow – First Flush[c] DOC
200 S 400 N	1.02 (0.48)[d]	2.39 (2.19)	-
300 N 300 W	-	23.69 (18.97)	55.33 (54.24)
800 N 150 W	-	19.14 (19.31)	32.95 (20.53)
1000 N 200 W	-	25.74 (33.32)	46.45 (39.34)
1250 N 200 W	-	11.48 (13.85)	31.13 (25.15)
1300 N 200 W	-	11.76 (6.78)	16.97 (13.71)
1400 N 200 W	-	26.38 (26.27)	98.43 (85.39)
1800 N 200 W	1.59 (2.01)	7.89 (6.84)	-

[a] DOC concentrations are in units of mg C L^{-1}
[b] Baseflow samples were not collected at outfall sites
[c] First flush condition only applies to outfall sites
[d] Standard deviation reported in parentheses

Table 3-5. Mean and standard deviation of calculated fluorescence indices[a].

Sample Location	Baseflow[b]			Combined Flow and Stormflow			Stormflow – First Flush[c]		
	FI	**HIX**	**BIX**	**FI**	**HIX**	**BIX**	**FI**	**HIX**	**BIX**
200 S 400 N	1.62 (0.04)[d]	5.95 (6.33)	0.76 (0.07)	1.60 (0.06)	5.09 (2.25)	0.71 (0.06)	-	-	-
300 N 300 W	-	-	-	1.56 (0.06)	4.28 (0.83)	0.71 (0.06)	1.54 (0.02)	5.03 (1.05)	0.65 (0.07)
800 N 150 W	-	-	-	1.50 (0.03)	3.93 (0.58)	0.74 (0.06)	1.51 (0.06)	4.45 (0.76)	0.67 (0.09)
1000 N 200 W	-	-	-	1.48 (0.05)	6.14 (1.52)	0.65 (0.09)	1.47 (0.05)	6.67 (1.61)	0.61 (0.11)
1250 N 200 W	-	-	-	1.52 (0.08)	5.86 (2.73)	0.71 (0.11)	1.51 (0.07)	6.29 (1.19)	0.63 (0.06)
1300 N 200 W	-	-	-	1.51 (0.05)	4.40 (1.41)	0.78 (0.11)	1.60 (0.08)	4.97 (1.38)	0.76 (0.13)
1400 N 200 W	-	-	-	1.47 (0.06)	6.31 (1.72)	0.67 (0.13)	1.46 (0.02)	8.23 (1.85)	0.55 (0.08)
1800 N 200 W	1.62 (0.03)	5.43 (3.89)	0.77 (0.05)	1.53 (0.04)	6.14 (2.24)	0.68 (0.10)	-	-	-

[a] All index values are unitless

[b] Baseflow samples were not collected at outfall sites

[c] First flush condition only applies to outfall sites

[d] Standard deviation reported in parentheses

Table 3-6. Calculated $SUVA_{254}$[a] values for each sampling location and flow condition.

Sample Location	Baseflow[b]		Combined Flow and Stormflow		Stormflow - First Flush[c]	
	Median	**Mean**	**Median**	**Mean**	**Median**	**Mean**
200 S 400 N	2.06	2.53 (1.45)[d]	2.06	2.45 (1.58)	-	-
300 N 300 W	-	-	3.44	4.91 (4.61)	3.81	11.69 (23.10)
800 N 150 W	-	-	2.13	2.14 (0.45)	1.86	2.44 (3.27)
1000 N 200 W	-	-	2.81	2.82 (0.60)	2.99	2.90 (0.61)
1250 N 200 W	-	-	3.52	6.51 (8.55)	2.97	5.02 (7.69)
1300 N 200 W	-	-	2.64	2.69 (0.70)	1.51	1.52 (0.62)
1400 N 200 W	-	-	3.02	3.07 (0.62)	2.60	2.71 (0.83)
1800 N 200 W	2.10	2.48 (1.53)	2.66	3.18 (2.57)	-	-

[a] $SUVA_{254}$ values are in units of L mg C^{-1} m^{-1}
[b] Baseflow samples were not collected at outfall sites
[c] First flush condition only applies to outfall sites
[d] Standard deviation reported in parentheses

Figures

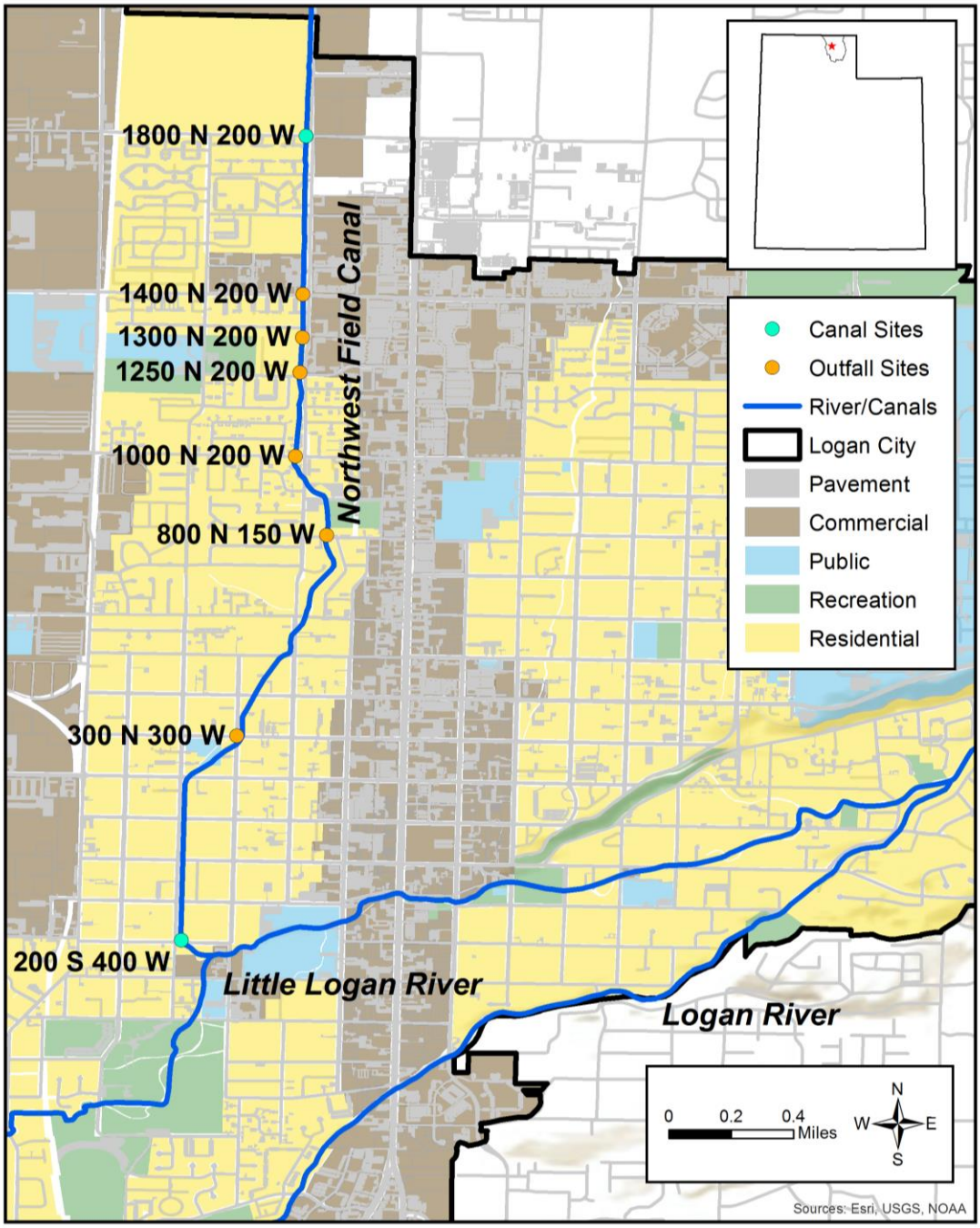

Figure 3-1. Site map of the Northwest Field Canal showing locations of sampling sites and land use categories.

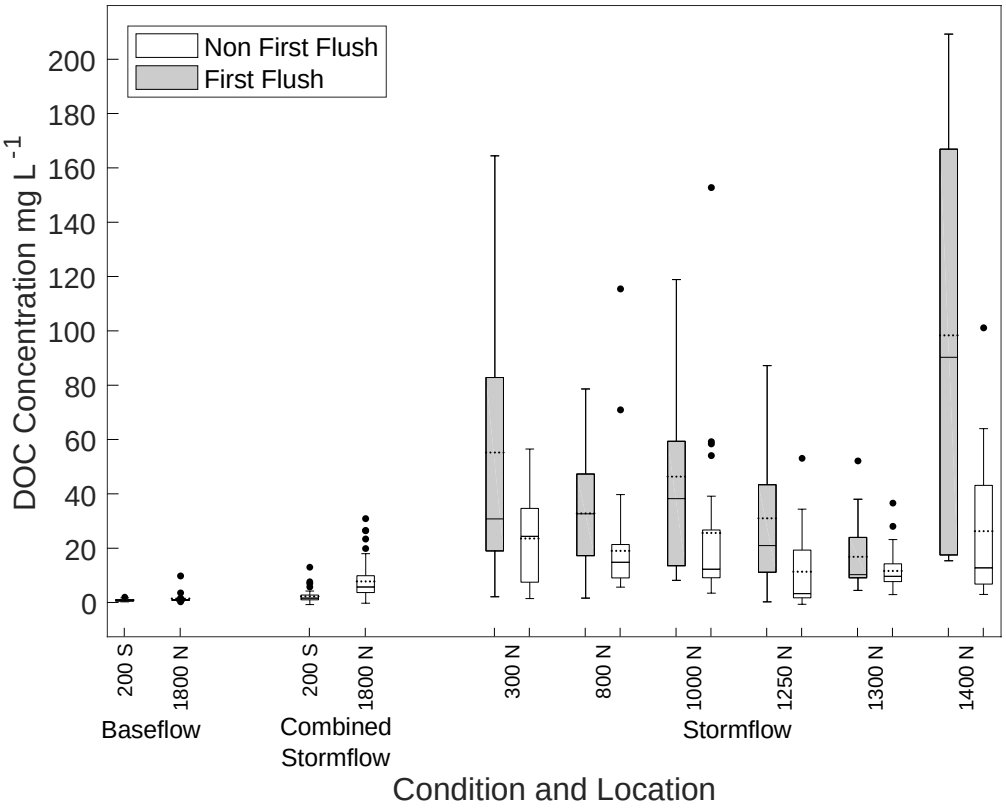

Figure 3-2. Box and whisker plot of DOC concentrations in the Northwest Field Canal under baseflow and stormflow conditions. Solid horizontal lines represent the median value while dotted horizontal lines represent the mean value.

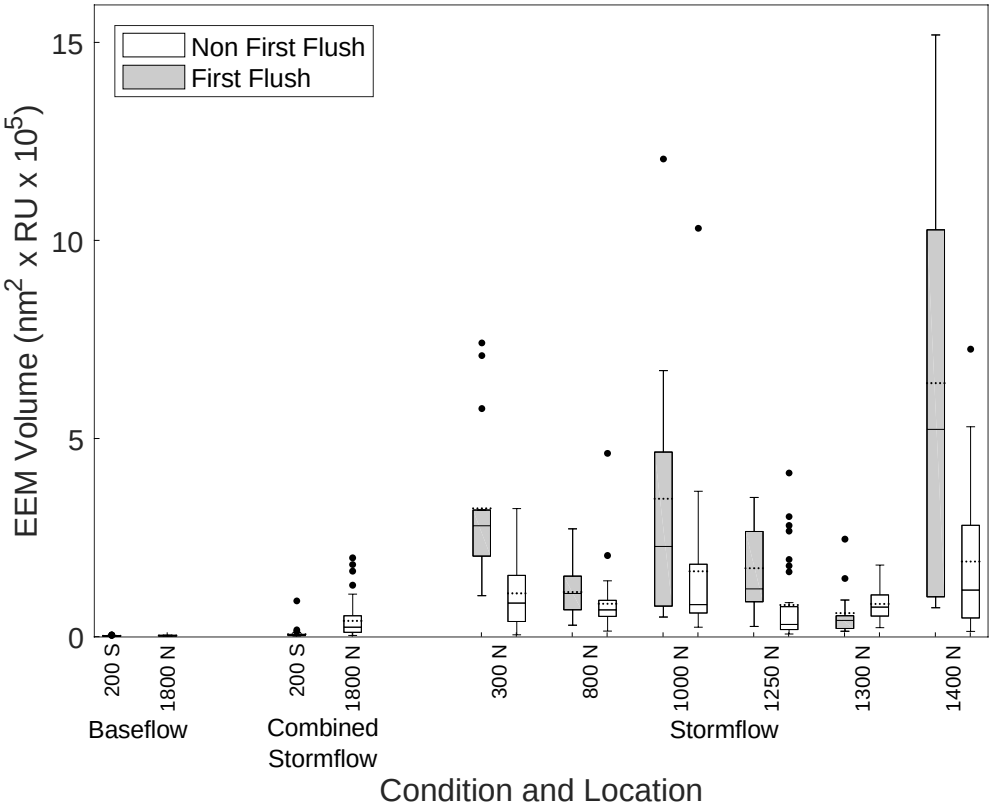

Figure 3-3. Box and whisker plot comparing the calculated volumes under the EEM for sampling locations and flow conditions. Solid horizontal lines represent the median value while dotted horizontal lines represent the mean value.

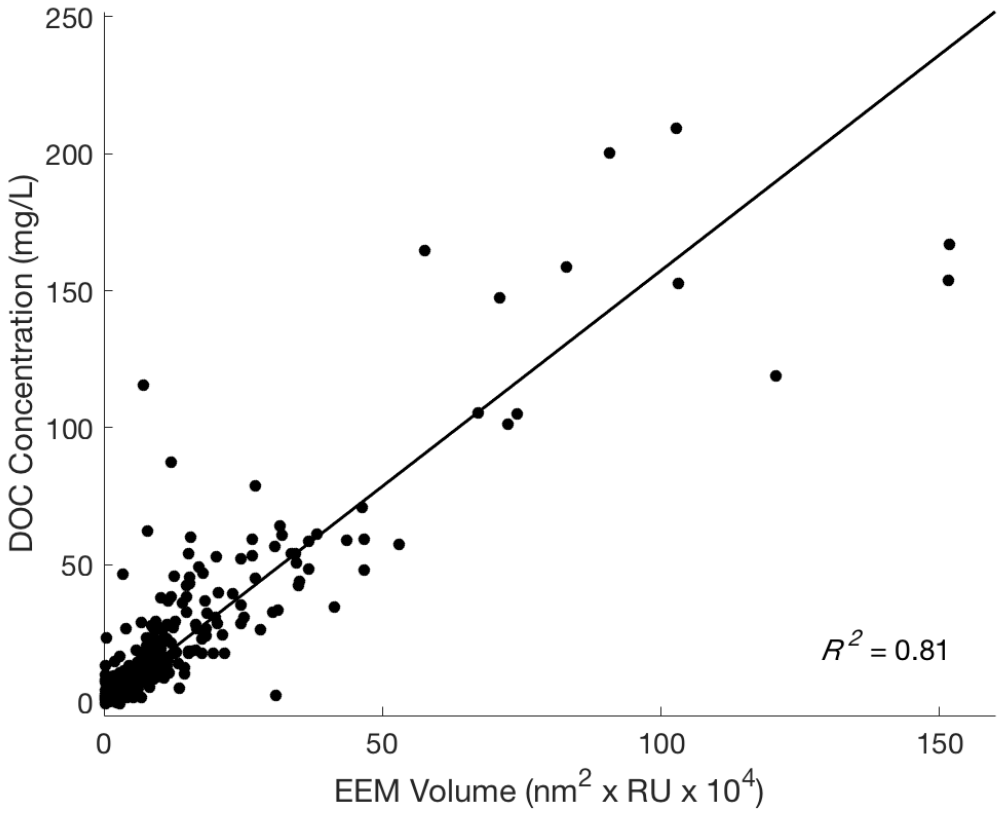

Figure 3-4. Correlation between EEM fluorescence volume and DOC concentrations.

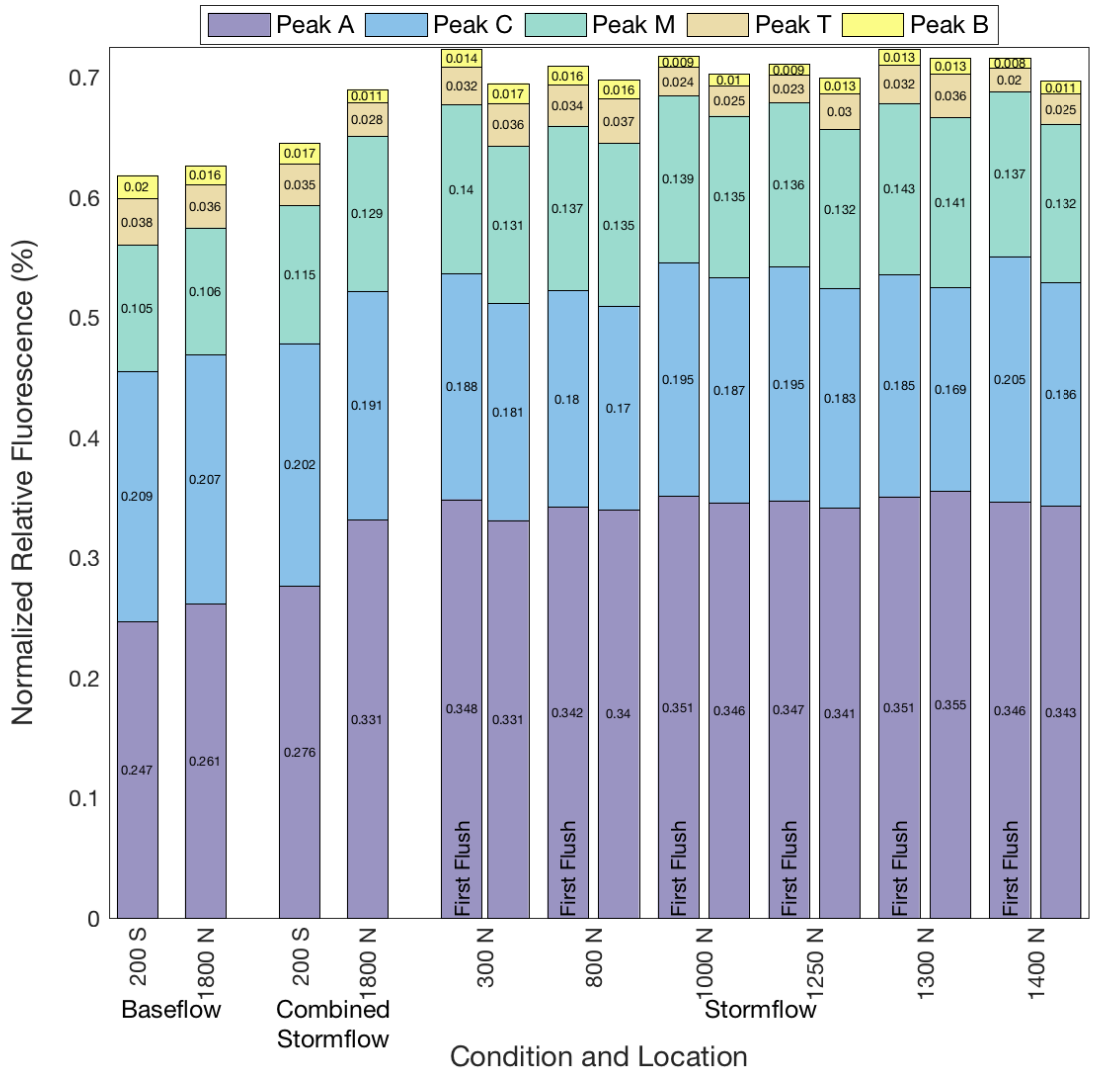

Figure 3-5. Change in relative contributions of known EEM peaks across sampling locations and flow conditions.

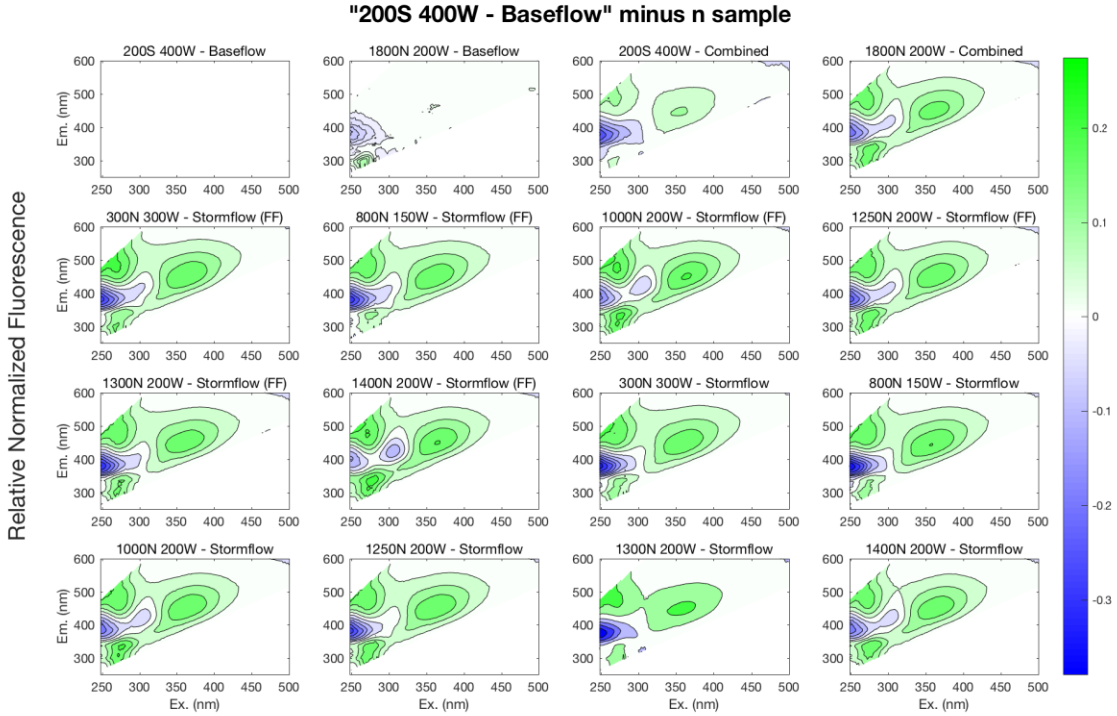

Figure 3-6. Subtraction of normalized EEMs for each flow condition from the normalized baseflow EEM at the 200 S site. First flush samples are indicated by (FF) in subplot titles.

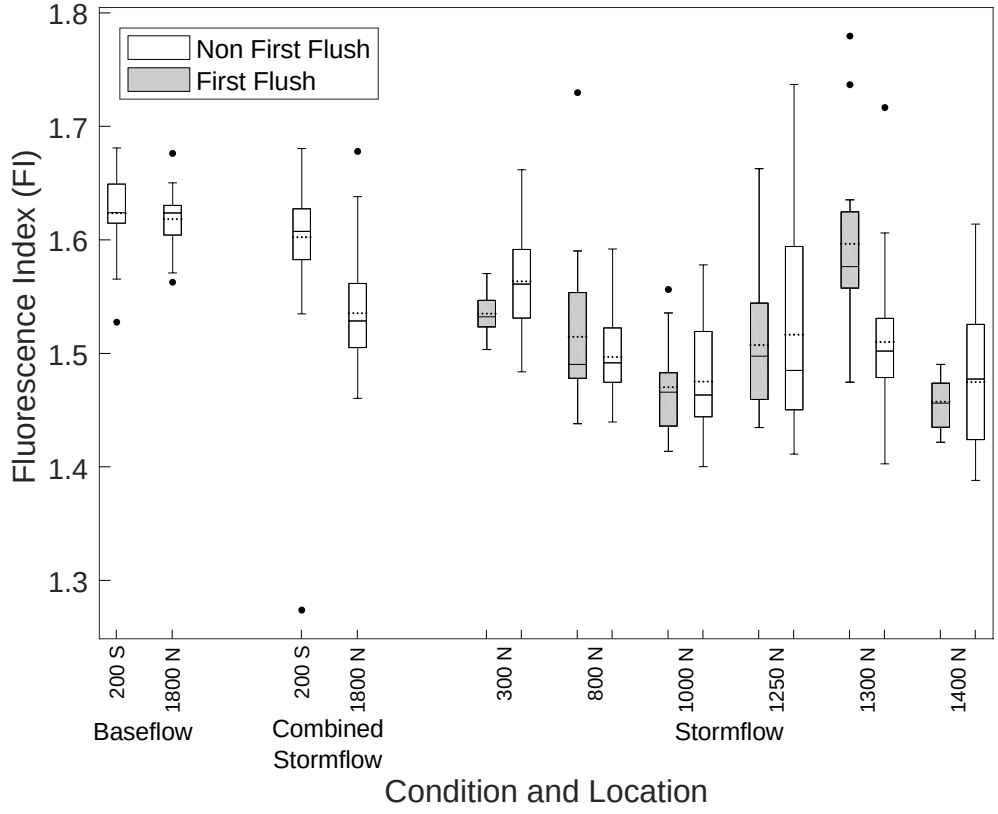

Figure 3-7. Box and whisker plot of the FI values in the Northwest Field Canal under baseflow and stormflow conditions. Solid horizontal lines represent the median value while dotted horizontal lines represent the mean value.

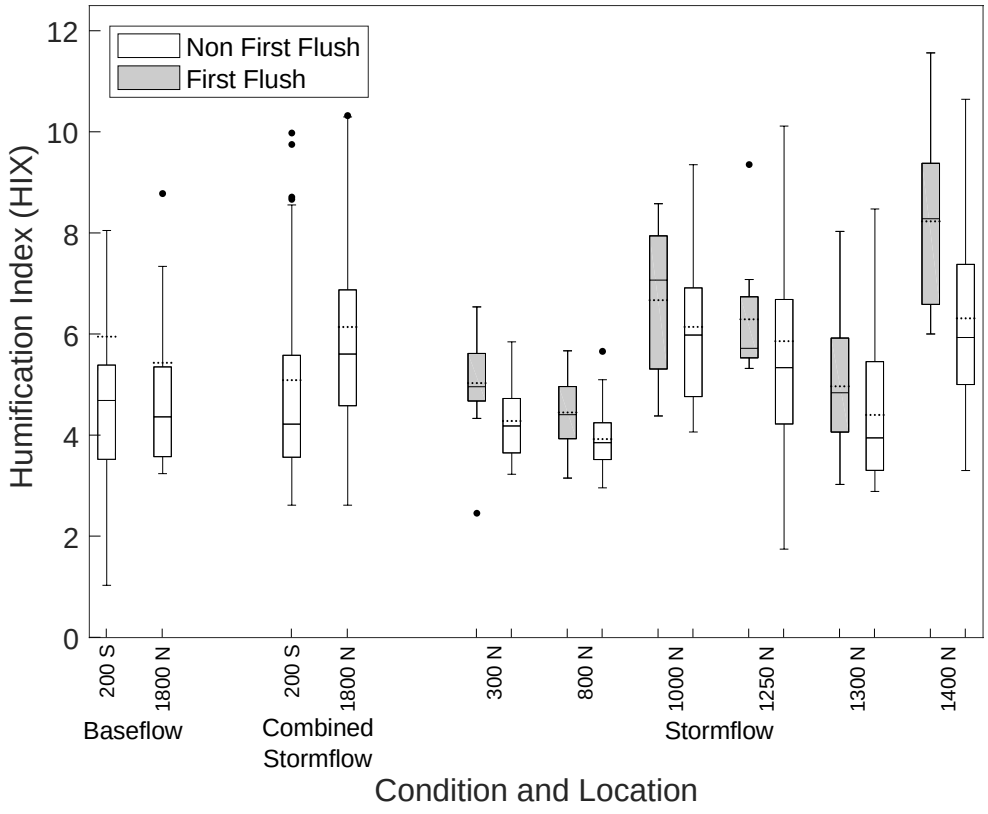

Figure 3-8. Box and whisker plot of HIX values in the Northwest Field Canal under baseflow and stormflow conditions. Not all outliers are shown given the y-axis scale. Solid horizontal lines represent the median value while dotted horizontal lines represent the mean value.

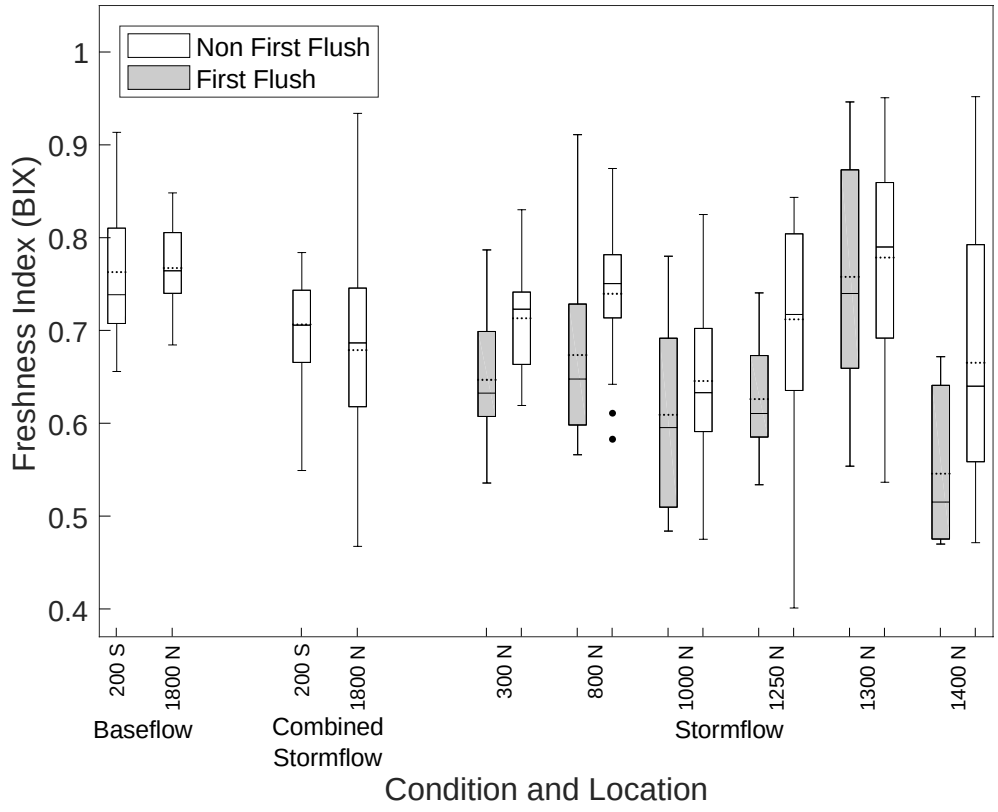

Figure 3-9. Box and whisker plot of BIX values in the Northwest Field Canal under baseflow and stormflow conditions. Solid horizontal lines represent the median value while dotted horizontal lines represent the mean value.

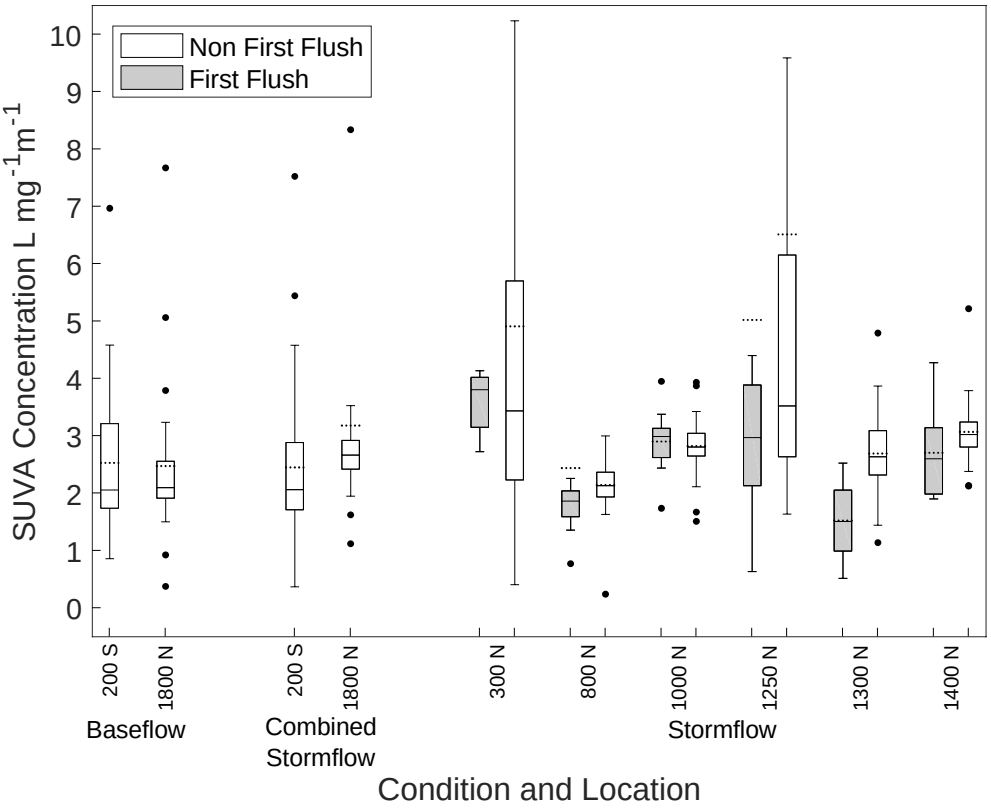

Figure 3-10. Boxplot of $SUVA_{254}$ values in the Northwest Field Canal under baseflow and stormflow conditions. Solid horizontal lines represent the median value while dotted horizontal lines represent the mean value. Not all outliers are shown given the y-axis scale.

CHAPTER 4

HIGH FREQUENCY MEASUREMENTS REVEAL SPATIAL AND TEMPORAL PATTERNS OF DISSOLVED ORGANIC MATTER IN AN URBAN WATER CONVEYANCE

Abstract

Stormwater runoff events in urban areas can contribute high concentrations of dissolved organic matter (DOM) to receiving waters, which has the potential to cause impairment to the aquatic ecosystem of urban streams and downstream water bodies. Compositional changes in DOM due to storm events in forested, agricultural, and urban landscapes have been well studied, but *in situ* sensors have not been widely applied to monitor stormwater contributions in urbanized areas, leaving the spatial and temporal characteristics of DOM within these systems poorly understood. In this study, we deployed fluorescent DOM (FDOM) sensors at upstream and downstream locations within a study reach to characterize the spatial and temporal changes in DOM quantity and sources within an urban water conveyance that receives stormwater runoff. Baseflow FDOM decreased over the summer season as seasonal flows upstream transported less DOM. FDOM fluctuated diurnally, the amplitude of which also declined as the summer season progressed. During storm events, FDOM concentrations were rapidly elevated to values orders of magnitude greater than in baseflow measurements, with greater concentrations at the downstream monitoring site, revealing high contributions from stormwater outfalls between the two monitoring locations. Observations from custom, *in situ* fluorometers resembled results obtained using laboratory methods for identifying

DOM source material and indicated that DOM transitioned to a more microbially derived composition as the summer season progressed, while stormwater contributions contributed DOM from terrestrial sources. Deployment of a mobile sensing platform during varying flow conditions captured spatial changes in DOM concentration and composition and revealed contributions of DOM from outfalls during stormflows that would have otherwise been unobserved.

4.1 Introduction

Dissolved organic matter (DOM) plays an important role in the aquatic environment and can have significant effects on aquatic organisms. The concentration of DOM in stream ecosystems can change seasonally and at shorter temporal scales based on geographical, hydrological, and biological conditions of a region (Creed et al., 2015). Quantifying these changes can be important in better understanding potential water quality issues and the effects of anthropogenic DOM contributions to receiving waters. Stormwater runoff can be a significant source for loading of water quality constituents (i.e., DOM) given that concentrations of these constituents in stormwater runoff can be much higher than those in the receiving water body (McElmurry et al., 2014; Saraceno et al., 2009). In urban environments, this can be even more significant due to land use characteristics such as imperviousness and directly connected flow paths that allow pollutants to be transported directly to a stream, bypassing natural riparian buffers (Hatt et al., 2004). With most contributions of organic matter in urban areas being flushed out during brief and potentially infrequent stormwater runoff periods, short episodes of hypoxia in receiving streams and downstream water bodies can occur (Mallin et al.,

2006) due to the oxygen demand exerted by decomposing organic matter (Boyd, 2000; Keith et al., 2014). However, characterizing the concentrations of constituents like DOM in stormwater runoff can be challenging due to the timing and flashiness of events. It is logistically difficult to collect measurements sufficient to characterize runoff from an event using standard grab sampling methods across many stormwater outfalls. The use of *in situ* sensors can help in overcoming this challenge by allowing for continuous monitoring of changes in water quality and the ability to better capture runoff from storm events.

The purpose of this study was to improve the understanding of spatial and temporal patterns in DOM concentration in an urban stream subject to stormwater runoff events. More specifically, we used high frequency, *in situ* data collection to detect changes in the composition and concentration of DOM in the Northwest Field Canal (NWFC), a water conveyance in Logan, Utah, USA that was originally built for conveying diverted river water for agricultural irrigation and that is now also used as a conveyance for urban stormwater. Understanding the quantity and quality of DOM and how it changes during storm events may lead to more informed management decisions and more accurate assessment of compliance with water quality standards set by state and federal regulatory agencies.

The NWFC discharges into Cutler Reservoir, which is listed as having impaired water quality in the State of Utah's list of impaired waters compiled by the Utah Department of Environmental Quality (DEQ), Division of Water Quality (DWQ), in compliance with Section 303(d) of the Clean Water Act (Utah DWQ, 2004; Utah Office

of Administrative Rules, 2017). A total maximum daily load (TMDL) study was recently completed that targeted excess total phosphorus loading to the reservoir as a primary cause of the water quality impairment (Utah DWQ, 2010). However, Cutler Reservoir was listed for low dissolved oxygen (DO) concentrations within the reservoir, and potential effects on aquatic organisms were identified as the driver for the TMDL. While excess phosphorus is a primary water quality concern, DOM contributions during storm runoff events may also be of concern for both the quality of the water in the canal with respect to what is desirable for canal water users and with respect to potential downstream effects in Cutler Reservoir. This is a pattern that is repeated in many western cities where population centers grew within areas historically used for agriculture and where agricultural canals now serve dual purpose as both agricultural and stormwater conveyances (City of Grand Junction, 2016; City of Logan, 2016; City of Sequim, 2016). Indeed, urban stormwater runoff has proven to be a major contributor of sediment, nutrients, and other pollutants to receiving water bodies in many areas of the U.S. (National Research Council, 2009).

In this study, we deployed a suite of fluorescent DOM (FDOM; also synonymous with colored DOM, i.e., CDOM) sensors in the NWFC over the course of two summer irrigation seasons (May – October) at the upstream and downstream ends of a study reach. Using *in situ* measurements we sought to: 1) determine the spatial and temporal patterns in FDOM during baseline flow conditions over the irrigation seasons (i.e., water diverted into the NWFC for irrigation purposes, referred to from here on as “baseflow”), 2) determine the influences of stormwater runoff on FDOM concentrations and how

concentrations change spatially within the study reach, and 3) examine the changes in DOM composition during baseflow and stormflow conditions.

4.2 Methods

4.2.1 Study Area

Logan, Utah, located in the state's northern region, has a population of about 50,371 (U.S. Census Bureau, 2016), making it the largest city in Utah's Cache County. The Logan River enters city boundaries from the east as the river finishes its course through Logan Canyon. The Logan River watershed (United States Geological Survey Hydrologic Unit Code 1601020303) is part of the larger Bear River basin. Stormwater runoff in Logan is primarily directed into four agricultural irrigation canals that are diverted from the Logan River, run north, then west, and eventually empty into Cutler Reservoir. The study site for this research included the Logan City urban water system, but focused on the Northwest Field Canal (NWFC – Figure 3-1), which is the irrigation canal located farthest west in Logan. This canal was selected specifically because it receives runoff from a variety of land uses within its drainage area.

The Logan River enters the city from the east and runs through what is known as the Logan "Island" district. At River Hollow Park, a portion of the Logan River is diverted into a mixed natural/lined channel called the Little Logan River. The Little Logan River then travels through the heart of the city, receiving stormwater from notable city features such as Merlin Olson Park and the Main Street City Center. The Little Logan River then flows west to Logan High School. Just west of Logan High School, the

Little Logan River is diverted into the NWFC. The NWFC flows north, first through residential and mixed residential neighborhoods and then through primarily commercial and mixed-use, receiving stormwater from much of Logan's city center and commercial zones. Drainage subcatchments in Logan City are bordered by the four irrigation canals, with stormwater traveling primarily from east to west. Many Logan City residents have the option of irrigating their lawns and gardens with canal water, thus irrigation water is diverted from the canals and is conveyed through the city's gutters. Water is diverted from the canal east of a neighborhood and either returns directly or is applied for irrigation and later runs off into the canal to the west.

4.2.2 Sampling and Laboratory Analysis

The NWFC was monitored from the 200 South 400 West intersection (upstream) to the 1800 North 200 West intersection (downstream) in Logan (Figure 3-1), a distance of approximately 2.7 miles. Monitoring sites along the canal consisted of stormwater outfall sites and canal sites. Canal monitoring sites were installed at the upstream and downstream ends of our study reach. Between the upstream and downstream canal sites, stormwater outfall sites were located at stormwater discharge points in the canal. The instrumentation of both canal and stormwater outfall sites is listed in Table 4-1.

We devised a sampling protocol that included both canal and stormwater outfall monitoring sites aimed at characterizing the DOM of baseflow in the canal, flow from stormwater outfalls, and combined flows within the canal during storm conditions. Periodic grab sampling was conducted during baseflow conditions to characterize water diverted from the Logan River for irrigation purposes. Samples were collected on a

weekly basis, when possible, throughout the two irrigation seasons. Baseflow sampling was postponed during storm events or when storm runoff was influencing the conditions in the canal.

Stormwater sampling was carried out using automated samplers capable of collecting 24 – one Liter samples at a time at both stormwater outfall and canal sites. Stormwater outfall sites and canal sites were configured to work in pairs, such that the upstream canal site was associated with the more upstream outfall site and the downstream canal site was associated with the further downstream outfall site. Threshold criteria were developed for automated sample collection during storm flows based on weather conditions (Table 3-1). Samples were collected during periods where all threshold conditions were satisfied. If any of the criteria fell below its threshold, sampling was postponed. Once thresholds at a stormwater outfall site had been met, an automated signal was sent to its associated canal site initiating sampling at that site. Sampling intervals at stormwater outfall sites were varied to capture the bulk of the first flush of an event and the falling limb of the storm hydrograph. This resulted in a sampling interval of every 3 minutes for the first 5 samples, followed by a sample every 15 minutes for the rest of the storm or until all 24 of the sample bottles had been filled. Outfall sampling intervals reflect the short and intense nature of many storms experienced in Logan and were set after monitoring several storms to determine the extent and duration of first flush effects.

After receiving a stormwater runoff event flag from an outfall site, the canal sites were programmed to initiate adaptive, event-based sampling. Samples were collected at

canal sites according to a turbidity threshold sampling procedure. During storm events, samples were triggered as turbidity values rose above or fell below predefined thresholds. Threshold values were determined using methods described by Lewis (1996). A more detailed description of coordinated sampling procedures in the canal is provided by Melcher and Horsburgh (2017).

Physical samples were taken to the lab and analyzed for excitation emission matrix spectroscopy (EEMS) using an Aqualog spectrofluorometer (Horiba Jobin Yvon, Edison, New Jersey) and dissolved organic carbon (DOC) concentration. All samples were filtered using type GF/F (0.7 μm pore size) filters prior to analysis. EEMs were collected in ratio mode (sample/reference) to account for non-uniform output of the lamp over the excitation range (Cory et al., 2010). Excitation wavelengths spanned from 248 nm to 830 nm at 2 or 6 nm increments and were integrated from 0.5 to 4 seconds, depending on the sample. Emission wavelengths were collected between approximately 250 nm and 828 nm at a low charge-coupled device (CCD) gain and 8 pixel (~ 4.12 nm) increment. Some samples were analyzed at the University of Utah using a different model Aqualog while the Aqualog at USU was being repaired. Excitation wavelengths remained the same but emission wavelengths spanned between approximately 245 nm and 825 nm (~ 2.3 nm). These data were integrated to the same emission wavelengths measured by the USU Aqualog before analysis. Since two different instruments were used in the collection of EEMs, intensity calibration was performed to convert data to Raman units (RU), as discussed below.

Corrections were performed on the resulting EEM of each sample to account for differences in spectral, absorbance, and intensity properties of samples. Milli-Q blanks were collected daily before running samples. EEM scans were corrected for instrument specific response by the Aqualog as the ratio of the corrected reference signal to the corrected emission detector signal, resulting in a spectral corrected EEM after each measurement. Sample EEM's were corrected for the inner filter effect (Lakowicz, 2006). Milli-Q blank and sample EEM's were Raman-normalized by dividing the EEM by the area under the water-Raman curve at an excitation of wavelength 350 nm, converting the arbitrary units to RU(Lawaetz and Stedmon, 2009). Raman-normalized EEM's were then blank subtracted and corrected for dilution.

EEM's were used to characterize the source of DOM in collected samples by calculating the fluorescence index (FI). The FI is commonly calculated from EEMs as the ratio of the emission intensities at 470 nm and 520 nm with excitation intensity at 370 nm and is used to indicate changes in DOM production sources, with higher values representing more microbially derived DOM and lower values indicating more terrestrially derived DOM (McKnight et al., 2001).

4.2.3 Continuous Data Collection

Measurements of water quality parameters at the continuously monitored canal sites (Table 4-1) were recorded every 15 minutes during baseflow conditions and every 5 minutes during stormflow conditions (i.e., "event data"). Parameters at the outfall sites were measured once every minute and recorded at this interval during stormflow conditions but were only recorded every 15 minutes during baseflow conditions (i.e.,

when the storm drains were not discharging stormwater runoff). At any time throughout the study period there were two stormwater outfall sites installed, and a total of six different outfall sites were monitored during this study.

The EXO2 FDOM and C6 CDOM sensors were calibrated to quinine sulfate units (QSU) using a 300 ppm QSU solution and procedures recommended by the sensor manufacturers. The two custom fluorometers were calibrated using raw fluorescence units in blank subtracted mode (RFUB), per the recommendation of the manufacturer. Sensors were calibrated at the start of monitoring seasons and were cleaned and re-calibrated as needed throughout the field data collection seasons.

We used custom fluorometers with excitation-emission wavelengths specifically chosen for the purpose of measuring the FI *in situ* ($FI_{in\text{-}situ}$). Each Turner Designs C6 was outfitted with two custom fluorometers (denoted as #1 and #2), which were optically centered at 470 nm (±10 nm) and 520 nm (±10 nm) in emission, respectively, and both at 380 nm (±15 nm) in excitation, where the value in parenthesis is the range of the bandpass filter. These specifications were selected based on a balance between our needs for calculating the $FI_{in\text{-}situ}$ and the manufacturer's ability to build the custom sensors. The values reported in this paper for $FI_{in\text{-}situ}$ are the direct ratio of the quality controlled observations from the two custom fluorometers. The lab measured FI values were calculated from EEMS with resulting units in RU, whereas $FI_{in\text{-}situ}$ values were calculated from the two individual fluorometers measuring in RFUB; because of this, the $FI_{in\text{-}situ}$ values have a different range and scale than typical FI values derived from EEMs, which typically fall between 1.2 and 1.8. Given that the relative trends or differences in FI

values, irrespective of the absolute value of the FI, can be interpreted to represent changes in the source of DOM (Cory et al., 2010), we chose to calculate FI values using the native units of the custom, *in situ* fluorometers as we were mainly interested in how FI values changed under different flow conditions in the canal.

4.2.4 Mobile Sensing Platform

Data were also collected using a mobile sensing platform (Figure 4-1). The mobile platform was deployed along select canal transects during baseflow and stormflow conditions to capture spatial changes in water quality with high resolution and reveal contributions from unmonitored outfalls that would have otherwise gone unmeasured. We conducted multiple baseflow and stormflow sampling events, all of which occurred during the 2016 monitoring season. Most deployments were made between 1250 N and 1800 N because this section of the NWFC had the easiest access (much of the canal upstream of 1250 N is surrounded on both sides by private residences limiting access) and the smallest number of obstructions that would require portaging of the sensor platform. Baseflow events were conducted multiple times to characterize any changes in baseflow conditions over the course of the summer. Stormflow events were conducted for several storm events in efforts to measure storms with differing characteristics.

During each sampling event, the sensing platform was allowed to float along the length of the transect at the speed of the water flowing in the canal. Measurements were recorded on a 2 second interval with the exception of turbidity, which was measured every 30 seconds. These recording intervals reflect the fastest speed with which

individual observations could be obtained from the individual sensors. During the deployment of the mobile platform, the Turner C6 was removed from the upstream canal monitoring site and installed on the mobile platform; all other instrumentation for the mobile platform was already installed (Table 4-2).

4.2.5 Data Analysis

Data from the continuous monitoring sites were transmitted via radio telemetry and backed up to a server located on the USU campus and stored in an instance of the Consortium of Universities for the Advancement of Hydrologic Science, Inc. (CUAHSI) Observations Data Model (ODM) Version 1.1.1 relational database (Horsburgh et al., 2008). Continuous data for all measured variables at the upstream and downstream canal sites were quality controlled and adjusted for calibration shifts, fouling and instrument drift, and value anomalies using the ODMTools software (Horsburgh et al., 2015).

All data presented here from the YSI EXO2 FDOM, Turner Designs C6 CDOM, custom fluorometer #1, and custom fluorometer #2 were corrected for temperature and turbidity influences using Equations 1 and 2, which were adopted from Watras et al. (2011) and Lee et al. (2015):

$$FDOM_{temp} = \frac{FDOM_{raw}}{1\text{-}0.017(Temp_m - Temp_{ref})} \quad (1)$$

$$FDOM_{corr} = \frac{FDOM_{temp}}{0.82e^{(-0.005\ Turb_m)}+0.18} \quad (2)$$

where $FDOM_{raw}$ is the uncorrected FDOM, $Temp_m$ is the corresponding measured water temperature, $Temp_{ref}$ is the reference temperature of 20° C, $FDOM_{temp}$ is the temperature corrected FDOM, $Turb_m$ is the corresponding measured turbidity, and $FDOM_{corr}$ is the

final corrected result. Figure 4-2 shows an example of the application of these equations to our FDOM measurements and illustrates that the shape and magnitude of FDOM is altered due to temperature and turbidity effects during a storm event. DOC observations from samples collected during this period are superimposed for comparison.

The coefficients presented in Equations 1 and 2 were chosen after we conducted a comparison of multiple sets of coefficients from the literature (Watras et al., 2011; Downing et al., 2012; Lee et al., 2015; Saraceno et al., 2017). Additional coefficients for turbidity corrections from Saraceno et al (2016) and Saraceno et al. (2017) were obtained via personal correspondence, as they are not available in published literature. We corrected our FDOM data using each set of coefficients and then compared corrected FDOM values to observed DOC concentrations. We chose the coefficients that produced the best linear fit (in terms of R^2) between corrected FDOM and our DOC observations. Temperature coefficients selected were from Watras et al. (2011) and turbidity coefficients were from Lee et al. (2015). Based on our review of the literature, all of the experimental temperature correction coefficients were similar, and all of the experimental turbidity-FDOM attenuation curves were nearly the same for turbidity values less than 300 NTU, above which some discrepancies have been observed (Saraceno et al., 2017). Given the similarity in the temperature correction coefficients, the fact that 99.98% of our observed turbidity values were below 300 NTU, and the fact the we saw only negligible differences in R^2 values in regressions between corrected FDOM and DOC using the different sets of correction coefficients, we felt that using existing coefficients produced results adequate for our study.

Data obtained using the mobile platform were quality controlled by removing data during times when the platform was out of the water before and after deployment, while avoiding shallow riffle sections through which the platform would not float freely during lower flows, and during times when we had to portage around low bridges and culverts through which the platform could not pass during high flows. Distances along the sampling transect were based on a projection method that aligned the GPS coordinates to the channel centerline by calculating the shortest perpendicular distance from the GPS coordinates to the centerline. This helped us account for both error in the GPS coordinates and the fact that the platform did not always track the exact centerline of the channel as it floated downstream. Turbidity observations, which were recorded at 30 second intervals, were linearly interpolated to two second intervals to match the rest of the data collected by the mobile platform so that fluorescence data could be corrected for temperature and turbidity effects as mentioned above.

4.3 Results

4.3.1 Temporal Changes of DOM

In situ monitoring revealed that early season flows had higher FDOM and that, overall, FDOM values generally declined over the summer irrigation seasons (Figure 4-3). Monthly FDOM values for baseflow conditions are summarized in Table 4-3. Baseflow FDOM measurements decreased between May and October by 78% at the upstream monitoring location and by 71% at the downstream site. In contrast, FDOM measurements during stormflows were orders of magnitude greater than baseflow FDOM

values, with a storm event average of 20.5 (± 12.9 STD) QSU and a peak as high as 81.3 QSU at 200 S and a storm event average of 69.8 (± 58.7 STD) QSU and peak as high as 501.5 QSU at 1800 N. Elevated values during storms reverted to baseflow values shortly after the subsidence of rain (i.e., on the order of hours – Figure 4-3).

Diurnal cycles were also observed in the *in situ* fluorescence data, which have been reported in similar work (Saraceno et al., 2009; Spencer et al., 2007). Figure 4-4 shows the monthly changes in the diurnal variability of measured FDOM during baseflow conditions at the two continuous monitoring locations during the 2016 field season. To create a relatively small number of bins that show how the diurnal cycles changed over the course of the irrigation season, FDOM values were binned by month and then by time of day at 15 min increments. The mean and standard deviation were then calculated for each time of day for each month to get the mean and standard deviation of FDOM over a 24-hour period (n = 96). The overall decline in FDOM throughout the season, shown in Figure 4-4, is consistent with results shown in Figure 4-3. The diurnal variability in baseflow FDOM also declined throughout both seasons (2016 shown in Figure 4-4), but was visually different between the upstream and downstream monitoring locations. Similar diurnal changes were observed (i.e., seasonal decline and dampening of diurnal amplitudes in FDOM) when comparing the canal sites to an upstream FDOM sensor located on the Logan River at the Utah Water Research Laboratory (iUTAH GAMUT Working Group, 2017).

The $FI_{in\text{-}situ}$ (FI determined from continuous measurements made by our custom fluorometers) during baseflow conditions increased over the course of the 2016

monitoring season at both the upstream and downstream monitoring sites but had large variability (Figure 4-5). The $FI_{in\text{-}situ}$ increased between May and October by approximately 4% at the upstream monitoring location and by approximately 16% at the downstream site. We attempted to verify this result by examining the seasonality observed in lab measured FI, which also showed an increase in FI throughout the monitoring seasons for both sites (data not shown), and by directly comparing $FI_{in\text{-}situ}$ with lab measured FI, which we expected to be highly correlated. Correlation between $FI_{in\text{-}situ}$ and lab measured FI was higher during stormflow conditions ($R^2 = 0.73$ for the data presented in Figure 4-6; $R^2 = 0.57$ for the same date range as Figure 4-6 at the 200 S monitoring location, not shown) than it was during baseflow conditions ($R^2 = 0.29$ at 200 S and $R^2 = 0.04$ at 1800 N for all FI data, not shown).

4.3.2 High Resolution Spatial Variability of DOM

Results from the mobile platform during baseflow conditions were consistent with our seasonal analysis of FDOM in that the overall FDOM values decreased in subsequent runs throughout the season (Figure 4-7). In addition, each of the four baseflow runs we performed show a slight increase in FDOM along the transect reach. Stormflow boat runs had higher FDOM values compared to those of baseflow runs. Figure 4-8 shows that the largest increases in FDOM during stormflow runs were associated with the locations of outfalls along the canal transect. It is important to note that two runs were conducted on 21-Sep-2016, one in the morning and one at night, under distinctly different flow

conditions, and, thus are referred to as 21-Sep-2016 AM and 21-Sep-2016 PM for clarification.

$FI_{in\text{-}situ}$ was also monitored using the mobile platform. Figure 4-9 shows the responses of FDOM and $FI_{in\text{-}situ}$ during a single storm event. To help visualize the trend of the data, a smoothed curve of the calculated $FI_{in\text{-}situ}$ series (created using the "smooth" function with the rloess method in MATLAB) is plotted in addition to the raw data. Drops in FI during the stormflow run correspond to increases in FDOM at outfall locations, with the most dramatic responses at the 1400 N and 1610 N outfalls.

4.4 Discussion

4.4.1 Continuous FDOM Measurements

Stream flows originating from high alpine regions, such as the mountains in Northern Utah, are mainly sustained by snowmelt, with peak runoff occurring in the late spring and declining throughout the summer season as the remaining snow melts. It has been observed that spring flows from these types of streams exhibit diurnal fluctuations in discharge, and, once the snowpack within a basin is mostly depleted, the amplitude of the diurnal fluctuations is significantly less or ceases all together (Laudon and Slaymaker, 1997; Lundquist and Cayan, 2002; Marsh and Woo, 1981). Net radiation is a dominant driver for snowpack melt off (Mazurkiewicz et al., 2008), leading to these observed discharge fluctuations.

Spring snowmelt driven flows have been shown to increase the transport of DOC in snowmelt dominated streams (Burns et al., 2016; McKnight et al., 2001). This is

consistent with our results where we observed the highest FDOM values early in the season corresponding with spring snowmelt runoff. The patterns we observed in FDOM are similar to those noted by others for seasonal stream flow characteristics of snowpack dominated watersheds, where values were higher during snowmelt and slowly decreased throughout the summer. The seasonal patterns we observed in FDOM concentration were likely driven by changes in high elevation snowmelt, soil moisture, and hydrologic connectivity, which would be expected to decrease throughout the summer as snowmelt decreases. As high elevation snowpack decreases, followed by a decline in soil moisture content, connectivity of organic-rich upper soil horizons to shallow flowpaths linked to the Logan River (the water source for the NWFC) likely declines, resulting in less DOM being contributed to active streams and less DOM transport as the season progresses (Pellerin et al., 2012).

The decline in the observed diurnal variability of FDOM over the course of the monitoring seasons is likely linked to snowmelt as well, where the daily pulse of DOM from snowmelt would be reduced as fewer shallow flow paths exist later in the season due to dryer soil moisture conditions. In addition to snowmelt driven diurnal fluctuations, factors such as photodegredation and microbial activity (i.e., phytoplankton and zooplankton) have been attributed to diurnal fluctuations in FDOM (Spencer et al., 2007). The shape and timing of the diurnal trends presented here are consistent with those observed by Spencer et al. (2007), where FDOM was rising overnight and declining throughout the day with the start of decline shortly after sunrise. At the start of each irrigation season, the NWFC channel was mostly free of vegetation, but throughout the

season riparian vegetation, macrophytes, and bottom algae become abundant, particularly at the downstream monitoring location (1800 N), which could explain the slightly greater variability observed at the downstream site (Figure 4-4). When Spencer et al. (2007) observed diurnal variability in FDOM, they concluded that it was independent of river flow because they did not observe diurnal fluctuations in discharges. However, their study was conducted over a short period of time in late summer on a river that originates predominately from agricultural return flows, and, therefore, would not be expected to have significant diurnal fluctuations. It has also been observed that urban streams, which may have been straightened, piped, or line, may retain less organic matter than other streams because they lack the more complex benthic environment of more natural streams. This could, conceptually, limit biological activity (Paul and Meyer, 2001), resulting in less diurnal fluctuations. Therefore, we hypothesize that the drivers for diurnal fluctuations change seasonally, with spring snowmelt driving the variability early in the season and photodegredation dominating the much smaller diurnal fluctuations observed in the late summer and early fall.

The characteristics of FDOM observed over the course of a storm event are similar to the findings made by Saraceno et al. (2009), where FDOM had a sharp rise with the onset of runoff followed by a gradual decline (e.g., Figure 4-2). However, in our system FDOM returned to pre-event values relatively quickly (on the order of hours), whereas Saraceno et al. (2009), who studied a larger watershed with more varied land use, observed elevated levels for over a week before returning to pre-event values. The peak concentration of FDOM varied by storm event but did not have any noticeable

seasonal patterns, indicating that FDOM concentrations during storm events are most likely a factor of rainfall intensity and duration, as illustrated by Figure 4-3.

The two seasons monitored were characteristically different due to factors such as seasonal snowpack and rainfall, which both affect the transport of DOM in aquatic systems. Between the two seasons, FDOM appears to be higher at the downstream site in 2015 but is lower at the downstream site in 2016 (Figure 4-3). However, these differences are small relative to the accuracy of the FDOM sensors, and we attribute this phenomenon to sensor calibration differences. If anything, we would expect the downstream site to have higher FDOM values due to potential return flows to the canal from the irrigation of lawns and gardens between the two sites (either from overspray transported through the stormwater conveyances to the canal or from excess flood irrigation that returns via surface runoff), transporting organic matter rich soil water. This is supported by the results presented in Chapter 3 of this thesis, which showed that DOC concentrations were slightly elevated at the downstream monitoring location compared to the upstream site during baseflow conditions.

4.4.2 Custom Fluorometers for in situ FI

The application of custom fluorometers to measure the FI in the type of aquatic environment we studied has only emerged in the past several years. Comparison with additional studies is necessary to verify the effectiveness and repeatability in this relatively new method. Our search of the literature found only one study that used custom fluorometers for estimating FI values (Carpenter et al., 2013), which we use here for comparison with our results. Due to manufacturer availability, the custom fluorometers

we used were centered at an excitation wavelength of 380 nm as opposed to 370 nm for the custom fluorometers used by Carpenter et al. (2013) for their study. This difference makes it harder to compare results and was not ideal given that the excitation wavelength used to calculate the FI from an EEM is 370 nm (McKnight et al., 2001). However, the bandpass filters on our custom fluorometers were narrower, which, should allow for a more discrete signal to be measured by the two sensors we used. In general, our results are similar to the observations made by Carpenter et al. (2013) in that the custom fluorometers used to measure $FI_{in\text{-}situ}$ correlated well with the Cyclops – 7 standard CDOM sensor. This was expected since all three sensors are centered around the Peak C region of the EEM spectrum but have slightly different spectral and bandpass filter parameters.

The values of $FI_{in\text{-}situ}$ in this study ranged between 0.65 and 0.95, which are slightly lower than the values reported by Carpenter et al. (2013), likely due to the slight differences in the spectral parameters of the sensors. This range is also considerably less than the range of commonly reported FI values from the literature (i.e., 1.2 -1.8). However, as mentioned earlier, the absolute value of the FI would be expected to differ because of differences in spectral properties between fluorescence measurement methods and spectrofluorometers. Despite this, changes in FI values can be interpreted to represent changes in the source of DOM.

The custom fluorometer data had high variability, even within short time periods under baseflow conditions, which was also observed by Carpenter et al. (2013). This noise could be caused by several factors, including: 1) true variability in DOM

concentrations; 2) interference from other water quality constituents like turbidity; and 3) instrument noise. Additional research is needed to better characterize and potentially correct for the noise we observed.

We hypothesize that the increase in $FI_{in\text{-}situ}$ over the course of the 2016 monitoring season at both canal sites was due to changes in DOM contributions upstream at higher elevations in the watershed. DOM transported to the stream during snowmelt runoff is likely to come from upper soil horizons with DOM characteristic of vegetation sources, with lignin-derived phenols and plant derived carbohydrates (Kaiser et al., 2004). Thus, as soil moisture declines throughout the summer, the hydrologic connectivity of soils to the stream during snowmelt decreases and less plant derived DOM is transported from the hillslopes to the river. This results in a shift in instream DOM toward microbial sources, as evidenced by higher FI values. This hypothesis is supported by Burns et al. (2016), who showed that DOM composition during the snowmelt period was strongly attributed to soil water contributions.

Within the NWFC at the upstream and downstream monitoring locations, the $FI_{in\text{-}situ}$ was consistently lower at the downstream site, with the exception of October. Our hypothesis for the spatial differences is similar to our interpretation of the seasonal changes observed for the $FI_{in\text{-}situ}$. We believe that irrigation of lawns and gardens adjacent to the NWFC had an effect similar to that of high elevation snowmelt in that irrigation increased the hydrologic connectivity of soils adjacent to the canal, resulting in contributions of organic rich soil water between the two monitoring locations. While we

believe that irrigation practices lowered the $FI_{in\text{-}situ}$ between the two sites, changes in high elevation contributions of DOM still influenced the overall trend throughout the season.

The results from $FI_{in\text{-}situ}$ during single storm events indicated rapid changes in DOM composition over short periods of time. Over one particular several day episode of storms, the $FI_{in\text{-}situ}$ was quite variable at the start with both high and low values (May 6-7; Figure 4-6), while later storms caused a more significant decrease in the $FI_{in\text{-}situ}$ and reverted to higher values shortly after the subsidence of runoff (May 10, Figure 4-6). Carpenter et al. (2013) reported that the $FI_{in\text{-}situ}$ increased with the onset of rain and attributed this to the potential suspension of decaying algae in the river. We believe that this could explain some of the variability at the beginning of the several day rain event, with any algae being flushed out after the first event and, therefore, having less of an influence on subsequent stormflows within this short period of many rain events.

Overall, lab measured FI had a high positive correlation with $FI_{in\text{-}situ}$ during storm events, but had a much lower degree of correlation when baseflow conditions were considered for either of the two monitoring locations. A potential explanation for the overall low correlation could be due to differences in measurable resolution or sensitivity between the benchtop spectrofluorometer and custom, *in situ* fluorometers. It could also be possible that the spectral parameters of the custom, *in situ* fluorometers should be altered, such as narrowing the bandpass filters or shifting the center of the light source (i.e., from 380 nm to 370 nm in excitation), in order to better correspond with lab measured FI. More research is needed to determine whether better agreement can be obtained between fluorescence intensity values from discrete EEM regions measured in

the lab and fluorescence intensity values measured using custom, *in situ* fluorometers. Aside from the FI, other research has shown that peak picking may also be a viable method for detecting slight changes in DOM composition (Chapter 3 of this thesis) and has been used for determining wastewater contributions to receiving streams (Goldman et al., 2012) and as a surrogate for BOD (Hudson et al., 2008). These methods could potentially be applied using custom, *in situ* fluorometers for future research and monitoring applications.

4.4.3 High Resolution Spatial Characteristics

Although many mobile water quality sensing platforms have been used for mapping water quality and environmental parameters in surface water bodies (Casper et al., 2012; Dunbabin and Grinham, 2010; Podnar et al., 2010; Low et al., 2009), this is the first study to implement one for collecting water quality measurements during urban stormwater runoff events. The boat traveled with the streamflow and, therefore, provided a Lagrangian context (e.g., following an individual fluid parcel) for the movement of a parcel of water through the system. The high spatiotemporal sampling frequency revealed contributions from unmonitored outfalls that would have otherwise gone unmeasured.

The slight increases in FDOM measured in the downstream direction during baseflow mobile platform deployments may be due to shallow groundwater contributions or trickling outfalls caused by irrigation practices and return flows. It is also possible that the disturbance and suspension of sediment that occurred during our interactions with the platform during a run (e.g., portaging the platform around bridges and culverts) may have

contributed to this. We minimized this to the extent we could; however, it was necessary for us to intervene at times to keep the platform moving and to avoid getting it stuck under bridges.

The measured FDOM responses at outfall locations were strongly influenced by the timing in deploying the mobile platform, and, therefore, are not easily comparable across stormflow runs. For example, if the first flush of the storm had already happened before we deployed the platform, the initial FDOM values in the canal would already be elevated and responses from outfalls less pronounced. This occurred in three of the stormflow condition runs (not shown), where FDOM concentrations were already elevated, and the profile of FDOM along the transect was relatively flat. The differences in deployment timing can be seen in Figure 4-8, where the run on 13-Sep-2016 has a higher initial FDOM than the run on 21-Sep-2016 PM. The run on 13-Sep-2016 was deployed a few hours after rain had initially begun and subsided but at the start of another storm cell that also generated runoff, while the run on 21-Sep-2016 PM was deployed right after the onset of flows from the outfall at 1250 N had started. Deploying the platform right at the first flush (21-Sep-2016 PM) resulted in our highest FDOM values out of any stormflow run.

We observed that the first flush of a storm event has the highest concentrations of FDOM; however, catching the storm right at the first flush is not necessarily why the 21-Sep-2016 PM stormflow run had higher FDOM values compared to other runs. Storm characteristics such as intensity, duration, and locality also highly influenced the responses observed in FDOM along the study reach. The storm on 21-Sep-2016 was very

intense and generated a lot of runoff. The combined differences in storm characteristics and timing can be seen in Figure 4-8, where some outfalls generated a response in FDOM during one run but did not in the other run. Additionally, increases in FDOM occurred in sections were there are no outfalls (e.g., before Penny Ln on 21-Sep-2016 PM), which may indicate overland flows directly into the canal.

On average, the $FI_{in\text{-}situ}$ values during baseflow deployments of the mobile platform were higher than $FI_{in\text{-}situ}$ values during stormflow runs. This indicates that there is a shift to more allochthonous and terrestrially derived DOM composition due to the contributions of DOM from outfalls. This was expected as composition of DOM during stormflows should be more terrestrially driven due to saturated soils and runoff driving values of $FI_{in\text{-}situ}$ down. During stormflows, the $FI_{in\text{-}situ}$ exhibited a drop in response to outfall contributions, which was consistent with lower lab FI values that have been reported due to stormwater contributions from outfalls in the NWFC (Chapter 3 of this thesis)

4.5 Conclusions

The results show that the concentrations of FDOM change temporally and spatially throughout irrigation seasons, with major drivers for baseflow DOM concentrations likely being snowmelt and hydrologic connectivity in soils at higher elevations upstream of Logan City. A decline in FDOM was observed at the stationary sites in the canal and was also observed across four subsequent baseflow runs of the mobile sensing platform. Compositional changes in DOM throughout the field season inferred from FI values indicate that less terrestrially derived DOM is being contributed

to the river from which the NWFC is diverted. Lastly, FI was consistently lower at the downstream monitoring location due to return flows into the canal generated by irrigation practices adjacent to the NWFC.

The downstream monitoring site had significantly higher FDOM concentrations compared to the upstream site during stormflow conditions due to the contributions from outfalls between the two sites. During stormflow conditions, the mobile sensing platform confirmed that contributions of DOM were associated with the locations of outfalls discharging runoff into the canal and revealed spatial changes in DOM composition and concentration along canal transects. Short duration drops in FI after the onset of runoff indicate that contributions of DOM derived from terrestrial sources are being added to the system, changing the composition of DOM within the NWFC during stormflow conditions.

Our study showed that DOM contributions to the NWFC during storm events are well above the DOM concentrations during baseflows. The implications of these stormwater contributions and the changes in composition could result in rapid declines in DO concentrations over short periods of time in the canal as well as longer term stresses on the already impaired downstream water body of Cutler Reservoir. Understanding the relationships between DOM concentrations and compositions to DO and estimating DOM loading rates during stormflows in the NWFC is the next logical step in determining the true implications to downstream water users and could provide crucial information for future management of stormwater runoff that can potentially lead to the improvements of water quality in downstream water bodies

Acknowledgments

This work was supported by funding from the Utah Water Research Laboratory at Utah State University and from United States National Science Foundation grant 1208732. Any opinions, findings, and conclusions or recommendations expressed are those of the authors and do not necessarily reflect the views of the National Science Foundation.

References

Boyd, C. E. (2000), *Water quality: An introduction*. Kluwer Academic Publishers, Boston, MA.

Burns, M. A., H. R. Barnard, R. S. Gabor, D. M. McKnight, and P. D. Brooks (2016), Dissolved organic matter transport reflects hill slope to stream connectivity during snowmelt in a montane catchment, *Water Resour. Res. 52*, 1–20, doi: 10.1002/2015WR017878.

Carpenter, K. D., T. E. C. Kraus, J. H. Goldman, J. F. Saraceno, B. D. Downing, B. A. Bergamaschi, G. McGhee, and T. Triplett (2013), Sources and characteristics of organic matter in the Clackamas River, Oregon, related to the gormation of disinfection by-products in treated drinking water. U.S. Geological Survey Scientific Investigations Report 2013-5001, 78.

Casper, A. F., B. Dixon, E. T. Steimle, M. L. Hall, and R. N. Conmy (2012), Scales of heterogeneity of water quality in rivers: Insights from high resolution maps based on integrated geospatial, sensor and ROV technologies, *Appl. Geog.*, *32*(2), 455–464, doi: 10.1016/j.apgeog.2011.01.023.

City of Grand Junction (2016), *Grand Junction Municipal Code Volume II: Development Regulations; Title 28: Stormwater Management Manual; Chapter 28.52: Irrigation/Drainage Structures.* Grand Junction, Colorado. <http://www.codepublishing.com/CO/GrandJunction/html2/GrandJunction28/GrandJunction2852.html#28.52> (Feb. 8, 2017).

City of Logan (2016), *Storm Water Management Plan*. Logan, Utah. <http://www.loganutah.org/SWMP%20Document%20Less%20Appendices_Final.pdf> (Feb. 8, 2017).

City of Sequim (2016), *Storm and Surface Water Master Plan*. Sequim, Washington <http://www.sequimwa.gov/DocumentCenter/View/7735> (Feb. 8, 2017).

Cory, R. M., M. P. Miller, D. M. McKnight, J. J. Guerard, and P. L. Miller (2010), Effect of instrument-specific response on the analysis of fulvic acid fluorescence spectra, *Limnol. Oceanogr. Methods*, *8*, 67–78, doi: 10.4319/lom.2010.8.0067.

Creed, I. F., D. M. McKnight, B. A. Pellerin, M. B. Green, B. A. Bergamaschi, G. R. Aiken, D. A. Burns, S. E. G. Findlay, J. B. Shanley, R. G. Striegl, B. T. Aulenbach, D. W. Clow, H. Laudon, B. L. Mcglynn, K. J. Mcguire, R. A. Smith, and S. M. Stackpoole (2015), The river as a chemostat : fresh perspectives on dissolved organic matter flowing down the river continuum, *Can. J. Fish. Aquat. Sci.*, *14*, 1–14, doi: 10.1139/cjfas-2014-0400.

Downing, B. D., B. A. Pellerin, B. A. Bergamaschi, J. F. Saraceno, and T. E. C. Kraus (2012), Seeing the light: The effects of particles, dissolved materials, and temperature on in situ measurements of DOM fluorescence in rivers and streams, *Limnol. Oceanogr. Methods*, *10*, 767–775, doi: 10.4319/lom.2012.10.767.

Dunbabin, M., and A. Grinham (2010), Experimental evaluation of an autonomous surface vehicle for water quality and greenhouse gas emission monitoring, paper presented at: *IEEE International Conference on Robotics and Automation (ICRA)*, 5268–5274, May 3-8, Anchorage, AK, doi: 10.1109/ROBOT.2010.5509187.

Goldman, J. H., S. A. Rounds, and J. A. Needoba (2012), Applications of fluorescence spectroscopy for predicting percent wastewater in an urban stream, *Environ. Sci. Technol.*, *46*, 4374–4381, doi: 10.1021/es2041114.

Hatt, B. E., T. D. Fletcher, C. J. Walsh, and S. L. Taylor (2004), The influence of urban density and drainage infrastructure on the concentrations and loads of pollutants in small streams, *J. Environ. Manage.*, *34*(1), 112–124, doi: 10.1007/s00267-004-0221-8.

Horsburgh, J. S., D. G. Tarboton, D. R. Maidment, and I. Zaslavsky (2008), A relational model for environmental and water resources data, *Water Resour. Res.*, *44*, W05406, doi: 10.1029/2007WR006392.

Horsburgh, J. S., S. L. Reeder, A. S. Jones, and J. Meline (2015), Open source software for visualization and quality control of continuous hydrologic and water quality sensor data, *Environ. Modell. Software*, *70*, 32–44, doi: 10.1016/j.envsoft.2015.04.002.

Hudson, N., A. Baker, D. Ward, D. M. Reynolds, C. Brunsdon, C. Carliell-Marquet, and S. Browning (2008), Can fluorescence spectrometry be used as a surrogate for the Biochemical Oxygen Demand (BOD) test in water quality assessment? An example from South West England, *Sci. Total Environ.*, 391(1), 149–158, doi: 10.1016/j.scitotenv.2007.10.054.

iUTAH GAMUT Working Group (2017), iUTAH GAMUT Network Quality Control Level 1 Data at Logan River at the Utah Water Research Laboratory west bridge (LR_WaterLab_AA), HydroShare, http://www.hydroshare.org/resource/1b87fe7452624e82a54fa57432b17583.

Kaiser, K., G. Guggenberger, and L. Haumaier (2004), Changes in dissolved lignin-derived phenols, neutral sugars, uronic acids, and amino sugars with depth in forested Haplic Arenosols and Rendzic Leptosols, *Biogeochemistry*, *70*(1), 135–151, doi: 10.1023/B:BIOG.0000049340.77963.18.

Keith, M. K., S. Sobieszczyk, J. H. Goldman, and S. A. Rounds (2014), Investigating organic matter in Fanno Creek, Oregon, Part 2 of 3: Identifying and quantifying sources of organic matter to an urban stream, *J. Hydrol.*, *519*, 3010–3027, doi: 10.1016/j.jhydrol.2014.07.027.

Lakowicz, J. R. (2006), *Principles of fluorescence spectroscopy*, 3rd Ed., Springer USA, New York, NY, doi: 10.1007/978-0-387-46312-4.

Laudon, H., and O. Slaymaker (1997), Hydrograph separation using stable isotopes, silica and electrical conductivity: an alpine example, *J. Hydrol.*, *201*, 82–101, doi: 10.1016/S0022-1694(97)00030-9.

Lawaetz, A. J., and C. A. Stedmon (2009), Fluorescence intensity calibration using the raman scatter peak of water, *Appl. Spectrosc.*, *63*(November), 936–940, doi: 10.1366/000370209788964548.

Lee, E.-J., G.-Y. Yoo, Y. Jeong, K.-U. Kim, J.-H. Park, and N.-H. Oh (2015), Comparison of UV-VIS and FDOM sensors for in situ monitoring of stream DOC concentrations, *Biogeosciences*, *12*(10), 3109–3118, doi: 10.5194/bg-12-3109-2015.

Lewis, J. (1996), Turbidity-controlled suspended sediment sampling and load estimation, *Water Resour. Res.*, *32*(7), 2299–2310, doi: 10.1029/96WR00991.

Low, K. H., G. Podnar, S. Stancliff, J. M. Dolan, and A. Elfes (2009), Robot boats as a mobile aquatic sensor network, paper presented at: *Workshop on Sensor Networks for Earth and Space Science Applications (ESSA)*, Apr. 16, San Francisco, CA.

Lundquist, J. D., and D. R. Cayan (2002), Seasonal and spatial patterns in diurnal cycles in streamflow in the Western United States, *J. Hydrometeorol.*, *3*, 591–603, doi: 10.1175/1525-7541(2002)003<0591:SASPID>2.0.CO;2.

Mallin, M. A., V. L. Johnson, S. H. Ensign, and T. A. MacPherson (2006), Factors contributing to hypoxia in rivers, lakes, and streams, *Limnol. Oceanogr.*, *51*(1, part 2), 690–701, doi: 10.4319/lo.2006.51.1_part_2.0690.

Marsh, P., and M.-K. Woo (1981), Snowmelt, glacier melt, and high arctic streamflow regimes, *Can. J. Earth Sci.*, *18*(8), 1380–1384, doi: 10.1139/e81-127.

Mazurkiewicz, A. B., D. G. Callery, and J. J. McDonnell (2008), Assessing the controls of the snow energy balance and water available for runoff in a rain-on-snow environment, *J. Hydrol.*, 354(1–4), 1–14, doi: 10.1016/j.jhydrol.2007.12.027.

McElmurry, S. P., D. T. Long, and T. C. Voice (2014), Stormwater dissolved organic matter: Influence of land cover and environmental factors, *Environ. Sci. Technol.*, *48*(1), 45–53, doi: 10.1021/es402664t.

McKnight, D. M., E. W. Boyer, P. K. Westerhoff, P. T. Doran, T. Kulbe, and D. T. Andersen (2001), Spectrofluorometric characterization of dissolved organic matter for indication of precursor organic material and aromaticity, *Limnol. Oceanogr.*, *46*(1), 38–48, doi: 10.4319/lo.2001.46.1.0038.

Melcher, A. A., and J. S. Horsburgh (2017), An urban observatory for quantifying phosphorus and suspended solids loads in combined natural and stormwater conveyances, *Environ. Monit. Assess.*, *2017,* 189-285, doi: 10.1007/s10661-017-5974-7.

National Research Council (2009), *Urban Stormwater Management in the United States Committee on Reducing Stormwater Discharge Contributions to Water Pollution*. The National Academies Press, Washington, DC, doi: 10.17226/12465.

Paul, M. J., and J. L. Meyer (2001), Streams in the urban landscape, *Annu. Rev. Ecol. Syst.*, *32*(1), 333–365, doi: 10.1146/annurev.ecolsys.32.081501.114040.

Pellerin, B. A., J. F. Saraceno, J. B. Shanley, S. D. Sebestyen, G. R. Aiken, W. M. Wollheim and B. A. Bergamaschi (2012), Taking the pulse of snowmelt: In situ sensors reveal seasonal, event and diurnal patterns of nitrate and dissolved organic matter variability in an upland forest stream, *Biogeochemistry*, *108*(3), 183–198, doi: 10.1007/s10533-011-9589-8.

Podnar, G., J. M. Dolan, K. H. Low, and A. Elfes (2010), Telesupervised remote surface water quality sensing, paper presented at: *IEEE Aerospace Conference*, 1–9. Mar. 6-13, Big Sky, MT, doi: 10.1109/AERO.2010.5446668.

Saraceno, J. F., B. A. Pellerin, B. D. Downing, E. Boss, P. A. M. Bachand, and B. A. Bergamaschi (2009), High-frequency in situ optical measurements during a storm event: Assessing relationships between dissolved organic matter, sediment concentrations, and hydrologic processes, *J. Geophys. Res.*, *114*, G00F09, doi: 10.1029/2009JG000989.

Saraceno, J. F., J. B. Shanley, and B. Aulenbach (2016), Multi-site field verification of laboratory derived FDOM sensor corrections: The good, the bad and the ugly, abstract H11B-087 presented at: 49th Annual AGU Fall Meeting, Dec. 12-16, San Francisco, CA.

Saraceno, J. F., J. B. Shanley, B. D. Downing, and B. A. Pellerin (2017), Clearing the waters: Evaluating the need for site-specific field fluorescence corrections based on turbidity measurements, *Limnol. Oceanogr. Methods*, *15*(4), 408-416. dio: 10.1002/lom3.10175.

Spencer, R. G. M., B. A. Pellerin, B. A. Bergamaschi, B. D. Downing, T. E. C. Kraus, D. R. Smart, R. A. Dahlgren, and P. J. Hernes (2007), Diurnal variability in riverine dissolved organic matter composition determined by in situ optical measurement in the San Joaquin River (California, USA), *Hydrol. Processes*, *21*(23), 3181–3189, doi: 10.1002/hyp.6887.

U.S. Census Bureau, Population Division (2016), Annual Estimates of the Resident Population: April 1, 2010 to July 1, 2015. <https://factfinder.census.gov/faces/tableservices/jsf/pages/productview.xhtml?src=bkmk> (Apr. 26, 2017).

Utah Depatment of Environmental Quality, Division of Water Quality (2004), *Utah's 2004 303(d) List of Impaired Waters*, Salt Lake City, UT.

Utah Depatment of Environmental Quality, Division of Water Quality (2010), *Middle Bear River and Cutler Reservoir Total Maximum Daily Load (TMDL)*, Salt Lake City, UT.

Utah Office of Administrative Rules (2017), *R317-2. Standards of Quality for Waters of the State*. Salt Lake City, UT.

Watras, C. J., P. C. Hanson, T. L. Stacy, K. M. Morrison, J. Mather, Y.-H. Hu, and P. Milewski (2011), A temperature compensation method for CDOM fluorescence sensors in freshwater, *Limnol. Oceanogr. Methods*, *9*, 296–301, doi: 10.4319/lom.2011.9.296.

Tables

Table 4-1. Instrumentation at the canal and outfall monitoring sites.

Site Type	Instrumentation	Function / Variable
Continuously Monitored Canal Site	Campbell Scientific CR800 Datalogger	Data logging
	Campbell Scientific TE525WS Rain Gage	Rainfall
	Campbell Scientific CS451 Pressure Transducer	Gage Height
	Teledyne ISCO 3700	Automated Sample Collection
	Forest Technology Systems DTS-12	Turbidity
	Sontek SL3000 Side looking ADVM	Water Flow (Upstream Canal Site)
	YSI EXO2 Multiparameter Sonde	Specific Conductance
		Water Temperature
		pH
		Dissolved Oxygen
		FDOM
	Turner Designs C6 Multi-sensor Platform	Water Temperature
		Water Depth
		Cyclops – 7 Standard CDOM
		Cyclops – 7 Custom Fluorometer #1
		Cyclops – 7 Custom Fluorometer #2
Continuously Monitored Stormwater Outfall Site	Campbell Scientific CR800 Datalogger	Data logging
	Campbell Scientific TE525WS Rain Gage	Rainfall
	Teledyne ISCO 3700	Automated Sample Collection
	Teledyne ISCO 2150	Water Depth
		Water Velocity
		Water Temperature
		Water Flow
		Water Volume

Table 4-2. Instrumentation of the mobile sensing platform.

Instrumentation	Function / Variable Measured
Campbell Scientific CR6 Datalogger	Data logging
Garmin GPS16X-HVS GPS Receiver	Latitude
	Longitude
	Altitude
	Course
	Speed
YSI EXO2 Multiparameter Sonde	Specific Conductance
	Water Temperature
	pH
	Dissolved Oxygen
	FDOM
Turner Designs C6 Multi-sensor Platform	Water Temperature
	Water Depth
	Cyclops - 7 Standard CDOM
	Cyclops - 7 Custom Fluorometer #1
	Cyclops - 7 Custom Fluorometer #2
Forest Technology Systems DTS-12	Turbidity

Table 4-3. Summary of monthly FDOM statistics for baseflow conditions at the upstream and downstream continuous monitoring locations during 2015 and 2016 combined.

Site	Parameter	May	Jun	Jul	Aug	Sep	Oct
200 S	Min	8.14	3.92	1.44	1.93	1.76	1.85
	Mean	22.16	10.7	6.41	5.43	4.87	4.94
	Max	28.77	22.88	12.8	9.23	9.83	9.47
	STD	3.54	5.3	2.78	2.38	2.45	2.72
	Median	22.16	9.78	7.76	6.9	3.25	2.95
1800 N	Min	12.66	6.06	3.95	3.73	2.88	3.84
	Mean	18.27	12.15	6.89	6.58	7.22	6.4
	Max	26.38	20.45	13.14	12.82	13.89	10.3
	STD	3.26	3.03	2.1	2.2	2.43	1.65
	Median	17.59	12.44	5.91	5.54	8.56	7.04

Figures

Figure 4-1. Operation of the mobile sensing platform during stormflow conditions.

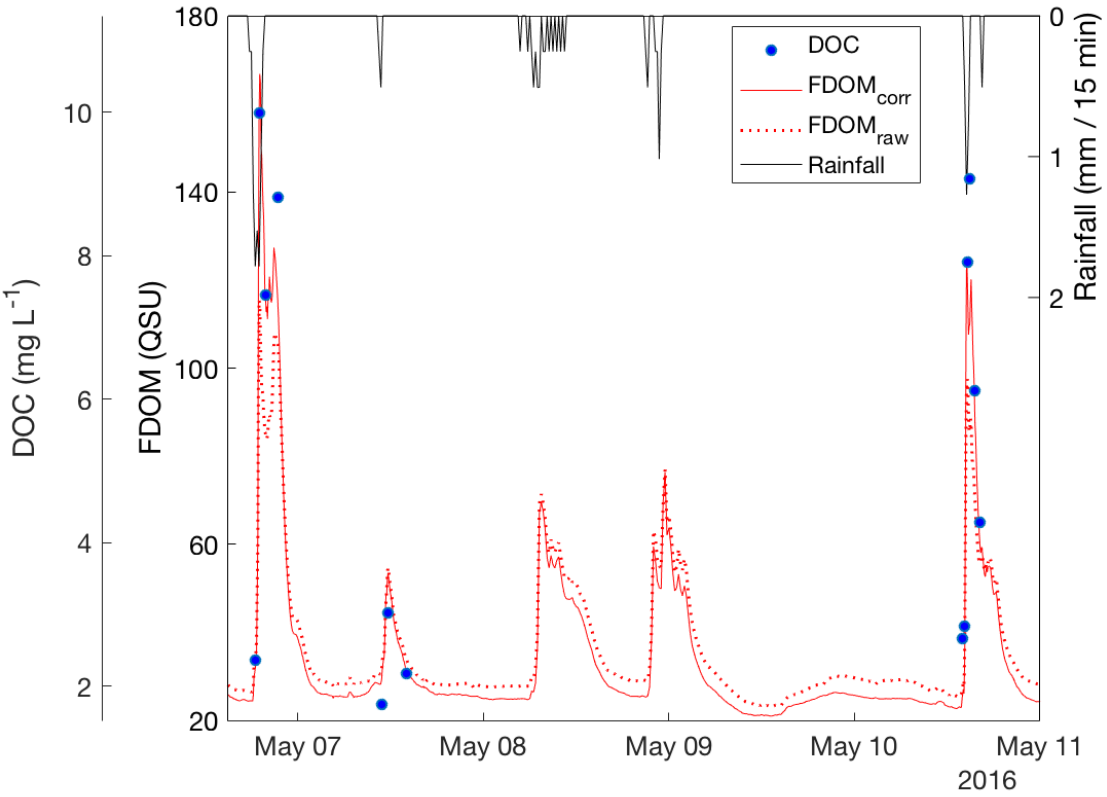

Figure 4-2. Comparison of raw and corrected FDOM with DOC samples during a storm event at the 1800 N monitoring location.

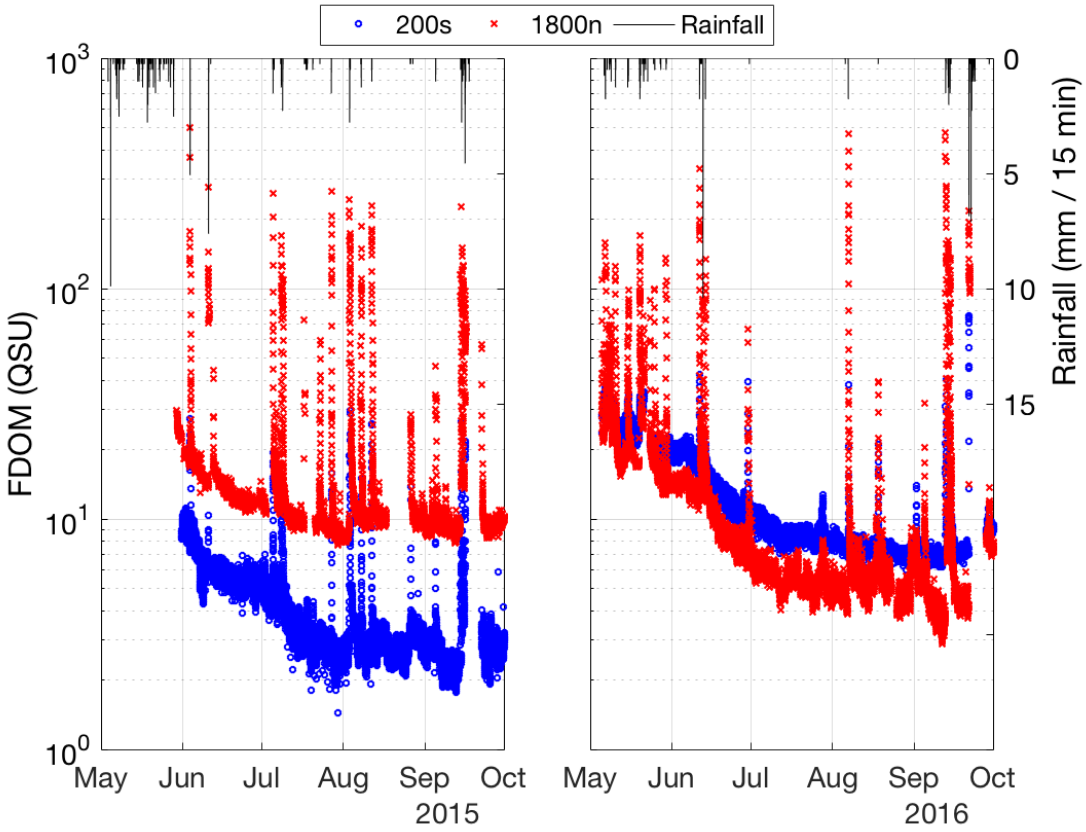

Figure 4-3. *In situ* measurements of FDOM in log scale and rainfall during the two irrigation seasons in the NWFC. Data is in 15 minute increments.

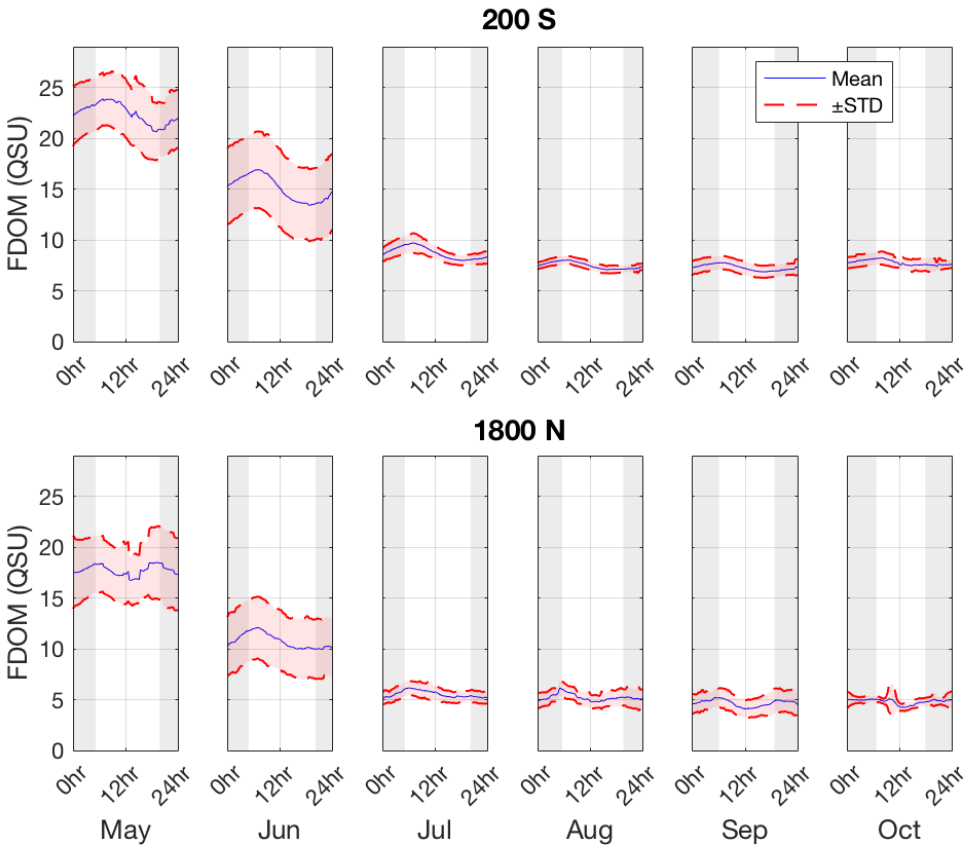

Figure 4-4. Mean and standard deviation of the diurnal cycle of FDOM during baseflow conditions for each month at the continuous canal monitoring sites during the 2016 field season. Gray shading indicates nighttime periods based on the sunrise and sunset times (MST) in Logan, UT for the 15th day of the month.

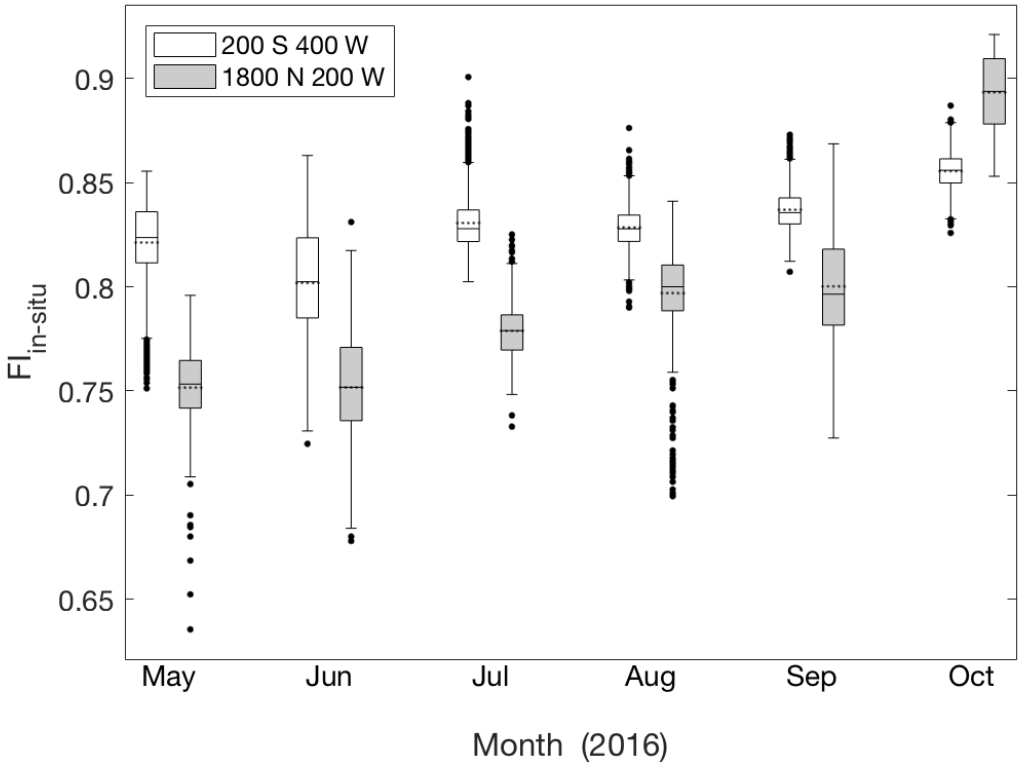

Figure 4-5. Monthly change of $FI_{in\text{-}situ}$ measured in the NWFC at the upstream and downstream monitoring locations during baseflow conditions.

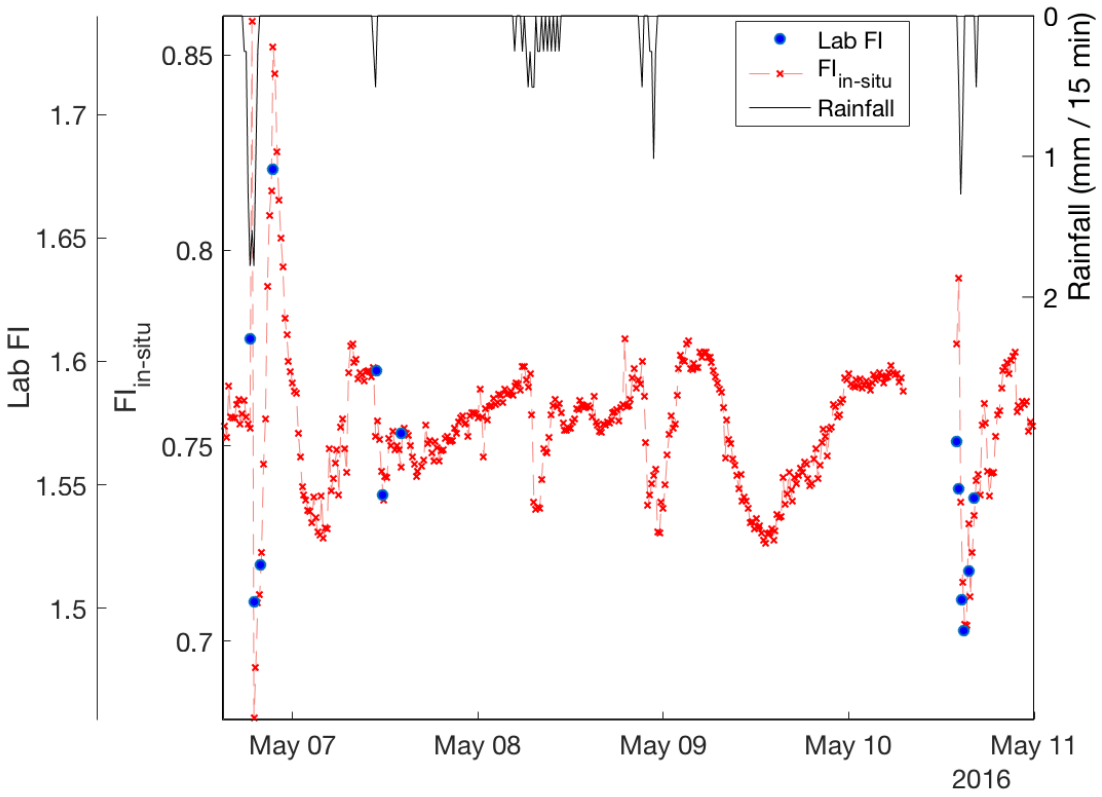

Figure 4-6. Comparison of lab measured FI and $FI_{in\text{-}situ}$ (FI determined from continuous measurements made by our custom fluorometers) values during a storm event at the 1800 N monitoring location.

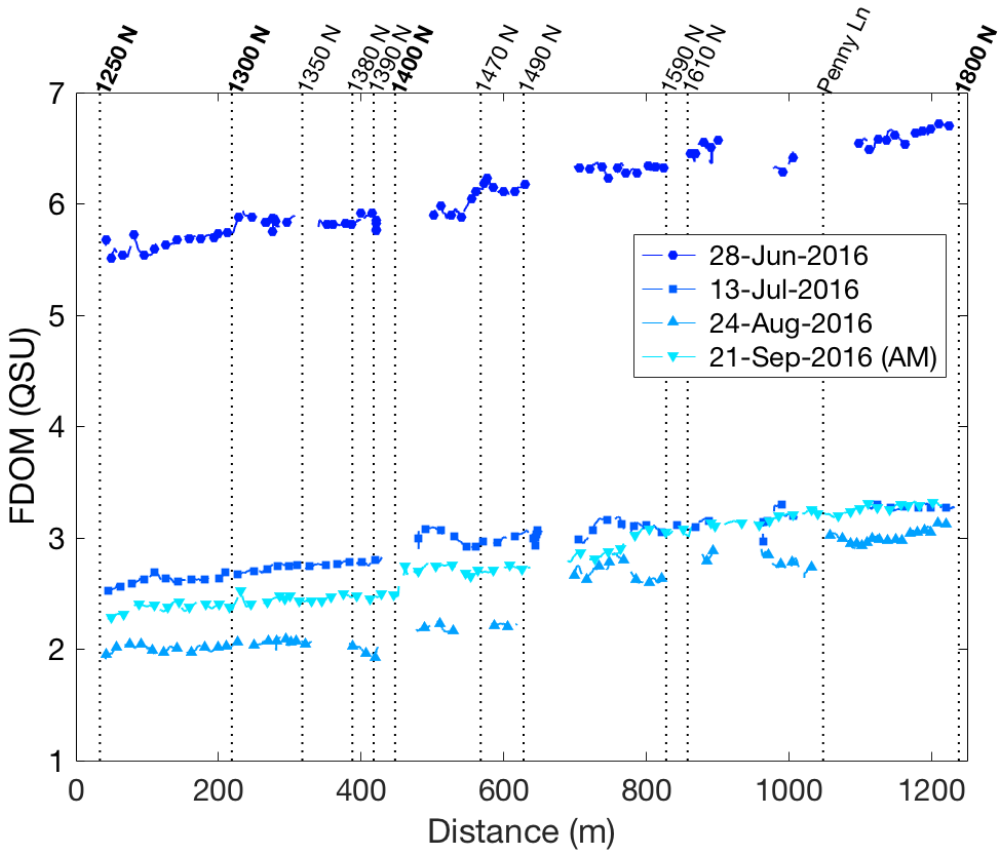

Figure 4-7. Baseflow runs with the mobile sensing platform. Dotted vertical lines indicate the location of outfalls along the reach with monitored sites in bold font.

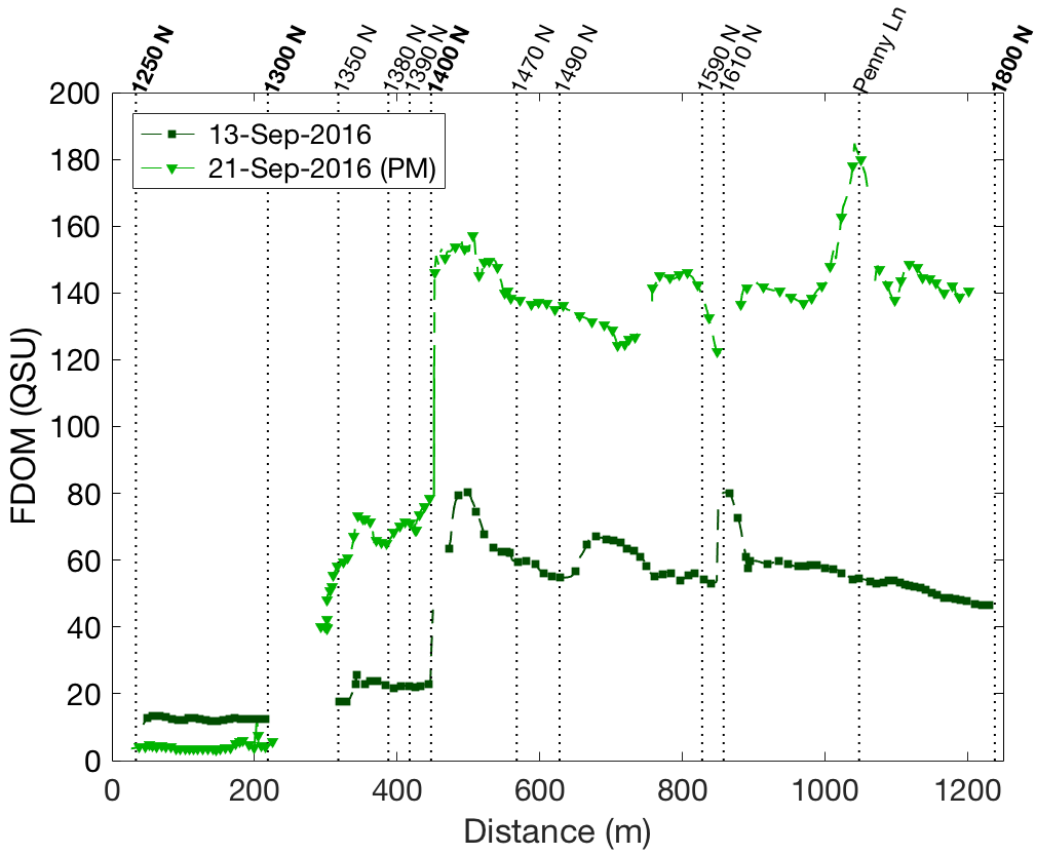

Figure 4-8. Two stormflow runs with the mobile sensing platform where spikes in FDOM are associated with the locations of outfalls discharging into the canal. Dotted vertical lines indicate the location of outfalls along the reach with monitored sites in bold font.

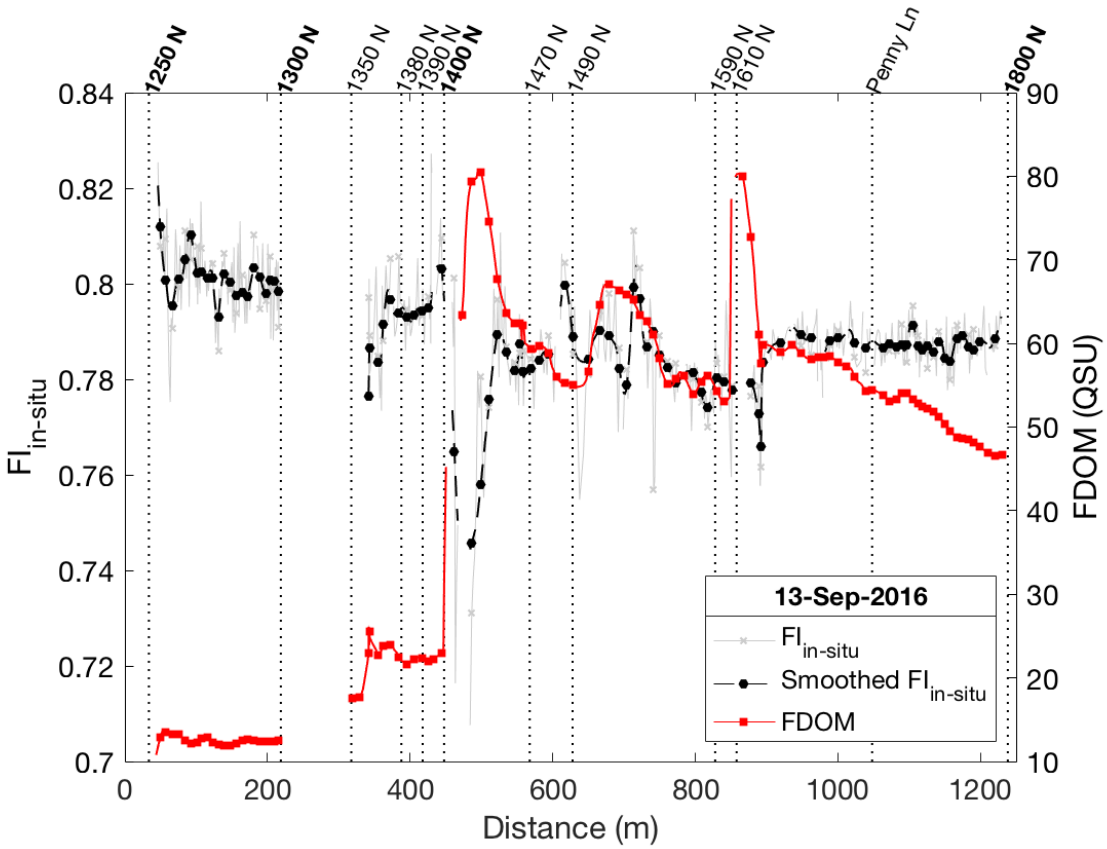

Figure 4-9. Comparison between the response of FDOM and $FI_{in\text{-}situ}$ to outfall contributions during a stormflow run with the mobile sensing platform. Dotted vertical lines indicate the location of outfalls along the reach with monitored sites in bold font.

CHAPTER 5

SUMMARY AND CONCLUSION

The characteristics of dissolved organic matter (DOM) contributions during two irrigation seasons and several stormwater runoff events in the Northwest Field Canal (NWFC) have been presented in this thesis. Results were grouped into two main chapters. First, Chapter 3 shows how DOM changed spatially and temporally within the NWFC using excitation emission matrix spectroscopy (EEMS) and dissolved organic carbon (DOC) concentration analysis from physical samples collected in the canal and from storm drains that were later analyzed in the laboratory. Chapter 4 then illustrates results from using *in situ* monitoring techniques to determine the spatial and temporal patterns in fluorescent DOM (FDOM) and the use of custom fluorometers to detect compositional changes in DOM.

Results in Chapter 3 showed that baseflow concentrations of DOC were low and did not change significantly between monitoring sites at the upstream and downstream ends of the NWFC. However, during storm events, DOC concentrations in the canal were elevated due to runoff being discharged from outfall sites, with the majority of DOC contributions being exported during the first flush (first 15 minutes) of runoff. These discharges subsequently altered the in stream DOM composition.

Comparison between the volume under the EEM absorbance surface and DOC concentrations indicated that the largest changes in DOM within the canal were concentration related (i.e., concentrations were much higher in flows from stormwater outfalls and in the combined flows within the canal under stormflow conditions than they

were in baseflow). However, our examination of the EEMs on a relative scale using a peak picking analysis showed that there were also compositional changes between the flow conditions. Relative changes in peaks characteristic of certain classes of organic compounds indicated that the DOM pool during storm events increased in humic-like composition, while protein-like chemical contributions decrease minimally or do not change. The changes were more significant at the downstream monitoring locations, revealing that changes in DOM composition in the canal are driven by the contributions from the stormwater outfall sites during storm events.

A EEM subtraction procedure was applied to our data in an attempt to identify potential differences in EEM peaks between stormflow and baseflow samples. However, this procedure did not appear to reveal any new information about differences in EEM peaks within the examined excitation and emission wavelength ranges that we did not see using other methods. There are other, more sophisticated methods that can be used to analyze EEM peaks, including principle components analysis (PCA) and parallel factor analysis (PARAFAC) modeling, that may reveal additional structure in our EEMs samples that we were not able to observe using the simpler methods we used.

Calculation of EEM indices allowed for further characterization of the DOM. The fluorescence index (FI) showed that during baseflow conditions the DOM is of a more autochthonous composition. During combined flow (i.e., stormwater plus canal water) conditions FI values were less than baseflow FI and exhibited a drop in FI between the upstream canal sites suggesting additions of more terrestrially derived DOM composition within the study reach. FI values of stormwater from outfall sites had lower FI values compared to the combined stormflow FI, indicating that runoff discharges are driving the

drop in FI within the canal. The findings from calculating the humification index (HIX) and the freshness index (BIX) provided consistency to what was observed with the FI. HIX values suggest that there are differences in the degree of microbial processing among the different land uses that drain to individual outfalls within the study reach. BIX values indicated that DOM from stormwater inputs is of older and more terrestrially derived DOM, which may indicate that organic matter is stored in the storm drains until flushed out with the onset of additional runoff. Stormflow values for FI, HIX, and BIX at 1000 N and 1400 N always exhibited the greatest difference from baseflow, while 300 N and 800 N always had smaller differences, indicating that the fluorescence properties of DOM being contributed during storm events are site specific. $SUVA_{254}$ values were elevated in the canal during stormflow, indicating a change in chemical structure of the DOM to more aromatic compounds, which are less labile in nature. The high variation in $SUVA_{254}$ values may have been caused by metal contamination, and therefore, only median values were analyzed for $SUVA_{254}$.

The results from Chapter 4 show that the concentrations of FDOM declined throughout the season at both upstream and downstream monitoring sites, likely driven by reductions in spring snowmelt driven flows throughout the summer. The two monitoring sites had relatively similar FDOM measurements during baseflow conditions, which is consistent with the results from the DOC analysis. Storm events resulted in contributions of FDOM that were orders of magnitude greater than the highest concentrations observed during baseflow conditions. During stormflow conditions, the downstream monitoring site had significantly higher FDOM measurements than the

upstream monitoring site, likely due to the contributions from outfalls between the two sites during storm events, which is also consistent with analysis presented in Chapter 3.

Custom fluorometers deployed at the continuous monitoring sites were used to measure the FI *in situ* ($FI_{in\text{-}situ}$). The results for $FI_{in\text{-}situ}$ showed that the composition of DOM changed throughout the season to a more microbially derived DOM, indicated by the gradual increase in $FI_{in\text{-}situ}$ values throughout the summer. The values observed for $FI_{in\text{-}situ}$ were consistently lower at the downstream monitoring location compared to the upstream site, which we attribute to return flows into the canal generated by irrigation practices adjacent to the NWFC and are expected to have a more terrestrially derived DOM composition. Short duration drops in FI were observed after the onset of runoff, indicating that contributions of DOM derived from terrestrial sources are being added to the system during stormflow conditions. These $FI_{in\text{-}situ}$ results are similar to those observed in the lab measured FI, suggesting that, under some conditions, the use of custom fluorometers is effective in capturing continuous changes of DOM composition.

The implementation of a mobile sensing platform allowed for high frequency measurements that captured rapid changes in FDOM concentration and composition. Overall FDOM values declined in four subsequent baseflow runs, which is consistent with the seasonal analysis of FDOM observed at the two canal monitoring sites. During stormflow condition runs, spikes in FDOM were associated with the locations of outfalls discharging runoff into the canal, and certain stormflow runs depicted elevated values in FDOM where no outfalls are present, alluding to contributions to the canal from overland flow during intense rainfall periods. Overall, the application of the mobile sensing

platform was the best method to provide high spatial resolution measurements that revealed contributions from locations that would have otherwise gone unobserved.

Chapters 3 and 4 of this thesis provide insight into the spatial and temporal contributions of DOM to the NWFC throughout irrigation seasons and during storm events. Our results provide information about the source, quantity, and quality of DOM that is contributed to an urban water conveyance via stormwater runoff. We anticipate that the behavior we observed is likely similar to that of many urban systems in the intermountain western U.S. with land use types, climate, and urban water systems that are similar to the one we monitored. The implications of these stormwater contributions and the changes in composition could result in rapid declines in DO concentrations over short periods of time. In Cache County, this has the potential to cause further stresses on the already impaired downstream water body of Cutler Reservoir. These results provide better understanding of the composition of DOM in the canal system and may provide crucial information for future management of stormwater runoff that can potentially lead to the improvements of water quality in downstream water bodies.

CHAPTER 6

ENGINEERING SIGNIFICANCE

In the fields of environmental engineering and water resources, the assessment of water quality has commonly been conducted by measuring concentrations of select constituents. However, less attention has been given to quantifying the concentration and chemical composition of organic material, particularly in urban water systems. This is partially due to the difficulty and expense of collecting and analyzing individual samples and also because robust sensors for measuring organic material *in situ* have only been emerging for use in stream and riverine environments over the past several years. This thesis provides extensive data characterizing dissolved organic matter (DOM) within an urban water conveyance that receives stormwater runoff that have not been collected at the spatial and temporal scales presented here. The laboratory and *in situ* fluorescence measurement techniques applied in this work provide approaches for characterizing DOM concentrations and composition, for identifying the importance of particular stormwater outfalls with respect to impacts on water quality, and estimation of DOM loads in baseflow and from stormwater inputs. Furthermore, we demonstrated how the data can be refined, allowing for characterization of the DOM by certain classes of organic chemicals, age, and quality.

Understanding of the quantity and composition of DOM being contributed during stormwater runoff events has the potential to influence management of stormwater and the use of water in the canal by downstream water users. Stormwater managers could use the continuous data to identify priority areas for management practices aimed at

improving the quality of stormwater discharges. They might also use the data to identify illicit discharges to the stormwater system. Canal managers could use the data to alert downstream water users during times when water quality is impacted by stormwater.

The use of *in situ* data has become more frequent with advancements in technology. The benefits associated with continuous monitoring are numerous, including the ability to: 1) capture a much broader range of hydrologic conditions, 2) customize data collection frequency and create a much larger number of observations than could be analyzed in a laboratory, 3) identify and characterize short-term hydrologic events that are difficult to sample, and 4) reduce the cost per observation. The application of fluorescence monitoring in quantifying and characterizing DOM within urban water systems has yet to be thoroughly examined. This project advances the understanding and application of *in situ* FDOM measuring in freshwater systems.

Custom fluorometers are in the early stages of use, and, therefore, many applications are yet to be realized. The ability to identify seasonal and short term changes in sources of organic matter using *in situ* monitoring has many implications for the characterization of DOM throughout a watershed or across multiple watersheds. Advancement in surrogate relationships between observations from custom fluorometers and select regions of EEMS is of great interest for the potential use in monitoring for impacts from stormwater runoff or wastewater inputs. This research demonstrates that custom fluorometers are a promising advancement in the field of water quality monitoring, while acknowledging that improvements can still be made.

Monitoring of water quality constituents is commonly conducted at large spatial and temporal scales. Placements of monitoring sites are often a balance between idealized

measuring locations, ability to access an area of interest, and cost. This can be a challenge when it comes to identifying spatial changes in water quality, as there are often processes occurring at higher spatial resolutions that go unmeasured between stationary, *in situ* monitoring sites. The application of a mobile sensing platform to capture water quality measurements overcomes this challenge as indicated by the results shown in this thesis. The data obtained using a mobile platform are especially advantageous for enhancing the understanding of how DOM is contributed to (e.g., measuring contributions from ungaged stormwater outfalls) and processed within aquatic ecosystems. While we focused on results from the FDOM sensors, the platform is generic and can be used with any water quality sensors that can be integrated via a Campbell Scientific datalogger, lending itself to collection of higher resolution data over broader spatial areas. This method also has the potential to provide short term monitoring solutions to unmonitored aquatic ecosystems.

CHAPTER 7

RECOMMENDATIONS FOR FUTURE RESEARCH

The following is a list of additional or more advanced research ideas that could potentially supplement this work. These ideas are aimed at providing: 1) a better understanding of the compositional changes in dissolved organic matter (DOM) caused by stormwater inputs to urban water systems; 2) a better understanding of the total loads of organic matter contributed to these systems with stormwater; and 3) better understanding of the sources of DOM contributed to urban water systems via stormwater runoff.

1. Perform parallel factor (PARAFAC) analysis on the results of the excitation emission spectroscopy (EEMS) data that have already been collected. The peak picking methods applied in this work provide useful indications of DOM composition, but do not take full advantage of the information inherent in the measured EEM spectra. PARAFAC is a multiway analysis that has been referred to as a mathematical chromatography. The process decomposes the fluorescence signal of DOM into unique fluorescent groups (components) that represent a class of organic material whose abundance can be related to DOM precursor materials. PARAFAC may provide more information on discrete changes in component concentrations within the DOM pool than the peak picking analyses could.
2. Implement a robust burst sampling and outlier detection sampling schema for *in situ* measurements made with the Turner C6 multi-fluorometer platform to

reduce the noise and value anomies that were observed in this study. We used a simple burst technique for the data collected by this study using the Turner C6, but still observed significant noise in the fluorescence data, especially when compared to the YSI EXO2 FDOM. After consulting with representatives from YSI, it is our understanding that YSI sondes use a proprietary outlier detection and elimination algorithm during sampling before the measurement is sent via the SDI-12 interface to the data logger for recording in memory on the data logger. Implementing a similar algorithm to all measurement devices would provide more consistency within observations of the same type (i.e., fluorescence) within the monitoring network and may potentially reduce the time and effort required in quality control and interpretation of the data.

3. Further investigate relationships between lab measured fluorescence index (FI) and FI measured *in situ* ($FI_{in\text{-}situ}$). The results presented here demonstrated that $FI_{in\text{-}situ}$ is a viable method for detecting continuous changes in DOM sources. However, our $FI_{in\text{-}situ}$ results did not always have a high degree of correlation with lab measured FI values. $FI_{in\text{-}situ}$ was correlated with lab FI during storm events, but the correlation was not as strong during baseflow conditions. However, the number of samples collected during baseflow conditions was relatively small. Additional samples collected for laboratory EEMS during baseflow may help us determine whether sample size was an issue or whether there are other confounding conditions (e.g., noise in the custom fluorometer data). If the $FI_{in\text{-}situ}$ values could be reported on the same scale and as lab

measured FI, it would allow for greater comparability between FI values reported by other studies and represent the results in the scale that most readers will already be familiar with.

4. The mobile sensing platform should be tested in a different urban reach or other systems as additional case studies. As an example, the Jordan River, which is an urban river within Salt Lake City, UT, has several diversions and wastewater treatment return flows, making it a unique system to conduct mobile sensing deployments. The Jordan River faces problems with low dissolved oxygen, which has been attributed to organic matter inputs during stormwater runoff events. Deploying the mobile sensing platform in systems like the Jordan River has the potential to reveal critical zones of water quality impairment and identify locations of pervasive pollutant contributions during stormwater runoff events that have not been identified by grab sampling and continuous monitoring efforts to date.
5. Perform in house laboratory FDOM correction experiments for temperature and turbidity. While the coefficients found in the literature and used in this work were acceptable for our data, we acknowledge that there may be instrument or site specific characteristics in our system that could be better accounted for. Conducting FDOM correction experiments of our own would verify whether the corrections we adopted are robust or whether more specific corrections are needed.